SOME INVESTIGATIONS OF A MULTIPLE ARC PLASMA GENERATOR

By

EDWARD CHARLES POHLMANN, JR.

Bachelor of Science in Mechanical Engineering
Newark College of Engineering
Newark, New Jersey
1953

Master of Science in Mechanical Engineering
Northwestern University
Evanston, Illinois
1954

Submitted to the Faculty of the Graduate School of
the Oklahoma State University
in partial fulfillment of the requirements
for the degree of
DOCTOR OF PHILOSOPHY
May, 1964

SOME INVESTIGATIONS OF A MULTIPLE ARC PLASMA GENERATOR

Thesis Approved:

Donald R. Haworth
Thesis Adviser

J. B. Boggs

G. W. Grimmett

O. H. Hamilton

J. B. Boggs
Dean of the Graduate School

ACKNOWLEDGEMENT

The author wishes to express his gratitude to the many persons and institutions for their moral, educational, and physical support during the conduct of this thesis work.

The financial support, without which this work could not have been undertaken, was provided in part by National Science Foundation Grants 10161 and 20089, and by IIT Research Institute under project No. T 1046.

The general guidance of Dr. J. H. Boggs, Head of the School of Mechanical Engineering, and the individual instructive assistance of Dr. D. R. Haworth, Plasma Facility Project Leader, contributed significantly to the success of this work. The author is particularly grateful for the day to day help and encouragement of Dr. M. K. Jovanovic, former Plasma Facility Project Leader and close friend.

The manufacturing and operational problems encountered in the laboratory were lightened considerably by the constructive suggestions and physical assistance of Professor F. C. McQuiston Laboratory Supervisor, and his cooperative staff, J. A. McCandless, L. S. Benjamin, and G. M. Cooper. Mr. Benjamin was responsible for machining the many components used in the tests - a significant contribution, greatly appreciated. The author also wishes to express

his gratitude to the following persons: D. Chenault, D. Foss, and C. Smith, Mechanical Engineering students who helped from day to day on the project; S. Jordon who prepared the rough and final drafts of this thesis; and M. Avery and C. King who handled the paper work and records required in connection with the administration of the project.

TABLE OF CONTENTS

LIST OF FIGURES

CHAPTER I

INTRODUCTION

A plasma may be defined as a collection of ionized particles and electrons. This definition is usually restricted to those cases in which the number of positive charges is approximately equal to the number of negative charges. Usually, the positively charged particles are ionized atoms while the negatively charged particles are electrons. However, exceptions may and frequently do exist in small percentages. The word plasma was first applied to a collection of charged particles by I. Langmuir in the 1920's.

All states of matter represent different degrees of organization to which correspond certain values of binding energy. Thus, in the solid state the important quantity is the binding energy of molecules in a crystal. If the average kinetic energy per molecule exceeds the binding energy, the crystal structure breaks up either into a liquid or directly into a gas. A similar law operates in the case of liquids, and in order to change a liquid into a gas, a certain minimum kinetic energy per molecule is required to break the bonds of the intermolecular forces. If sufficient energy is added to gas, the atoms of the gas will be ionized, i.e., one electron or more will be dislodged from

the outer shell of electrons of the atom. Thus, ionized matter may be considered as belonging to a fourth state.

Examples of naturally occuring plasmas on earth are rather limited, but forms of partially ionized gases which constitute plasma include fire, lightning, the aurora borealis and aurora australis. In addition there are certain man-made plasmas. These occur in many lighting devices and the welding arc. Plasmas occur relatively very infrequently on the earth. However, beyond the earth, there are an overwhelming number of examples of the plasma state, i. e., the stars and the sun, and it is not surprising that probably more than 99. 9 percent of the matter in our universe is ionized and, therefore, in the plasma state.

Since plasmas may exist in many different forms, theoretical and experimental researches on plasmas have taken widely divergent paths. A large segment of this research is directed toward controlled nuclear fusion, and many plasma physicists are engaged in the solution of this problem. The electric arc discharge also produces a plasma, and this phenomenon is of interest to engineers and physicists.

The electric arc discharge has been studied in the laboratory for more than fifty years. During this time electric arc welding and the carbon arc lamp have been the major practical applications of the electric arc discharge. Within the last ten years, however, engineers and scientists have expressed renewed interest in the electric arc and particularly its application to the plasma jet.

The interest lies in the fact that the plasma jet can produce a high velocity jet of extremely hot gas. There are plasma spray devices used to apply thin coats of ceramic and refractory materials to the inside of rocket nozzles. The plasma jet has been used to cut and weld even the most difficult refractory materials.

The development of very high-speed flight vehicles has created a need for test facilities capable of simulating the conditions under which such vehicles will have to operate. Studies have shown that the important parameter determining the rate of transfer of heat to a surface is the enthalpy of the contiguous fluid. A hyperthermal test facility will usually simulate the stagnation enthalpy and stagnation pressure but not the free stream Mach number. Justification comes from the fact that simulation of heat transfer depends mainly on matching stagnation enthalpy and stagnation pressure. A hyperthermal wind tunnel is capable of operating for several minutes at a time. The multiple electric arc discharge device can provide the stagnation enthalpies required. The ablation of nose cone materials is of considerable interest, and the hyperthermal wind tunnel is particularly suited for studies of this nature where the stagnation enthalpy is again of prime importance. Although some ablation studies have been conducted, all the answers are not known, and there is still considerable interest in this problem.

Also of interest is the arc-jet plasma propulsion device in which the energy required to heat the gas to be ejected comes from

electrical arc heating. The arc-jet plasma engine is inherently capable of providing a specific impulse in the neighborhood of 2,000 seconds (1).* Although no device of this kind is presently capable of lifting a vehicle off the surface of the earth, the device can be used for flights in outer space not too far from the earth.

As the above examples imply, the plasma jet is capable of producing a gas jet of very high enthalpy; and it is obvious that some of the development work on plasma jets has been directly specifically toward increasing the enthalpy of the gas jet. To this end many schemes have been tried. One such scheme, the multiple arc, is the basis for this dissertation.

As the name implies the multiple arc consists of several electric arc discharges arranged in electrical series. Thus, the same current passes through each arc, and the number of arcs in operation can be changed by a suitable switch. The gas is made to pass through each arc in succession. If two arcs are used, the first may be considered a preheater, while the second is a superheater. By passing the gas stream through a series of arcs, it should be possible to raise the enthalpy of the gas jet to values not previously attained. The advantages of the series multiple arc over the single arc may be many, and the following advantages come to mind. The physical size of some of the components of the arc jet assembly depend on the amount of energy which must be dissipated in a unit

*Numbers in parentheses refer to references in the Bibliography.

time from the electrode surfaces. These components include the areas of the cathode and electrode spots, the size of the cooling water lines, and the size of the current carrying load wires and others. In general as the amount of current used increases as the size of the components increases. In the interest of the most compact design it is desirable to keep the size of these components small. However, if the current is reduced the maximum power input is also reduced, resulting in reduced enthalpy of the gas. The multiple arc makes it possible to reduce the amount of current input but to maintain the same power input (and therefore the same gas enthalpy). Stated another way, for the same available current, considerably more power can be put into the gas with the multiple arc than with the single arc. This should result in a gas jet of higher enthalpy. Furthermore, certain types of power supplies require a series ballast resistor in order to achieve stable operation. This ballast can waste a lot of power. The multiple arc reduces the size of the ballast required and consequently the power wasted. In general the multiple arc is useful in raising the enthalpy of the gas jet, and it is more suited to certain types of power supplies.

The purpose of the research program reported in this thesis was to develop a multiple arc jet device and to evaluate its operating characteristics. To this end it was necessary to determine the dependence of the energy conversion efficiency and the gas enthalpy on the current, arc potentials and gas flow rate, and to compare the multiple arc results with those obtained from the single arc jet.

CHAPTER II

REVIEW OF ARC DISCHARGES

This chapter is devoted to a brief description of the physical phenomena which occur in the electric arc discharge. Emphasis has been put on a physical description of these phenomena rather than a mathematical description. Discussed are such topics as the entire arc itself, establishing the arc, the various processes occuring at the anode and cathode junction, and the positive column phenomena. Because the high pressure, high current arc is the subject of this dissertation, the emphasis has been so directed in this review. High pressure means pressures such that the electrons, ions and atoms (or molecules) are all at the same temperature. High current in this case means one ampere or more.

General Description of Arc Discharges

The arc discharge is only one possible form of an electric discharge which may occur in a gas. During an electric discharge an electric current exists in the gas between two electrodes. The current exists in the form of positive and negative charged particles which drift in opposite directions under the influence of the electric field established in the space between the electrodes. This field is

the result of different potentials placed on the two electrodes. Figure 1 shows the possible regions of an electric discharge.

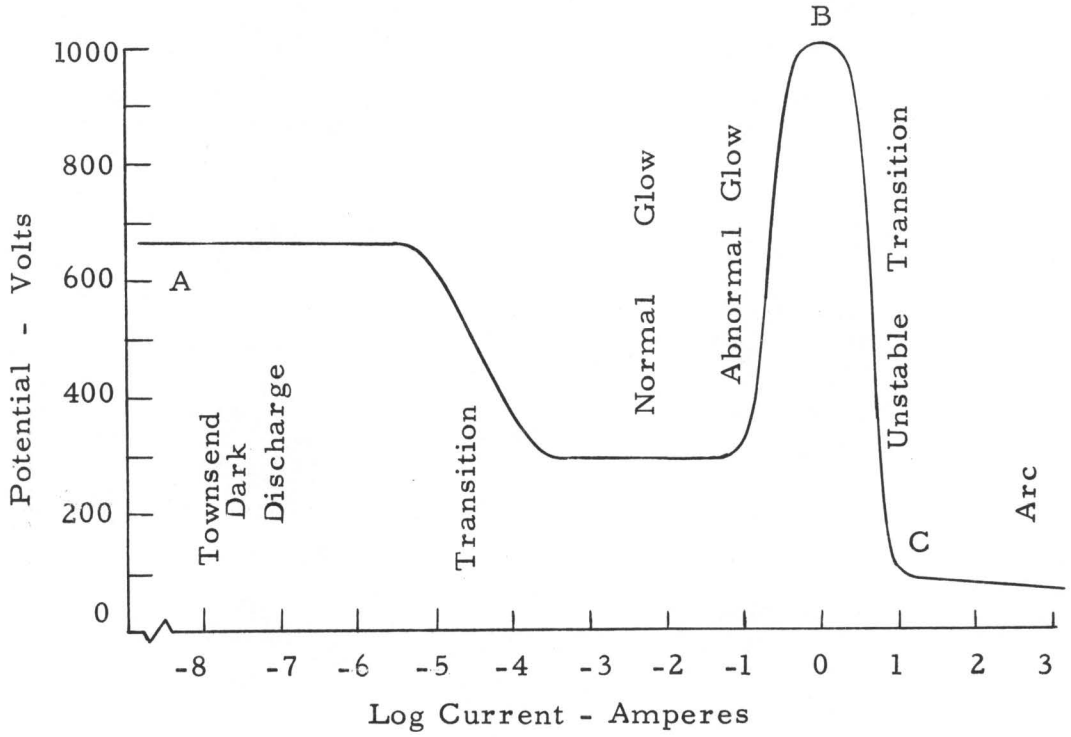

Figure 1 Possible Electric Discharges

It is assumed that the initial breakdown of the gas has occurred and that the current is held at a small value of 10^{-8} amperes, point A, by a current-limiting resistance which has been placed in series with the electrodes. As the current is increased, the voltage between the electrodes changes as shown by the curve, and the discharge passes through several different forms. Since this work is not concerned with these forms of discharge, little more will be said about them here. If the reader is interested, however, he may refer to Penning (2) for a brief introduction to all types of discharges, and to Loeb (3), Cobine (4), Von Engel (5), Von Engel and Steenbeck (6)

(in German), Meek and Craggs (7), Thomson and Thomson (8), Townsend (9), Handbuch der Physik (10) for a detailed treatment of these discharges.

Finally, as the current is increased, Point B of the diagram is attained. For a current larger than that corresponding to B, a sudden, usually unstable transition to a much lower voltage occurs (Point C). The stable arc discharge region now extends to the right of C. It is this region from C to D which is the subject of this thesis.

The curve of Figure 1 represents steady state discharges. Under certain conditions, such as a spark discharge, the transition from A to D may occur very rapidly (on the order of one microsecond) if a large voltage is suddenly applied to the electrodes without any resistance in series to prevent the current from rising quickly to the value at D. In such a case, there is very likely insufficient time for equilibrium to be attained in any of the intermediate states and the voltage may take a different course. This diagram, adopted from Somerville (11), is intended to indicate, in a general way only, the voltage-current characteristics of the different discharge processes. Numerical values of current and voltage have been inserted merely to indicate orders of magnitude. Factors which affect the voltage-current characteristics of an electrical discharge include the electrode size, shape, separation, and material, the gas and its pressure, and the proximity of the confining walls.

As stated above, the arc discharge is only one form of an electric discharge, and it may be regarded as the ultimate form of

discharge which will be reached under all conditions if the current through the gas is made large enough. A large enough current is usually one lying within the range 10^{-1} to 10 amperes (11). The term arc is usually applied only to stable or quasi-stable discharges and refers to a self-sustained discharge having a relatively low voltage drop and capable of supporting relatively large currents. Other characteristics include a volt-ampere curve which usually has a negative slope. In addition the gas temperature may be relatively high. If the high pressure arc burns horizontally, buoyant forces acting on the hot gases will cause the column to arch upwards, and it is probably due to this phenomenon that the arc discharge owes its name.

The arc itself is usually divided into three distinct regions for the purpose of study. These are designated as the cathode fall region, the positive column (or long column) and the anode fall region. Figure 2 is a graph of the potential of the arc versus the distance from the cathode, and the existence of the three regions is obvious. In order for the current to be passed from one electrode to the other, three things must happen.

(1) The current must be transferred across the gas-cathode junction. The cathode area through which the current flows, i.e., the location where the arc is actually attached to the physical surface, is called the cathode spot. There is also an anode spot. Across this junction a large electric gradient is established due to the space charge accumulation in this region. This results in a cathode fall of

potential of the order comparable to the ionization potential of the gas in which the arc burns, about 10 volts.

(2) The current must be conducted through the main body of gas called the positive column. For this to be possible, the normally neutral gas must be rendered conducting by the introduction of charge carriers, i.e., electrons and positive ions usually, or by their creation within it, or both. This is the region of the positive column, and in this region the electric gradient is much less than it is in the cathode and anode fall regions. The near constancy of the potential gradient in the positive column implies nearly equal numbers of ions and electrons. (It is assumed here that the ions are only singly ionized.)

(3) The current must be transferred across the anode-gas junction. Again a space charge accumulation results in an anode fall region for which the potential drop is less than that of the cathode fall.

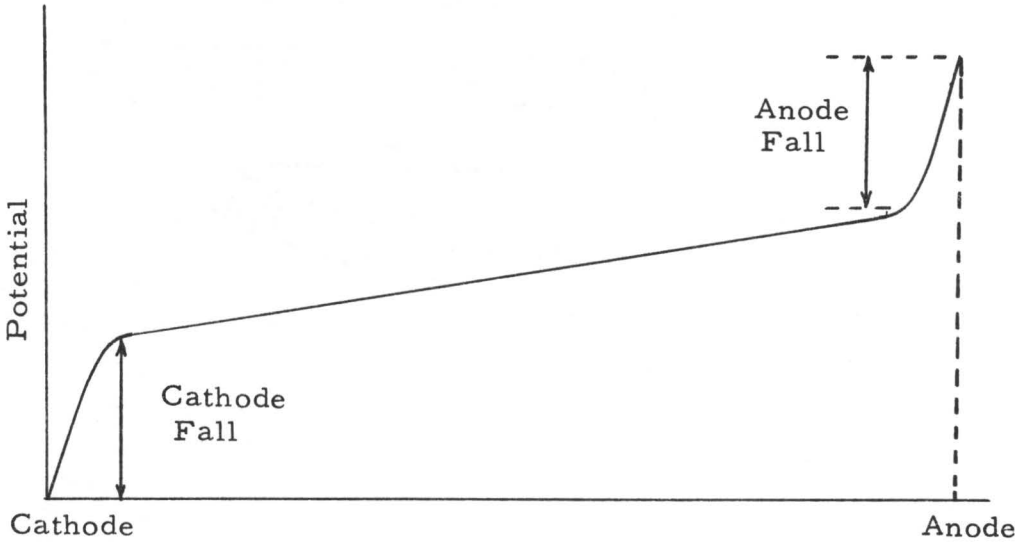

Figure 2 Potential Distribution in an Electric Arc

It is frequently necessary to distinguish between a low pressure arc and a high pressure arc. The most important difference between the low and the high pressure arc is the temperature of the positive column. In the high pressure column collisions of electrons with ions and neutrals are plentiful with the result that the directed energy an electron can acquire from the electric field between collisions is smaller than its random or thermal energy. Thus, any energy the electrons gain from the field is quickly transferred to the ions and neutral atoms or molecules because of the large number of collisions taking place. As a result, the ions, electrons and neutrals of the positive column are in thermal equilibrium. At low pressures there are fewer collisions, and the electron temperature may be rather high while the temperatures of the ions and neutrals are only a little above ambient. Figure 3 illustrates the effect of pressure on the temperature of the electrons and neutrals in an arc (12).

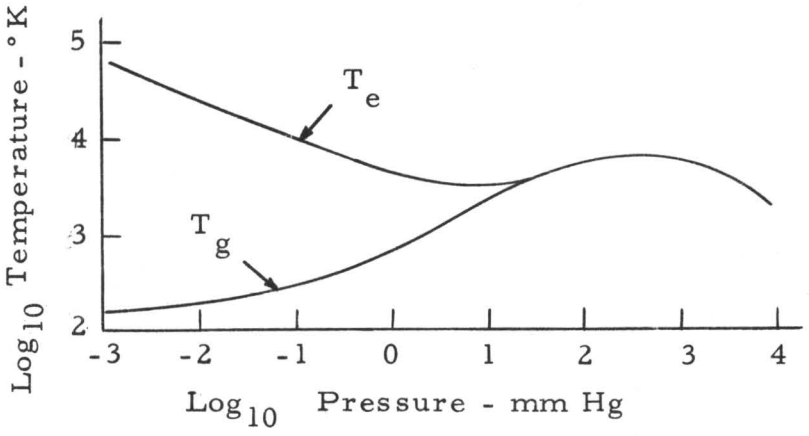

Figure 3 Electron and Gas Temperatures

A convenient dividing line between the low and high pressure arc would be that pressure at which the temperature of the electrons just equals that of the gas. From Figure 3 this appears to be at a pressure of about 25 mm or one inch of mercury. Of course, there is no sharp distinction between the low pressure and the high pressure regimes, but a rather gradual transition from one to the other.

An arc of some practical interest is the very short arc. The gap distances prevailing in these very short arcs are of the order of magnitude of the electron mean free path in gases at atmospheric pressure, so that many of the electrons will fall freely between the cathode and anode without making any collisions at all. This implies electrode separations of the order of 10^{-4} cm or less. The arc potential drop in short arcs is a little greater than the sum of the ionization potential of the metal vapor and the work function of the cathode surface. Obviously, a positive column does not exist in this type of arc, and the cathode and anode regions probably overlap.

Establishing the Arc

The establishment of the arc is a transient process which usually occurs in a relatively short time. Thus, many of the properties of the arc channel have achieved an almost quasi-steady state condition after a time of the order of 10 microseconds (13, 14). However, the approach to the ultimate steady state may take several minutes and even as much as 2 hours (15). The factors controlling the ultimate stabilization of the arc channel include the thermal

capacity of the electrodes, confining walls, if any, and the processes of convection and conduction of energy from the arc. These may require some time to come to steady state conditions, especially if the arc is unconfined.

The arc may be established by a transition from a high voltage low current type of discharge, by separating electrodes initially in contact, or by inserting between the electrodes sufficient quantities of current carrying elements to initiate the discharge. In all cases it is necessary to provide a sufficient number of ionized particles between the electrodes to initiate the discharge. If a continuous discharge is desired, it is also necessary to provide an external electrical circuit capable of maintaining the discharge once it commences.

(1) An arc may be established by a continuous or discontinuous transition from a low current stable discharge such as the glow. This process was discussed in the preceeding paragraph in connection with Figure 1. This transition may be effected very rapidly by means of a non-steady spark discharge. The arc is reached in this way when a discharge is initiated between electrodes in a gas at a pressure of about an atmosphere by a voltage source capable of breaking down the gap. No stable form of discharge exists until the arc form is reached. If the voltage source is not capable of maintaining the arc current, the discharge will extinguish. Clearly, the voltage between the electrodes is a function of current and time.

When the voltage across two electrodes is low, the gas is practically a perfect insulator. If the potential across the electrodes is gradually increased, a value is eventually reached for which the gas suddenly becomes conducting. This value of potential is called the breakdown or sparking voltage. The value of the sparking potential depends primarily on the gas, its pressure, and the electrode separation.

The processes occuring before the spark discharge are not completely understood, however the electrical breakdown can be considered to occur in two steps. These are called the statistical time delay and the formative time delay.

Suppose that a potential equal to or a little greater than the sparking voltage is applied across the electrodes. There is a finite time delay, called the statistical time lag, before the current starts to increase. The statistical time lag is the interval of time between the instant the breakdown voltage is applied and the instant one primary electron is formed in a suitable place by cosmic radiation, photo ionization, or other naturally occuring ionization processes.

Once an electron is produced in a suitable place, it is accelerated towards the anode by the electric field. However, a collision or collisions with neutrals occur producing additional electrons. These electrons are also accelerated towards the anode, but they engage in additional collisions which produce more electrons before they reach the anode. In this manner an electron avalanche is quickly established. After the number of ionized particles in the gap

has increased sufficiently, the voltage across the gap collapses very rapidly. The time elapsed from the appearance of the first electron until the voltage starts to collapse is called the formative time lag. The start of the voltage collapse is also the start of the non-stable discharge called a spark. These regions are indicated in a general way in Figure 4 (11).

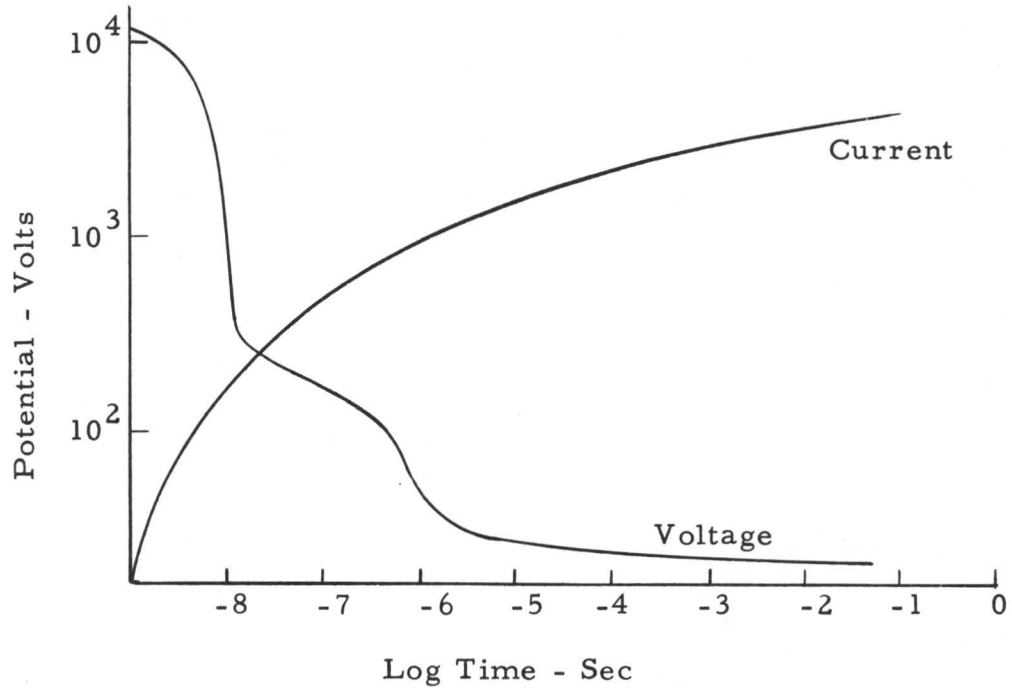

Figure 4 Electrical Breakdown History

The statistical time lag may be from 10^{-7} to 1 second, and the formative time lag ranges from 10^{-8} to 10^{-4} seconds (2, 5, 11). The formative time lag is shortened considerably when large overvoltages are used.

(2) An arc may be struck by drawing apart two touching electrodes through which a current is passing. When this is done, the

end points of contact between the electrodes dissipate some electrical energy, and a high temperature is developed in the region of the contact. As the pressure maintaining the contact diminishes, the resistance increases further, and the temperature rises to the point where the metal melts, forming a liquid metal bridge between the electrodes. As the electrodes are drawn apart the bridge lengthens until it finally ruptures explosively, either by vaporization at the hottest part or because the surface tension fails to maintain a coherent liquid bridge. The voltage across the bridge at the moment of rupture is usually of the order of one volt (11). After rupture an arc discharge is established between the electrodes. The discharge is sustained if the external electrical circuit is capable of maintaining the arc current; otherwise, the arc goes out.

A corollary of the drawn arc is the vacuum arc which may be struck between separating contacts in a highly evacuated space. This arc burns in the vapor of one or both of the electrode materials. The vapor is formed when the liquid metal bridge ruptures. The arc is frequently maintained in a manner similar to that of the very short arc.

(3) If two electrodes are separated by a few millimeters or more, and have impressed upon them a relatively low potential, about 125 volts, no arc discharge will result. However, if sufficient ionized species, obtained from an external source, are placed between the electrodes, an arc discharge will quickly form. Thus, electrons or ions or a mixture of both may be injected into the gas between the

electrodes to form a stable arc discharge. These may be obtained from electron or ion "guns." The ions are injected with sufficient energy to cause the required number of ionizing collisions in the gas separating the electrodes. On the other hand if electrons are injected they will be accelerated by the electric field, and even though it may be small, the electrons will gain enough energy from the field to cause a sufficient number of ionizing collisions.

A slightly ionized plasma may be injected between the electrodes, thus providing sufficient current carrying species to initiate an arc discharge. The plasma may be obtained from a plasma gun, and the degree of ionization need not be great probably one tenth of one percent being more than enough.

In addition the arc may be established by causing the gas between the electrodes to be broken down by a spark obtained from a separate auxiliary device. By this is meant a device whose electrical circuit is quite independent of the electrical circuit of the main electrodes. Such a device might be a RF discharge or the discharge from a Tesla coil or high voltage transformer. In addition a discharge from a pulsed high voltage source, such as used on internal combustion engines of the spark ignition type, may be used to establish the initial breakdown. The actual breakdown of the gas between the electrodes when these auxiliary devices are used is very similar to that described for the spark discharge. Since very little power is required by these sparking systems, they may be made rather compact and simplify the main electrode circuitry. Such auxiliary sparking devices are

very convenient to use when establishing arc discharges and are frequently used in present day experimental arc discharge devices (16, 17).

Electrode Processes

The phenomena occuring in regions of the electrode junctions between the positive column and the metal electrodes are not nearly so well understood as the phenomena of the positive column. These processes are more complex than those found in the column, and reliable experimental data are much more difficult to obtain. The cathode and anode fall regions are considered to have a thickness of the order of the electron mean free path. For the high pressure arcs this amounts to fractions of a millimeter. These fractions are very small for arcs operating at pressures of one atmosphere or larger. For this reason it is nearly impossible to insert any type of probe or even to get a good look at the region by optical techniques.

The electrode-column junctions are regions of sharp transition both electrically and thermally. Electrically, a transition must be made from a metallic conductor, in which the current is carried solely by electrons, to a gaseous conductor in which both electrons and ions carry current. At the anode, electrons may enter the metal from the gas, but, in general ions do not leave from the metal. At the cathode electrons must surmount a potential barrier in order to enter the gas. They may obtain the necessary energy to surmount the barrier in a number of ways. In general, the cathode

phenomena are more complex than those at the anode.

Because the processes occuring in the cathode fall region are different in many respects from those of the anode region, they will be treated separately in the following brief review. A more comprehensive review of present day theoretical understanding and experimental evidence may be found in Somerville's monograph (11).

Cathode Phenomena

The primary function of the cathode is to supply electrons to the gas. For purposes of discussion it is convenient to consider two distinct processes by which electrons may be liberated from the cathode surface. These are the thermionic emission and the field emission processes. The type of emission to be expected is determined largely by the particular metal used for the emitter surface. Ramberg (18) found from his experiments that arc cathodes of C, Ca, Mg, W are thermionic in nature, whereas those of Cu, Hg, Ag, Au are of the field emission type. Cathodes of Pt, Sn, Pb, Ni, Zn, Al, Fe, Cd seem to involve a modification of the field emission process, and the metals of this series having higher boiling points may combine the effects of thermionic and field emission. In practice, however, all metals may exhibit processes in which both mechanisms are at work, and such classification loses significance. In many cases the exact mechanisms involved are difficult to establish completely.

Strictly speaking, thermionic emission refers to that process by which electrons are emitted from a hot surface,

Richardson (19) derived an equation for thermionic emission of electrons as a function of the temperature of the emitter. The surface of the emitter may be heated by two distinct processes. (a) The emitter may be heated by some external source of energy such as an electric current heater as used in many electron tubes, or by means of a hot combustion flame. (b) In addition, the surface may be heated by bombardment of high energy particles such as electrons, protons, excited atoms, and by high energy radiation. These particle bombardment processes are the ones of interest in the arc discharge. Figure 5 is a schematic representation of the possible processes occuring at the surface of a thermionic arc.

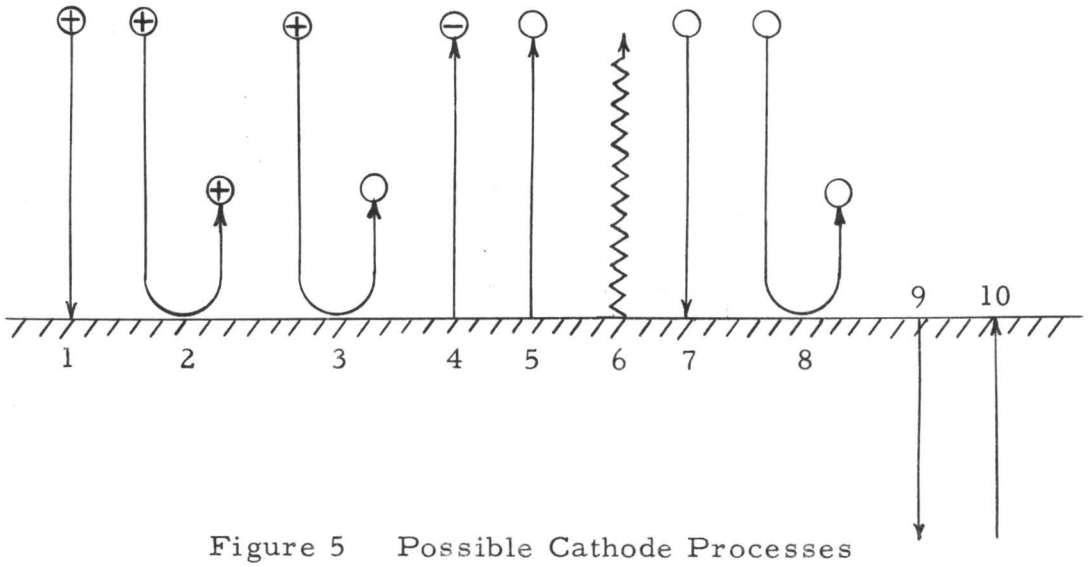

Figure 5 Possible Cathode Processes

In process (1) an ion has collided with the surface and has been absorbed by the surface. The energy absorbed by the surface, E_1, is composed of the ionization potential minus the work function

of the cathode surface plus the cathode fall potential (or some fraction of it if the ion has engaged in a collision within the fall region) plus the heat of condensation (or vaporization) of the neutral atom or molecule. For process (2) the ion may be reflected elastically or inelastically and without neutralization. It is, therefore, possible for heat to be added or removed from the surface, i.e., E_2 is plus or minus. Process (3) is similar to (2) except that the ion has been neutralized but not condensed on the surface. In process (4) electrons are emitted and cool the surface. Some material may be evaporated from the surface with a heat loss $-E_5$. Thermal radiation to or from the surface is $\pm E_6$. Neutral particles may be absorbed by the surface condensation process (7), with the liberation of energy E_7 or they may be reflected in such a manner that E_8 is positive or negative. This would represent conduction and convection processes. Heat E_9 may be conducted from the hot surface, or heat E_{10} may be added to the cathode from an external source.

An estimate of the fraction of the total cathode current carried by the electrons may be obtained by striking an energy balance among the processes occuring at the cathode surface. The analysis may be simplified considerably if, as a first approximation, it is assumed, as von Engel and Steenbeck (6) do, that the positive ions give to the cathode all the energy they gained in the cathode-fall space, and that the only heat loss is due to the emission of electrons.

The energy balance then becomes,

$$I_e \phi = I_i (V_c + V_i - \phi) \qquad (1)$$

where

I_e = the electron current

I_i = the ion current

ϕ = the work function of the surface

V_c = the cathode fall potential

V_i = the ionization potential

Since $I = I_e + I_i$ one gets after rearranging,

$$\frac{I_e}{I} = 1 - \frac{\phi}{V_c + V_i} \qquad (2)$$

with V_c and V_i each of the order of 12 and ϕ of 4 volts, this gives an electron current fraction of about 0.83. More complete analyses yield values between 0.64 and 0.99 (20, 21). Unfortunately, these figures cannot be checked easily for, as Somerville says (11), "there is no direct method of measuring the ratio of the electron to the positive ion current at the cathode." As implied above, the impinging ions are the chief source of energy required for thermionic emission. Some of these ions may come from the positive column, but most of them are probably produced in the cathode fall region. A self-sustaining cycle of events exists, and one may imagine a characteristic cathode cycle to take place as follows.

Once an electron is liberated from the cathode surface, it is accelerated toward the positive column by the large electric gradient which is of the order of 10^5 volts/cm. After the electron gains

sufficient energy it may collide with a neutral atom producing an electron and an ion. The original electron and the additional electron move off towards the positive column, while the ion is accelerated towards the cathode. Eventually the ion collides with the cathode surface atoms and may give up a part of its energy as described previously. The energy absorbed on the surface eventually is used to liberate additional electrons, and the cycle is complete. It is seen that the energy necessary to keep the cycle going comes from the work done on the ions and electrons by the external field. If positive ions are produced in the cathode-drop region, a high electron current density relative to the positive ion current density will be necessary to produce the positive ions essential to maintain the temperature. This is because the efficiency of ionization for a single collision is much less than 100 percent, and because the cathode fall region is assumed to be of the order of the mean free path of the electron, and therefore, many electrons cross the cathode drop region without making any collisions.

Present day understanding of cathode phenomena, especially in the high pressure arc, is hampered by a lack of reliable experimental data. Quantities of interest include the cathode current density, the ratio of the electron to the ion current, the cathode fall potential and the distance over which it takes place, the cathode surface temperature, and the gas or vapor pressure adjacent to the cathode. Measurements of these quantities are made very difficult by the high temperatures prevailing in the column and near the cathode by the

smallness of the distance over which the cathode fall occurs, and sometimes by the narrowness of the column itself at the point of attachment to the cathode.

Field emission is believed to be the the primary mechanism operating in cold cathode arcs. The term cold cathode is commonly applied to arcs with cathodes made of metals whose boiling points are below the temperature at which appreciable thermionic emission can be expected. An outstanding example is mercury. There is no generally accepted theory for the mechanism of electron emission from the cold cathode (11), but the most widely held view is that of the field emission theory. The process of field emission may be considered as one by which the electrons are literally pulled from the surface of the cathode. The required force comes from the intense electric field adjacent to the cathode. This theory requires a very high electric field as high as 10^7 volts/cm, which may be produced by the space charge of positive ions in the cathode fall space. Experimental data of the quantities of interest, such as current density, surface temperature, etc., are again rather scarce and unreliable for the field emission theory.

With a mercury cathode the emission of electrons is the result of the strong electric field adjacent to the cathode surface. If the cathode is tungsten, the emission is almost entirely thermionic. Between these two extremes, a combination of these processes probably occurs, and in many cases the exact mechanisms involved are difficult to establish.

Anode Phenomena

The primary function of the anode is to absorb the electrons which constitute the entire arc current at the anode surface. There are usually no ions emitted from the anode. Consequently there will be an excess of negative charges near the anode surface resulting in an anode fall region. In order that this be small, positive ions must be formed very close to the anode. The electric field of the anode fall attracts electrons from the positive column and repels the positive ions. Electrons accelerating in the anode fall pick up enough energy to generate positive ions by collisions. However, the positive ions accelerated in the opposite direction by the fall do not cause ionization of the gas but merely heat the gas thermally. The positive ion concentration increases toward the cathode. At the cathode end of the anode drop region the concentration of positive ions is high enough to neutralize the electron space charge, thus forming the plasma constituting the positive column. The history of the positive ion current differs from the electron current in that it does not originate in one of the electrodes but rather in the gas itself. The electrons, on the other hand, do originate in the cathode and actually flow into the anode.

The processes occuring at the anode are fewer in number, and therefore the heat balance is somewhat simplified. These processes are illustrated in Figure 6.

Process (1) is by far the most important process in the energy balance. It represents the absorption of an electron by the surface.

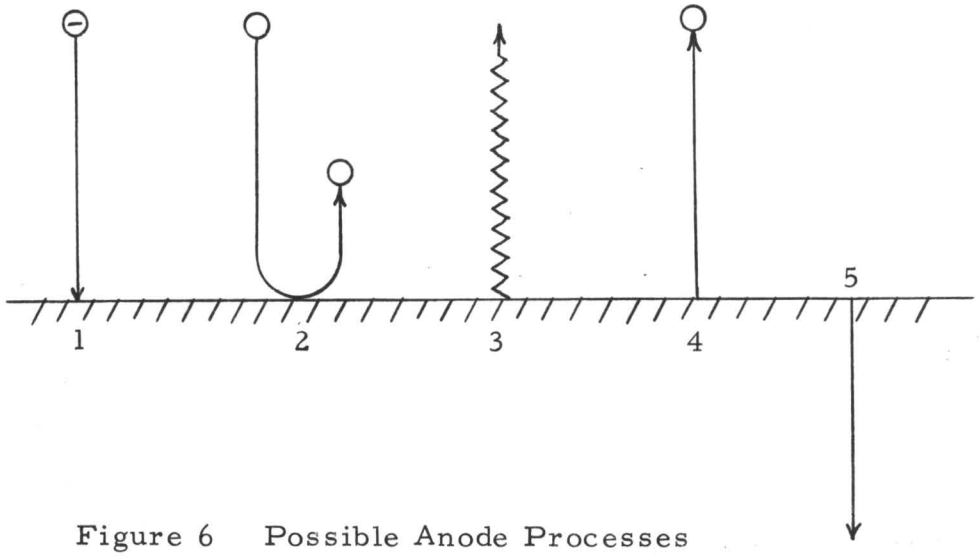

Figure 6 Possible Anode Processes

When this happens an energy, E_1, equal to the anode fall potential, or some fraction of it, plus the work function of the anode surface material is absorbed by the anode. Process (2) represents the energy, E_2, transferred to or from the anode surface by conduction and convection of neutral atoms only since, in general, ions do not come in contact with the surface. (Although an ion could engage in a collision very near the anode and receive a velocity toward the anode high enough for the ion to reach the anode, the probability of such an occurance is very low, and this possibility will not be considered. Special arcs, such as the Beck arc in which metallic salts have been introduced into the core of the anode, can emit ions, but these will not be considered either.) E_3 is the energy radiated to or from the surface. E_4 represents evaporation of neutral atoms of the anode material. E_5 is the heat removed by conduction through the anode. In general, $E_1 \approx E_5$ which is much greater than the energy lost by

conduction from the cathode. This explains why the cooling of the anode is the most critical of the two electrodes.

Measurements of quantities associated with the anode junction are made using the same techniques as used for the cathode measurements. Similarly, these measurements are difficult and uncertain, and they vary widely with arc parameters and conditions and from one observer to the next. Generally they can be compared with those at the cathode as follows. The contraction of the current channel is greater at the cathode than it is at the anode, and the anode current density is one or two orders of magnitude less. The anode spot temperature is somewhat higher than that of the cathode. The anode fall potential is somewhat less than the cathode fall. The anode fall thickness is the order of magnitude of an electron's free path.

Mobility and Diffusion

In the study of electric discharges of all types one frequently finds reference to the terms drift velocity, mobility, and diffusion coefficients. It will be helpful for future discussions to review only the basic concepts involved. Detailed treatment can be found in books by Loeb (23), Brown (24), von Engle (5) and others.

Ion Mobility

In a partially ionized gas there are charged and uncharged particles. The charged particles consist of positively and negatively charged ions as well as negatively charged electrons. Ordinarily,

these particles are moving in a completely random fashion with velocities distributed continuously in some manner which is related to the temperature of the gas as a whole. If the entire mixture is placed in an electric field, E, the random motion is altered. The positive ions will move in the direction of the field while the negative electrons will move in the opposite direction. The uncharged particles will not be directly affected by the field. The directed motion of the charged particles will be superimposed upon their random thermal motions, but will be hindered by collisions with other particles.

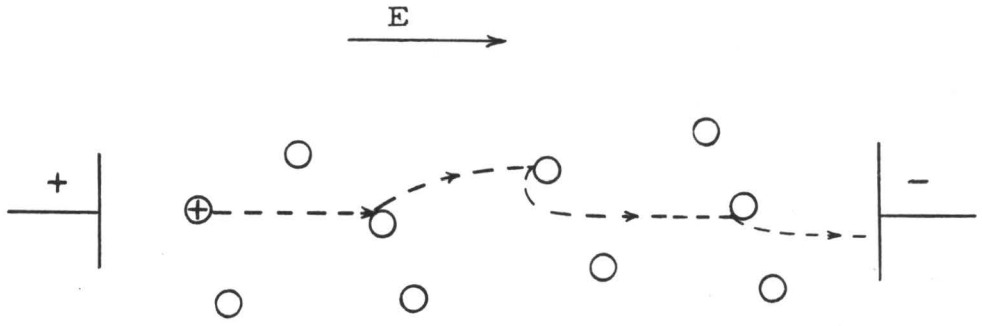

Figure 7 Ion Drifting in an Electric Field

If one considers the drift motion of a single positive ion, the effect of the electric field can be illustrated as shown in Figure 7. Each particle in Figure 7 also has a random thermal velocity which is not shown. After an impact the initial velocity of an ion is supposed to be the same as if it were a neutral gas molecule. However, the electric field tends to drive the particle towards the negative plate,

so that the ion moves along a parabolic path, exactly as a ball thrown in a gravitational field. Although the ion may start moving against the electric field, it proceeds on the average in the field direction. After a period of time, the ion will drift the same distance in any constant interval of time, on the average. Thus, it is possible to define a drift velocity, v. From this and the electric field, E, the mobility, K, is defined as the ratio of the drift velocity to the field. Thus,

$$K = \frac{v}{E} \tag{3}$$

Experiments have verified that the drift velocity of an ion is directly proportional to the field strength so long as the velocity gained by the ion from the field is less than the average thermal velocity of the gas through which the ions move. This is the case of interest in this work.

The slow motion of ions through a gas under the influence of an electric field is of considerable importance and readily lends itself to calculations that show the factors influencing the motion. In order to simplify the calculations the following assumptions are made: (1) the collisions between ions and neutral particles are perfectly elastic, (2) the ions do not exert forces on neutral particles, and (3) the mass of the ion is the same as the mass of the neutral particle.

An ion of charge e in the field E experience at every instant a force $f = Ee$ and an acceleration $a = Ee/m$, where m is the mass of the ion. If the time interval between collisions is τ, then the average

drift velocity is

$$v = 1/2a\tau. \tag{4}$$

The time between collisions is also given as the ratio of the mean free path L, and c, the average thermal velocity. Thus,

$$\tau = \frac{L}{c}, \tag{5}$$

and

$$v = 1/2 \frac{Ee}{m} \frac{L}{c} \tag{6}$$

from which

$$K = 1/2 \frac{eL}{mc} \tag{7}$$

Because of the statistical distribution of the mean free path, the mobility is

$$K = \frac{eL}{mc} \tag{8}$$

This is the basic solid elastic ion-mobility expression which yields only crudely approximate values of mobility. It neglects the fact that the initial directed velocity immediately after a collision may not be zero. Furthermore, it does not distinguish between the mass of the ion and the mass of the neutral particle.

There have been numerous solid elastic theories set up to correct these deficiencies. One of the more important is that derived by Langevin (22) on the basis of general and rigorous kinetic-theory analysis. The Langevin expression reads,

$$K = \frac{0.75eL}{mc} \left[\frac{m+M}{M}\right]^{1/2} \tag{9}$$

where

L = mean free path of (ions in the gas)

M = mass of the gas molecules

m = mass of the ions

c = average thermal velocity of the ions

It is seen from equation 9 that K is independent of E, but it varies inversely as density ρ or at constant temperature T as pressure P through the variation in L. Furthermore, K varies inversely as $\sqrt{T}$ through c.

It is useful to introduce the ratio E/P which in general governs the behavior of charge carries in gases. E is usually expressed in terms of volts/cm while P has the units of mm of Hg.

Experiment has established the independence of K with respect to E up to high values of E/P. At high values of E/P the kinetic energy of the drift, Eel, approaches the thermal energy, and equation 9 no longer applies. In inert gases below values of E/P = 5 and in other gases, such as H_2 and N_2 up to E/P 10 to 20, the ion gains relatively little energy from the electrical field (23). The values of E/P in the arc column of this investigation were less than 5. In the cathode and anode fall regions it is larger. Experiments have established the inverse pressure, or density, rule over very large ranges of pressure. However, like all solid elastic impact equations which neglect attractive forces between ions and neutrals, the equation incorrectly predicts the temperature variation of mobility. More elaborate derivations of mobilities can be found in Loeb (23).

Mobility of Electrons

In most cases electrons which move through a gas in a uniform electric field are not treated like ions of small mass. Since the electron's mass is so much smaller than the molecules or atoms of the gas in which they find themselves, they will lose only a small fraction of the energy during an elastic collision. The energy derived from the electric field will be scattered at random and will increase the electron temperature. Even in low fields the electrons may possess energies considerably above those of the surrounding gas molecules. For such cases, the energy distribution of the electrons may no longer be Maxwellian. Since the energies of electrons in fields in gases strongly affect their drift velocities, these should be studied together. Furthermore, the results of experiments have implied that it is hardly proper to speak of a mobility for electrons in gases, and in recent years it has become the custom to refer to the electron-drift velocity only. However, it is convenient to talk of electron mobility and to follow the simple kinetic theory approach.

In many cases for which the electron velocity distribution is Maxwellian, the electron mobility may be written as

$$K_e = B_1 \frac{eL_e}{m_e c_e} \tag{10}$$

where

e = electron charge

L_e = mean free path of electron

m_e = mass of electron

c_e = average thermal velocity of electrons

B_1 = constant

The value of the constant depends on the derivation used. Langevin's expression, equation 9, can be rewritten as

$$K_e = .75 \frac{eL_e}{m_e c_e} \sqrt{\frac{m_e + M}{M}} \tag{11}$$

Since $m_e \gg M$, this reduces to

$$K_e = .75 \frac{eL_e}{m_e c_e} \tag{12}$$

This expression is based on the assumption of elastic collisions and thermal equilibrium between electrons and gas molecules.

Diffusion

Particles are said to diffuse in a gas if they move from a region of high concentration to regions of low concentration. The origin of this motion is a purely thermal one. If n is the concentration of the particles, i.e., the number of particles per unit volume, and if n is a function of position only, the velocity of diffusion is

$$v = - \frac{D}{n} \nabla n \tag{13}$$

where D is the diffusion coefficient, and the negative sign indicates that the motion is in the direction of decreasing concentration. In one direction

$$v = - \frac{D}{n} \frac{dn}{dx} \tag{14}$$

Kinetic theory shows that in an ionized gas for which the velocity distribution of all particles is Maxwellian, the diffusion coefficient if given by

$$D = \frac{cL}{3} \tag{15}$$

where c is the average thermal velocity and L is the mean free path.

There is an important relation between the ionic mobility and diffusion coefficient. The mobility is given by equation 8, and the diffusion coefficient by equation 15. The ratio of these two is

$$\frac{3e}{mc^2} \tag{16}$$

Since

$$\frac{mc^2}{3} = kT \quad \text{and} \quad P = nkT, \tag{17}$$

the result is

$$\frac{K}{D} = \frac{e}{kT} = \frac{en}{P} \tag{18}$$

When electrons and positive ions of equal concentration are present in a gas on which an electric field acts, it is found that their motion can often be treated as if the collection of charges diffused with a common velocity. Electrons and ions will diffuse from the arc column in the radial direction. Since the mobility of the electrons is greater than that of the ions, the electrons will tend to move ahead of the ions. If this happened, the ion density would quickly become

much greater than the electron density. Of course such a separation of charges would result in large electrostatic forces, and the charge balance would be quickly restored. Therefore, the positive ions will control and limit the rate at which electrons can diffuse, and the ions and electrons will diffuse together. An average, or ambipolar, diffusion coefficient for the mixture of ions and electrons can be found (see Ref. 6 for example) to be

$$D_a = \frac{D_i K_e + D_e K_i}{K_e + K_i} \tag{19}$$

where subscript e stands for electron, and i for ion. If the ion and electron temperatures are the same, $K_e \gg K_i$, and substitution of equation 18 yields

$$D_a = \frac{2kTK_i}{e} \tag{20}$$

This is twice the diffusion coefficient of the ions (equation 18 with subscript i on K and D), but much less than D_e since $K_e \gg K_i$.

Arc Column

The arc column (sometimes called the positive column or the long column) serves to conduct electricity between the cathode and the anode. If the distance between the electrodes is of the order of an electron mean free path, the arc column does not exist and the anode and cathode fall regions overlap. However, for longer arcs a conducting column or channel of ionized gas will connect the electrodes. The column will conduct electricity because of the presence of charge

carriers of both signs. In most gases in the conducting state, these charge carriers are electrons and positive ions, and although negative ions may exist in some cases, they will not be considered here.

When the electrodes of a high pressure, high current electric arc discharge are separated, the voltage across the electrodes increases as shown in Figure 8. Experiments (for examples see references 4, 11, 25, 26, 27, 28, 29) indicate that over a considerable range of electrode separations, the voltage varies very nearly linearly with separation. An ideal positive arc column will be defined as one for which the voltage is linearly proportional to distance. In any arc, however, there is a certain small electrode separation over which the arc voltage does not vary linearly. This nonlinear voltage drop is the result of unique processes occurring throughout the cathode and anode fall regions. The distances over which the cathode and anode potential falls V_o take place are designated by a in Figure 8.

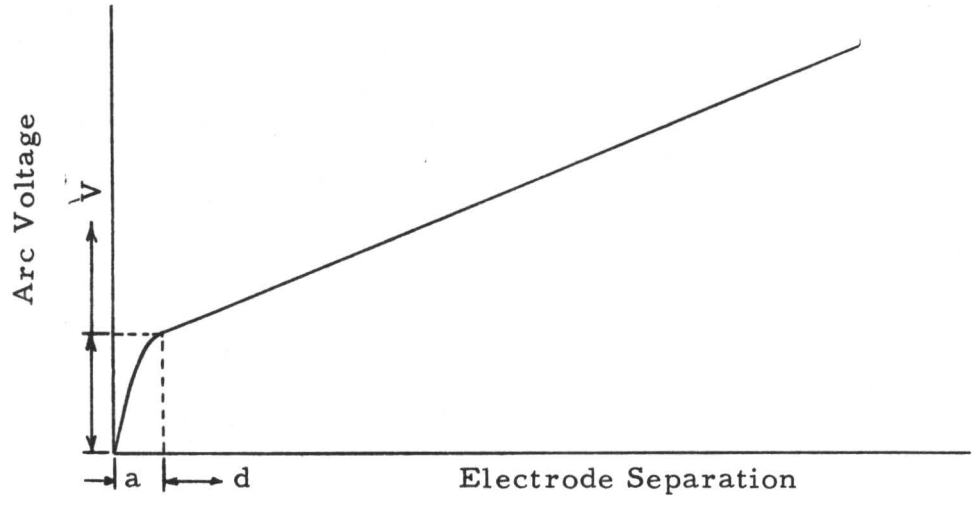

Figure 8 Arc Voltage-Electrode Separation Characteristic

In the positive column, the voltage varies linearly with distance, as assumed, and the slope of this curve is the constant electric intensity E. Thus,

$$E = \frac{dV}{dx} = \text{constant} \tag{21}$$

Where V is the potential and x is distance. From Poisson's equation for the one dimensional steady-state case,

$$\frac{dE}{dx} = 4\pi e(n_i - n_e) = 0. \tag{22}$$

where n_i and n_e represent the number of electrons and positive ions, respectively, in unit volume. Thus, the number of positive charges is equal to the number of negative charges. However, as yet there is nothing to prevent the number density from changing with position as long as $n_e = n_i$. The continuity equation for charges must be satisfied. Hence, in one dimension

$$\frac{\partial(n_e v_e)}{\partial x} + \frac{\partial n_e}{\partial t} = 0, \tag{23}$$

where v_e is the drift velocity of the electrons, The electron current density, j_e, is given as

$$J_e = e n_e v_e. \tag{24}$$

The current density may be considered as the ratio of the total current to the cross-sectional area through which the current flows. If the current is constant for any electrode separation, then the current density can only change if the cross-sectional area changes. The area of the arc is determined by the field, current, and gas within the arc.

If all these parameters are held fixed, there will be no change in the area from these effects. The area may also be changed by external means such as a change in pressure, the presence of cold surfaces, the application of a magnetic field, etc. However, none of these changes occur along the length of the arc or when the arc is merely elongated. Thus, there appears to be no reason to expect the cross-sectional area of the arc to change even if the electrode separation is varied. Also the electron current density will remain the same when the arc is stretched out, therefore,

$$\frac{d(J_e)}{dx} = \frac{d(en_e v_e)}{dx} = 0. \qquad (25)$$

The electron drift velocity is a function of the electron mass m, the root mean square velocity u, the mean free path L, and the electric field E. In general, u and L depend on E, but since E is the same throughout the positive column regardless of the electrode separation, the drift velocity remains the same. Finally, $dn_e/dx = 0$ for any electrode separation, and it also remains constant during the process of separating the electrodes.

As proved above, an arc column must be electrically neutral, This fact is nicely illustrated by an example in Sommerville's book (11) in which he assumes a mercury vapor arc at atmospheric pressure carrying a current of 6 amperes with a longitudinal gradient of 6 volts per centimeter, a channel diameter of 1.7 cm and a temperature of 5900°K. If the current were carried by electrons only, the radial

electric field at the periphery of the channel would produce a force of about 1700 tons acting on the electrons in each cubic centimeter.

Clearly, positive charge must be present in almost exactly equal density to neutralize this force. The magnitude of the forces involved in any departure from overall neutrality shows that the balance will be closely maintained automatically.

If there are n_e and n_i electrons and ions per cm^3 respectively, with charges -e and e, and if an electric field E(V/cm) is applied, these electrons and ions will move parallel to the field with average drift velocities v_e and v_i (cm/sec). The charge transport or current density in the direction of the field is

$$J = n_e e v_e + n_i e v_i \text{ (Amperes/cm}^2\text{)}. \qquad (26)$$

v_e is much greater than v_i because of the much greater mass of the ions. Hence, the current is carried almost entirely by electrons, the ions serving mainly to neutralize the space charge.

The normal tendency is for the relatively hot arc column to lose energy to the surroundings by means of conduction, convection, and radiation. These losses will cool the gas in the column and charges of opposite sign will recombine. In this way the conductivity of the column can be reduced until it can no longer carry a current, and the arc will be extinguished. In order to maintain a stable arc, these energy losses must be replaced from some external source, which in this case is the electric field of the arc column.

A steady state arc column can be maintained if the amount of

energy being lost from the column is equal to an amount of energy continually fed into the column from the external electric field. Work is done by the field in accelerating the electrons and ions in the channel. The amount of work done on any given particle is equal to the potential fall which the particle experiences. Both electrons and ions will fall through the same potential, but the electrons will do so much more quickly because of their smaller mass. Therefore, the main carrier by which the external electrical supply feeds power to the arc column is the electron constituent of the plasma. The electrons are accelerated by the field until they collide with plasma particles, neutral atoms and/or molecules, as well as with ions and other electrons. In such collisions the electron transfers the kinetic energy it acquired from the field to the particles with which it collides. The collisions may be elastic or inelastic, and if interactions between electrons and ions are ignored, then

$$JE = U_e + U_i \tag{27}$$

where J is the current density and U_e and U_i are the energies transferred to the gas atoms per cm^3 per second by elastic and inelastic collisions respectively.

The energy transferred elastically is in the form of kinetic energy and goes directly towards heating the gas. Only a small amount of energy can be transferred at an elastic collision. For inelastic collisions, relatively large amounts of energy may be transferred at a single collision.

At high pressures and densities collisions are very frequent, and because they are, electrons can gain only a small amount of energy from the external field between collisions. Consequently, the energy transferred at a collision is very small, and the collision is elastic Since elastic collision heat the gas, all plasma particles are at about the same temperature.

If the density is low, electrons can gain a considerable amount of energy between collisions, so that when a collision occurs it is frequently inelastic. With few elastic collisions the gas will be heated very little, and the electron temperature will be considerably above the ion and neutral atom temperatures.

There are two broad classes of energy transfer by which energy is lost from the arc column.

1. Energy may be transferred to the walls of a vessel in which the arc burns in several ways:

   a. By impact of gas molecules, ions and electrons with the wall. At high pressures energy is conveyed to the wall by the ordinary processes of thermal conduction and convection.

   b. Ambipolar diffusion may help to augment the convection losses, and ions and electrons which diffuse to the wall will give up their energy of ionization at the wall.

   c. Excited atoms and/or molecules may give up

their energy of excitation at the wall.

c. Dissociated molecules may re-associate at the wall.

2. A large variety of radiations may pass through the wall. The composition of the radiation depends on the nature of the gas and its degree of dissociation and ionization. However, at high pressures the gas is at a high temperature, and the largest portion of the energy is lost at the walls by convection and conduction, and the radiation losses are small.

On a macroscopic scale the arc is in static equilibrium when the energy balance is maintained. However, on a microscopic scale local deviations from equilibrium may occur. One can introduce a disturbance into the plasma state which will represent a departure from true equilibrium. This could be done simply by firing a particle into the plasma from a particle accelerator. After collisions with plasma particles, the injected particle becomes adjusted to its new environment. The time required for adjustment is the relaxation time. It is also possible for self-induced deviations from equilibrium to occur locally. Again the deviations will be damped out by collisions and equilibrium restored, and the time required is called the relaxation time.

Relaxation times in common arc plasmas for electrons are of the order of microseconds; for internal molecular excited states, one one-hundreth of a microsecond; for metastable atomic excited states, of the order of milliseconds; for the introduction of ordered motions,

of the order of microseconds (1). Thus, surge arcs, exploding wires, sparks, etc., which are considered short-time arc phenomena, do not last long enough for equilibrium to be established among electrons, ions, and gas particles, and it is probable that the column gradient is much higher for this type of phenomena.

It can be shown that at higher pressures the column must be in approximate thermal equilibrium with the gas molecules. The data of Somerville's example will be used. The random velocity of an electron in thermal equilibrium at 5900°K is 5.18×10^{7} cm/sec. The measurements of Brode (30) indicate the mean free path for electrons in mercury at atmospheric pressure is $L = 8.36 \times 10^{-5}$ cm. Substitution in equations (3) and (9) of these values together with those of E = 6V/cm, $e = 1.602 \times 10^{-19}$ coulomb and $m = 9.11 \times 10^{-28}$ gm gives $v_e = 1.28 \times 10^{4}$ cm/sec for the drift velocity. An electron drifting 1 cm parallel to the field will pick up a total of 6eV in a time $1/v_e = 7.8 \times 10^{-5}$ sec. In this time the electron will describe a nearly random path at least $5.18 \times 10^{7} \times 7.8 \times 10^{-5} = 4050$ cm long in the course of which it will make $3700/8.36 \times 10^{-5} = 4.85 \times 10^{7}$ collisions with mercury atoms. Consequently, in the steady state it has to pass on $6/4.5 \times 10^{7} = 1.24 \times 10^{-7}$ eV per collision. At 5900°K the mean electron energy is 0.76eV, so that at most an electron is required to pass on a fraction $\lambda = 1.24 \times 10^{-7}/0.76 = 1.63 \times 10^{-7}$ of its total energy at each collision. For elastic collisions it has been shown (31) that

$$\lambda = \frac{2.66m}{M} \left(1 - \frac{T_g}{T_e} \right) \qquad (28)$$

where m and M are the electronic mass and atomic mass respectively, and T_e and T_g are the electron and gas temperature. For mercury $\frac{M}{2.66m} = 1.39 \times 10^5$. Hence $(1-T_g/T_e) = 0.023$. Consequently, by elastic collisions alone the electrons can transfer to the gas all the energy they acquire, provided their temperature is a little as 2.3 percent above that of the gas. Since the inelastic processes of excitation and ionization also occur, T_e is even closer to T_g. At lower pressures the mean free paths becomes much larger, and it is possible for the electron temperature to exceed the gas temperature by a large amount. The pressure at which the electron temperature and gas temperature converge is about 1 inch Hg.

Since thermal equilibrium between all particles prevails, Saha's equation can be used to check the assumed temperature. If this is done, the assumed temperature of 5900°K is found to be sufficient to produce the ionization required to give the necessary conductivity. The correct value for the temperature can always be reached by a process of successive approximations.

A large amount of experimental data on the electric arc discharge has been collected in the last sixty years. The more important findings will now be presented.

For low values of current (less than 20 amperes) the gradient decreases as the current increases. Eventually a minimum is reached after which the gradient increases with current. The current at which the minimum gradient occurs depends on the electrode separation, electrode diameter, stabilizing gas and electrode material. For low

currents several investigators (15, 32, 34, 36) have found that for the entire arc

$$E \propto I^{-n} \tag{29}$$

The author found that an expression of the form

$$W = \frac{A}{R^B} + C \tag{30}$$

correlates the data of Edels (26) very nicely. In this expression

W = arc power = VI

R = arc resistance = V/I

A, B, and C are constants.

V = arc voltage

I = arc current

Edels data is displayed graphically and shows the arc voltage as a function of arc current. The four curves shown have a negative slope at lower current values, but the slope turns positive for currents above about 100 to 150 amperes.

The author found it much easier to fit curves to the data by using the arc power and arc resistance in the form given by equation 30 than by using arc voltage and current in any simple form, such as equation 29. However, for very large currents, Seelinger (35) found that the gradient could be expressed in terms of current by

$$E = c_1 I + c_2 I^{-1} + c_3 I^{-2} \tag{31}$$

where the c's are constants.

Because more energy is lost from the arc column by conduction and convection at higher pressures, an increase of pressure increases in the column gradient. The effect of pressure is given approximately as

$$E \propto p^m \tag{32}$$

where m varies with the gas and has values of 0.31 in Ne and 0.16 in A (8, 33, 36)

Suits (36) also foundwith copper electrodes that the average value of the voltage gradient decreases according to the condition of the electrode surface in the order polished, lathe turned, oxidized. Also, the column gradient decreases for metal electrodes in the order W, Ag, Zn, Fe, Al, Pb.

At high pressures, the gradient correlates with the heat transfer properties of the gas. For molecular gases dissociation helps increase heat transfer, and the gradient is greater in molecular gases than in atomic gases of comparable molecular weight. This explains why the total arc voltage of a nitrogen stablized arc is greater than that of an argon arc, other conditions remaining the same. This also may explain why welds made in argon show lack of penetration with no craters formed (37). In pure argon the heat transfer to the metal, being by conduction and radiation alone, is very poor. At the axis of the column of molecular gases most of the molecules are dissociated into atoms, while just outside the column, the gas is entirely in the molecular state. There will be strong concentration gradients causing

outward diffusion of atoms and inward diffusion of molecules. As the molecules diffuse in and reach a region of suitable temperature, they dissociate, absorbing energy from the hot gas. Diffusing out again as atoms, they re-associate and give up the dissociation energy. In this manner energy is transferred from hotter to cooler regions, not by true conduction which implies the transport of kinetic energy, but by the transport of dissociation energy. This mechanism results in a larger loss of energy from the column, and in order to replace the energy, the column gradient must be increased. This phenomenon does not occur in atomic gases, which will display a smaller gradient.

Suits and Poritsky (38) have applied the theory of free convection heat loss from solid bodies in fluids to the high-pressure arc column. The arc column is considered as a hot cylindrical body, and radiation is neglected. The equation for free convection is

$$\frac{hD}{k} = \text{const}\left(\frac{D^3 \beta \rho^2 g \Delta T}{\mu^2}\right)^a \left(\frac{c_p \mu}{k}\right)^b \qquad (33)$$

where h = coefficient of heat transfer

D = diameter of the cylinder, or arc column in this case

k = thermal conductivity

β = coefficient of volume expansion

ρ = density

g = acceleration due to gravity

μ = viscosity

c_p = specific heat

ΔT = temperature difference between the cylinder and the ambient fluid

and a and b are constants

All the fluid properties are evaluated at the arithmetic mean of the ambient and the cylinder temperatures. Since all groups are dimensionless, any consistent set of units may be used.

The heat lost at the surface of a cylinder per unit length is

$$W = \pi D h \Delta T \tag{34}$$

This loss is restored to the arc column by the electric field. Hence,

$$W = EI \tag{35}$$

If the arc current is assumed to be carried entirely by electrons,

$$I = \frac{\pi D^2}{4} e n_e K_e E, \tag{36}$$

where n_e = the electron concentration

K_e = electron mobility

e = electronic charge

Equations 34 and 35 can be combined to give

$$EI = 4\pi D h \Delta T \tag{37}$$

The film coefficient can be found from equation 33, and if D from equation 36 is substituted into equation 33 and equation 33 substituted into equation 37, there results after solving for E

$$E^q = \text{const}\ \ k\Delta T \left[\frac{\beta \rho^2 g \Delta T}{(e n_e K_e)^{3/2} \mu^2}\right]^a \left[\frac{c_p \mu}{k}\right]^b I^{q-2} \tag{38}$$

where $q = (3a + 2)/2$

At constant pressure the arc temperature may be assumed independent of the arc current, and since n_e is a function of temperature by Saha's equation, K_e is a function of pressure, and k, ΔT, β, ρ, g, μ, and c_p are constant, hence

$$E \propto I^{-n} \tag{39}$$

which agrees with equation 29.

The variation of the electron concentration n_e with gas pressure may be determined from Saha's equation, in which account must be taken of the variation of arc temperature with gas pressure, as

$$n_e = \text{const}\ P^j \tag{40}$$

where j = 1.44. The mobility varies inversely as the gas pressure, if the effect of temperature on the mean free path and average velocity of the electrons is neglected.

For an ideal gas

$$\rho = \frac{MP}{RT} \tag{41}$$

and

$$\beta = \frac{1}{T} \tag{42}$$

where M = molecular weight

R = universal gas constant

P = pressure

Equation 33 can then be written as

$$EI = \text{const}\ k\Delta T \left[\frac{D^3 M^2 P^2 g \Delta T}{T^3 \mu^2 R^2} \right]^a \tag{43}$$

If the dependence on temperature of the right-hand member of equation 43 is neglected,

$$EI \propto P^{2a} D^{3a} \tag{44}$$

If the current is fixed, substitution of E from equation 36 and n_e from equation 40 into equation 44 leads to

$$D \propto P^{-\gamma} \tag{45}$$

which is the same form as that found experimentally by Suits (39). An alternate combination of equations 36, 40, 44, again at constant current, gives

$$E \propto P^{m} \tag{46}$$

Equation 46 has the same form as equation 32 which was determined experimentally.

Thus, it appears that the theoretical treatment of the high pressure arc by the methods of Suits and Poritsky is useful for predicting the relation between various arc parameters.

The author has applied dimensional analysis to the problem of correlating the arc parameters. In general, the results can be made to agree with the theoretical and experimental conclusions discussed above. The dimensions assumed are

L = length

M = mass

θ = time

T = temperature

Q = charge

The variables of interest are

D = tube radius, L

d = electrode separation, L

P = pressure, $M/L\theta^2$

V = arc voltage, ML^2/θ^2Q

V_i = ionization potential of stabilizing gas, ML^2/θ^2Q

I = current, Q/θ

n = charge density, Q/L^3

e = electronic charge, Q

k = Boltzmann's constant, ML^2/θ^2T

T = temperature, T

Applications of the methods of dimensional analysis leads to five dimensionless groups, none of which contain the current, I. The groups are Vn/P, d/D, Vi/V, D^3n/e, and kT/D^3P. The functional relationship is assumed to be

$$\frac{Vn}{P} = C\left(\frac{d}{D}\right)^a \left(\frac{Vi}{V}\right)^b \left(\frac{D^3n}{e}\right)^f \left(\frac{kT}{D^3P}\right)^h \tag{47}$$

where a, b, C, f, h are assumed constants. Since V varies linearly with d, a must equal one. If the arc current is carried by the electrons only, then by equation 24

$$I \propto D^2 v_e n_e \tag{48}$$

If one imposes the same conditions as those imposed for the theoretical analysis of Suits and Poritsky, it is possible to find values for

b, f, and h such that

$$E \propto I^{-n} \tag{49}$$

$$D \propto P^{-\gamma} \tag{50}$$

and

$$E \propto P^{m} \tag{51}$$

in accordance with the experimental results.

The appearance of the group Vn/P is very interesting because this group was not found in the literature by the author. It will be referred to as the arc number in this work. The arc number can be expressed as Edn/P, and in this form a familiar parameter is noted. E/P is commonly used as an independent variable when it is desired to express the functional relationships of diffusion coefficients, mobilities, drift velocities, and collision frequencies. E/P can be thought of as the parameter which measures the energy gained per mean free path. The arc number may be thought of as the ratio of electric stress or pressure to hydrostatic pressure. Arguments for considering Vn or Edn as electric stress and another interesting ratio will now be considered.

If equation (21) is integrated

$$V = Ed \tag{52}$$

where V is the positive column potential drop only and d is the length of the positive column only.

Since the positive charge number density is the same as the negative charge density, let

$$n = n_i = n_e, \tag{53}$$

and then

$$V \cdot n = Ed \cdot n \tag{54}$$

The dimensions of the factors in this equation are

$$V = \text{volts} = \frac{\text{energy}}{\text{charge}} = \frac{ML^2}{\theta^2 Q}, \tag{55}$$

$$n = \frac{\text{charge}}{\text{volume}} = \frac{Q}{L^3} \tag{56}$$

where

Q = charge

L = length

M = mass

θ = time.

The product of the arc potential and the charge density is proportional to the time rate of energy dissipated (by diffusion in the simplest case) from the arc column, as is shown below. This energy must be supplied by the external power source and, more directly, by the field between the electrodes.

The product of the arc current and the positive column potential difference is equal to the energy supplied in unit time to the arc column. Under steady state conditions, the same energy is lost from the arc column. In the ideal case under discussion, this energy is used to replace the charged particles lost because of recombination and diffusion, and also to replace the energy lost by convection, conduction, and radiation. The rate at which the energy is supplied

is

$$W = VI \tag{57}$$

Since I, the current, can be written as

$$I = \frac{\pi D^2}{4} en (v_e + v_i) \tag{58}$$

the power is

$$W = \frac{\pi D^2}{4} enV (v_e + v_i) \tag{59}$$

Since the drift velocities do not change (E/ρ is constant),

$$Vn \propto W \tag{60}$$

i.e., Vn is proportional to the power required to maintain steady state conditions. Dimensionally, Vn may be considered as an electric stress, σ, because

$$Vn = \frac{ML^2}{\theta^2 Q} \cdot \frac{Q}{L^3} = \frac{M}{\theta^2 L} = \sigma \tag{61}$$

This stress results from the potential difference which exists between the electrodes and which supplies the energy necessary to maintain a constant degree of ionization. Within the arc column, there are other potentials which cause heat transfer and diffusion from the arc column, and therefore, energy loss from the column. This energy is replenished by the arc voltage during steady state operation. Thus, the potentials causing energy loss by diffusion and heat transfer induce an electrical potential difference in the arc column.

Next, assume that the sum of the anode and cathode fall distances, a of Figure 8 remains the same for any electrode separation. Then from equation 61,

$$\sigma a = Vna = Edna. \tag{62}$$

This can be rearranged to yield

$$\frac{\sigma}{d/a} = Ena = Y \tag{63}$$

Equation 63 is analogous to the simple Hooke's Law in elasticity. The symbol σ represents the stress as described above; d is the length of the positive column and represents the extension of the arc beyond the sum of the cathode and anode fall distances, a. According to the original assumptions, $\sigma = 0$ when $d = 0$, and the length a is analogous to the unstrained length of a beam. Equation 63 shows that the electric stress is proportional to the strain, d/a, in the positive column. The constant of proportionality, Y, is analogous to Young's modulus. For a given gas, pressure, and current, the product Ena is constant, and therefore, Y is also a constant. Note that the dimensionless group Vn/P can be easily written as

$$\frac{Ena}{a/d} \div P = \frac{Y}{P} \tag{64}$$

From the arguments presented during the derivation of equation 63, the ratio Vn/P or Y/P is at most a function of the particular gas and current. However, if the arc number is independent of current, then this dimensionless group characterizes the arc performance for any

given gas.

The application of dimensional analysis and the idea of electric stress as presented herein have not been noted in the literature by the author. While these ideas appear interesting and worthy of further study, nothing more has been done to develop them because they were considered outside the experimental scope of this dissertation.

CHAPTER III

PLASMA FACILITY AND AUXILIARY EQUIPMENT

A schematic of the plasma facility is shown in Figure 9. The major components of the facility are the main plasma generator, the test section, the multiple arc assemblies, the power supply, the gas supply and vacuum system, the cooling water system, and the associated controls and instrumentation. All of the equipment, except the motor generator set, the electronic control cabinet for the motor-generator set, and the ballast resistor are located in an air-conditioned room of the Mechanical Engineering Laboratory. Much of this equipment has been described in detail in Haworth's Ph. D. dissertation (16), and therefore, only the new equipment and the modifications to the equipment of Haworth's research will be discussed in detail.

Main Plasma Generator

The main plasma generator assembly designed by McQuiston (40) and used by Haworth in this work (16) proved to be poorly suited for the type of work anticipated. This older model assembly was composed of many individual parts and required many seals. Every time the generator was disassembled, it was necessary to break many of these seals. These seals were of paper gasket material and required some

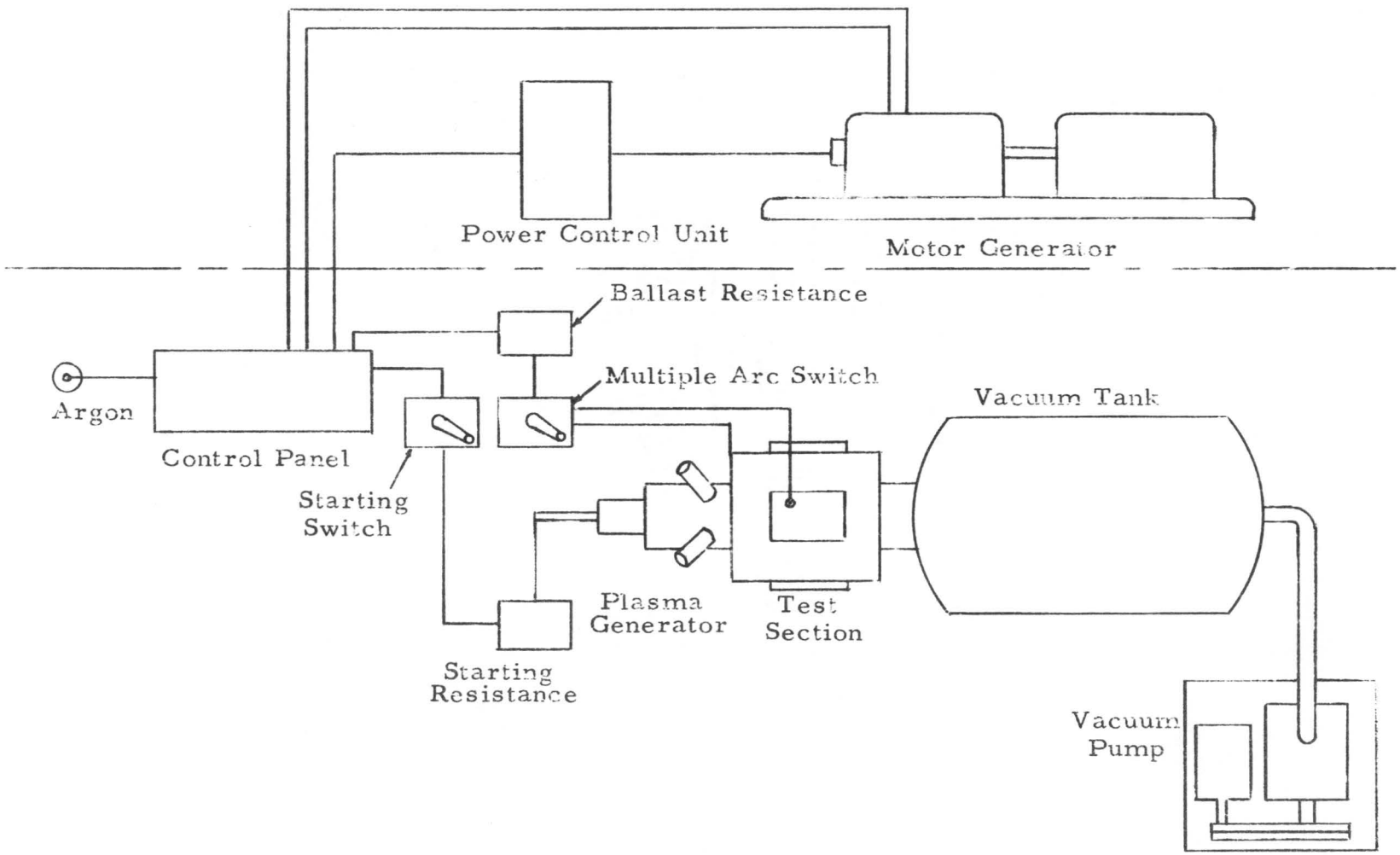

Figure 9 Schematic of Plasma Facility

kind of sealing compound. Even so, it was difficult to seal all joints. In addition, there were many gas, water and electrical connections which had to be broken and replaced every time the generator was disassembled. The time required for disassembly and re-assembly was considerable.

In order to eliminate these problems it was decided to design a new chamber such that all joints which would not have to be taken apart would be welded, and seals which must be broken frequently would be fitted with 0-rings and/or quick disconnect devices. In addition, the design of the main generator assembly would be such that the additional arc components could be attached easily to it.

After a period of time a suitable design was derived. This design Model D, was built and tested. An assembly drawing is shown in Figure 10. The main chamber in this design is water cooled and is composed of two concentric cylinders which form the water jacket. The cylinders are welded at the ends and to the nozzle support flange. The water enters at the upper left hand corner of the main chamber water jacket and circulates around the chamber. From here it flows into the nozzle cooling chamber, around the nozzle and out the exhaust. Tests with the previous chamber models indicated that very little water was required for cooling the main chamber. In order to minimize the number of cooling water circuits, the water is circulated through the main chamber before it does to the nozzle. The water which enters the nozzle cooling water jacket is essentially at the same

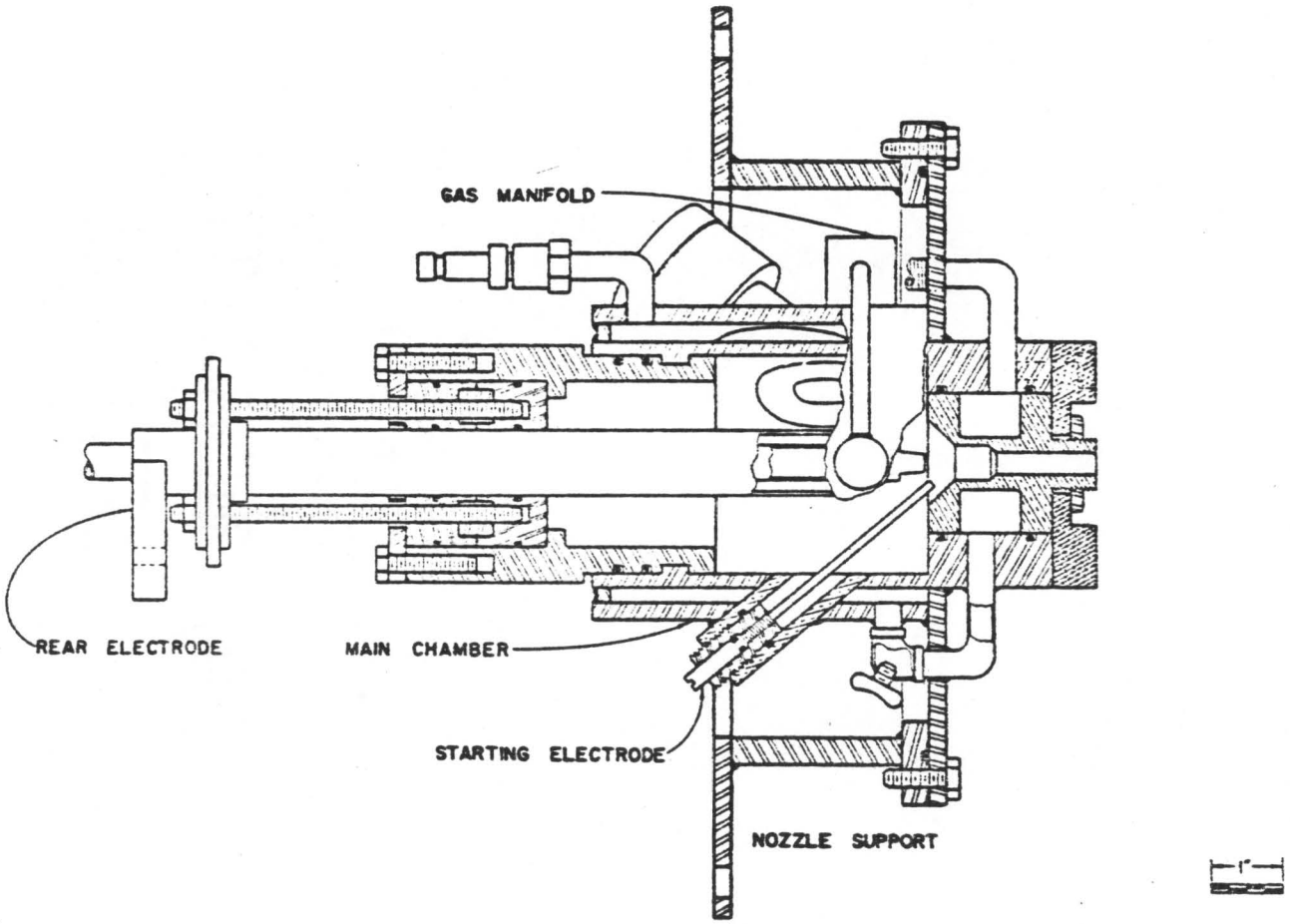

Figure 10 Model D Chamber Assembly

temperatures as it was when it entered the main chamber jacket.

As the drawing shows, the main chamber and the rear electrode support are both at the same electrical potential as the nozzle, which is grounded in the actual operation. Therefore, only the rear electrode is above the ground potential. The rear electrode support is fastened in the main chamber by a tongue and groove arrangement. There are four tongues or lips on the rear electrode support and four corresponding slots or grooves in the main chamber. This allows very quick disconnect action, and it is now only necessary to slip the rear electrode support into the rear end of the main chamber and rotate the support 1/8 turn. The starter electrode is now a brass rod fitted with an 0-ring and screwed into an insulating member which in turn is screwed into a metallic support.

The entire chamber is welded wherever possible. The nozzle support block, to the right in the figure, is fitted with four holes which are threaded. These take the support studs for the additional or the multiple arc assemblies (to be described later). The nozzle support flange is secured to the main flange by a series of bolts and is sealed by a single 0-ring. The main support flange was made in three different lengths so that the position of the nozzle can be varied by increments of two inches, either into or out of the chamber. This is to accomodate more or less additional arc assemblies and to insure that the last assembly will always be positioned in the same location within the test section, regardless of the number of additional arcs used. The structure was designed to withstand a pressure of 500 lbs/in^2

within the main chamber region.

Quick disconnects are used on all the water cooling lines. The gas is led to a common manifold from which it is distributed equally to two injection nozzles. In this design, the nozzles were made adjustable so that the angle relative to the center line of the chamber could be varied.

In order to obtain a water tight structure, it was necessary to weld the window holders, and the starter electrode holder both on the outside and on the inside shells of the double walled jacket of the main chamber. However, the inside diameter of the main chamber is relatively small, and the technician was required to exercise a great deal of skill in welding these components. In addition, because of the double walled chamber, excessive thermal stresses were set up. As a result, it was not possible to obtain water tight integrity.

Test Section

The test section is a rectangular steel box measuring 16 inches high, 16 inches wide, and 20 inches long. Three rectangular openings 6 inches by 12 inches long are in the top and sides. The two side openings are fitted with 5/8 inch thick Pyrex glass windows. The top opening is fitted with a plate to which are attached the electrical components required for the multiple arcs. The multiple arc assemblies are attached to the main plasma generator and extend into the test chamber. The test chamber is attached to a large tank which can be evaculated.

Power Supply

The main power supply for the Plasma Facility is the General Electric DC dynamometer system located in the Mechanical Engineering Laboratory. Only the motor-generator set and the control system are used. The elaborate control system is used to maintain the entire electrical system at some fixed operating condition and to prevent overloading any part of the system by excessive current variation. In practice the operator varies the amount of current passing through the arc(s) by changing the output voltage from the DC generator. The details of the control system are discussed in Haworth's thesis (16), and will not be repeated here.

Of interest at this point is the ballast and starting resistance circuits. These are shown schematically in Figure 11. The starting resistance is used to limit the initial surge current when the main arc is first started. The control box from a trolley car is used as a manual switch to reduce the starting resistance from a maximum value of one ohm to 1/16 ohm, and finally, a relay shorts out all of the starting resistance. However, a fixed ballast resistance of about 1/3 ohm remains in series with the arc(s).

The ballast resistance helps load the motor-generator more fully, because with the ballast, the fluctuations of the arc voltage become small compared to the total output voltage from the generator. Thus, a much more stable operation is achieved.

Another trolley car control box is used to switch in the additional arcs. A schematic of this circuit is shown in Figure 11. In the

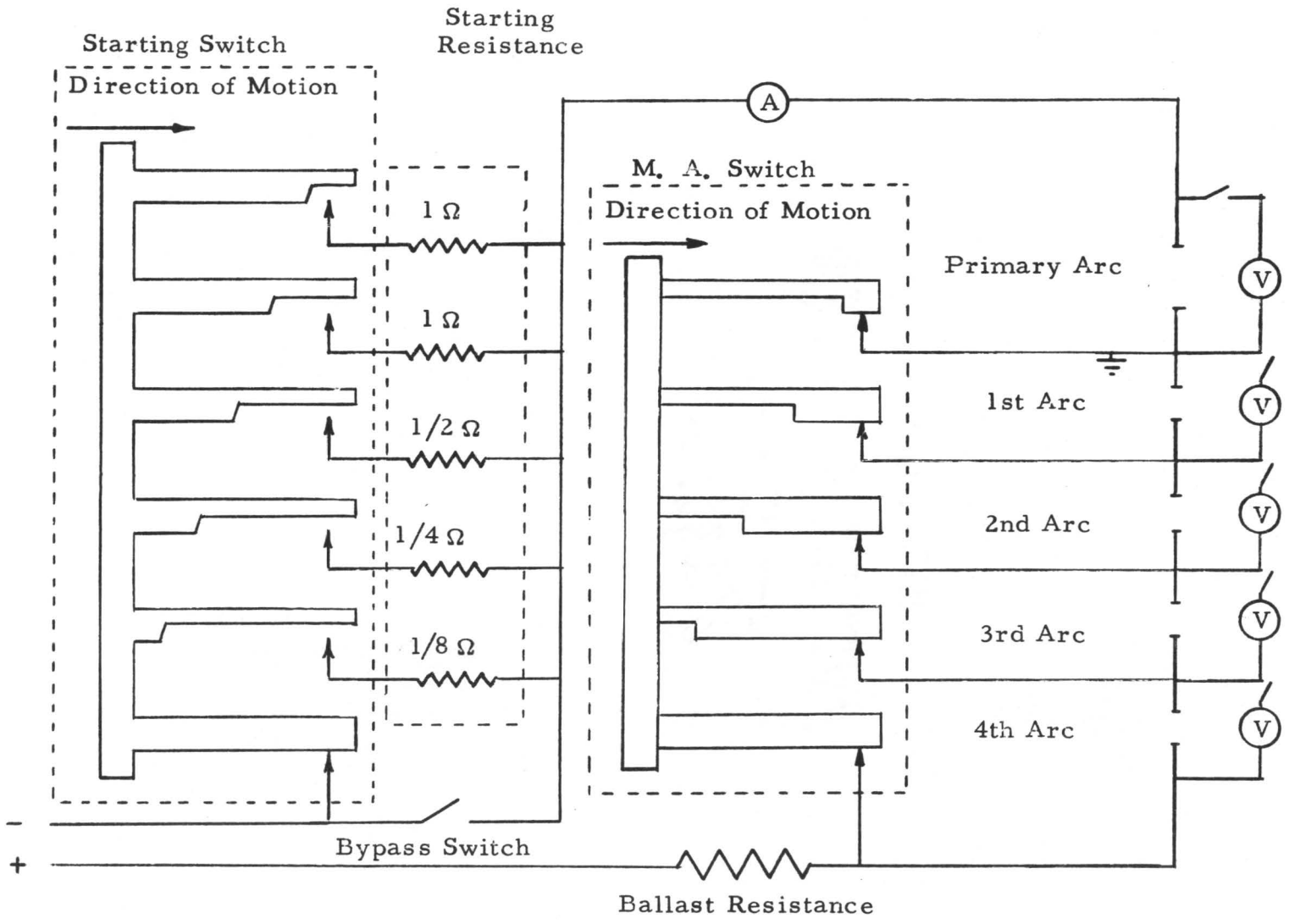

Figure 11 Multiple Arc Starting and Switching Schematic

closed position of the switch the additional arcs are all shorted out. As the switch is moved to the first position the shunt across the first additional arc electrodes is removed, and the only path available for the current is now across the electrodes. Since the gap between the electrodes of the second arc is filled with partially ionized gases from the first or primary arc, the second arc is readily established. As the switch is moved to the second position, the third arc is initiated. The multiple arc switch is capable of handling four additional arcs. For the tests reported herein only two additional arcs (three arcs total) were utilized.

The current is brought into and out of the test chamber by means of feed through conductors mounted in a plate which was positioned over the opening in the top of the test chamber. The details and assembly drawing of the feed through conductors are shown in Figures 12 and 13.

The current is measured by means of an 800 ampere, 50 millivolt shunt in conjunction with a Triplett ammeter. A Triplett voltmeter are used to measure the individual arc voltages. Each one of these voltmeters has associated with it a single pole, double throw spring loaded switch and a suitable resistance which allows either a 50 volts or a 100 volts full scale reading to be selected. A Weston meter with a range of 0-250 volts is used to measure the generator output voltage.

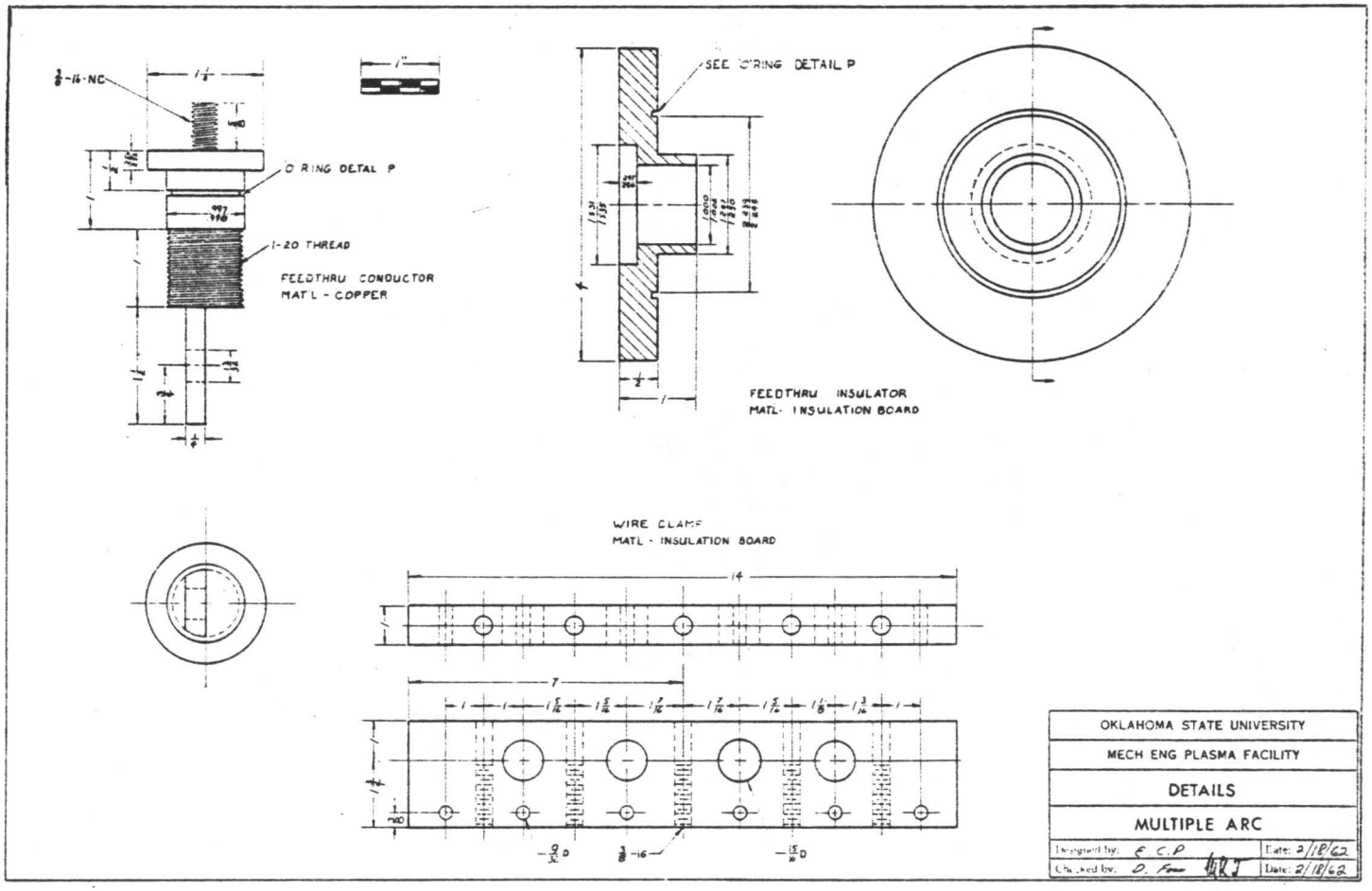

Figure 12 Current Feed Thru Details

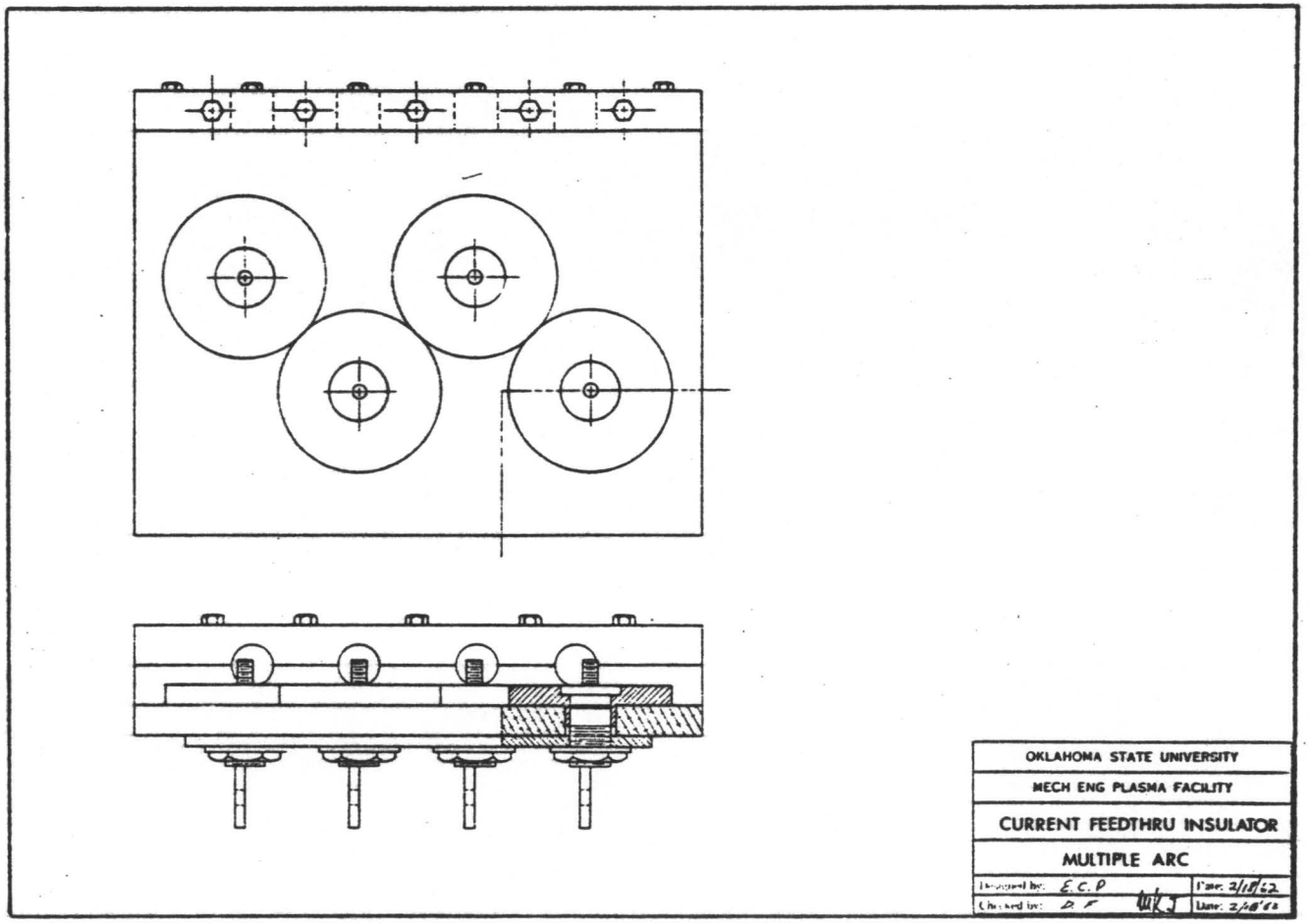

Figure 13 Current Feed Thru Assembly

Gas Supply and Vacuum System

The stabilizing gas, which was argon in all tests reported herein, flows from the high pressure gas cylinder through a pressure regulator to the main gas shut off valve. From here the gas flows through a sharp-edged orifice to the needle control valve, and then to the main chamber. The gas is distributed within the chamber by two nozzles fed from a common manifold. Instrumentation is provided to measure the gas bottle pressure, gas pressure and temperature immediately upstream of the sharp-edged orifice, and the differential pressure across the orifice.

The vacuum system for the Plasma Facility was designed to maintain an absolute pressure within the test section of one inch mercury absolute pressure, or less,for a flow rate of about nine pounds per hour of argon. The test section exhausts into a large cylindrical tank. A 2-inch and a 1/2 inch globe valve, connected in parallel to an opening in the tank, provide a means for varying the test section pressure. A mercury manometer is used to measure the test section pressure. The vacuum pump used is a Model KDH-220, Single Stage-Duplex Design, High Vacuum Pump made by the Kinney Manufacturing Company.

Cooling Water Supply

Cooling water is supplied to all electrodes. For the main chamber assembly the cooling water first passes through the rear

electrode (the anode) and then around the main nozzle (the cathode). The test chamber is fitted with quick disconnects which enable the multiple arc assemblies to be attached to the cooling water supply in a minimum of time. The water flow rate is controlled by valves located on the outlet side of the cooled equipment. A sharp edged orifice is used as the primary element for measuring the water flow rate to the main chamber assembly. Iron-constantan thermocouples sense the water outlet temperatures, and the signals are recorded as temperatures on a Brown Type 153x65 Electronic Multipoint Recorder. This instrument is wired so that every odd numbered point is the water outlet temperature from the main plasma generator assembly. The even numbered points are used to record the water inlet temperature, and the gas inlet temperature, temperatures which do not change rapidly. A calibrated venturi is used to measure the water flow rate from the multiple arc assemblies; Figure 14 shows the details of the venturi. A thermocouple senses the outlet temperature which is recorded continuously on a Leeds and Northrup Speedomax H AZAR strip chart recorder, Serial No. 63-34196-1-2.

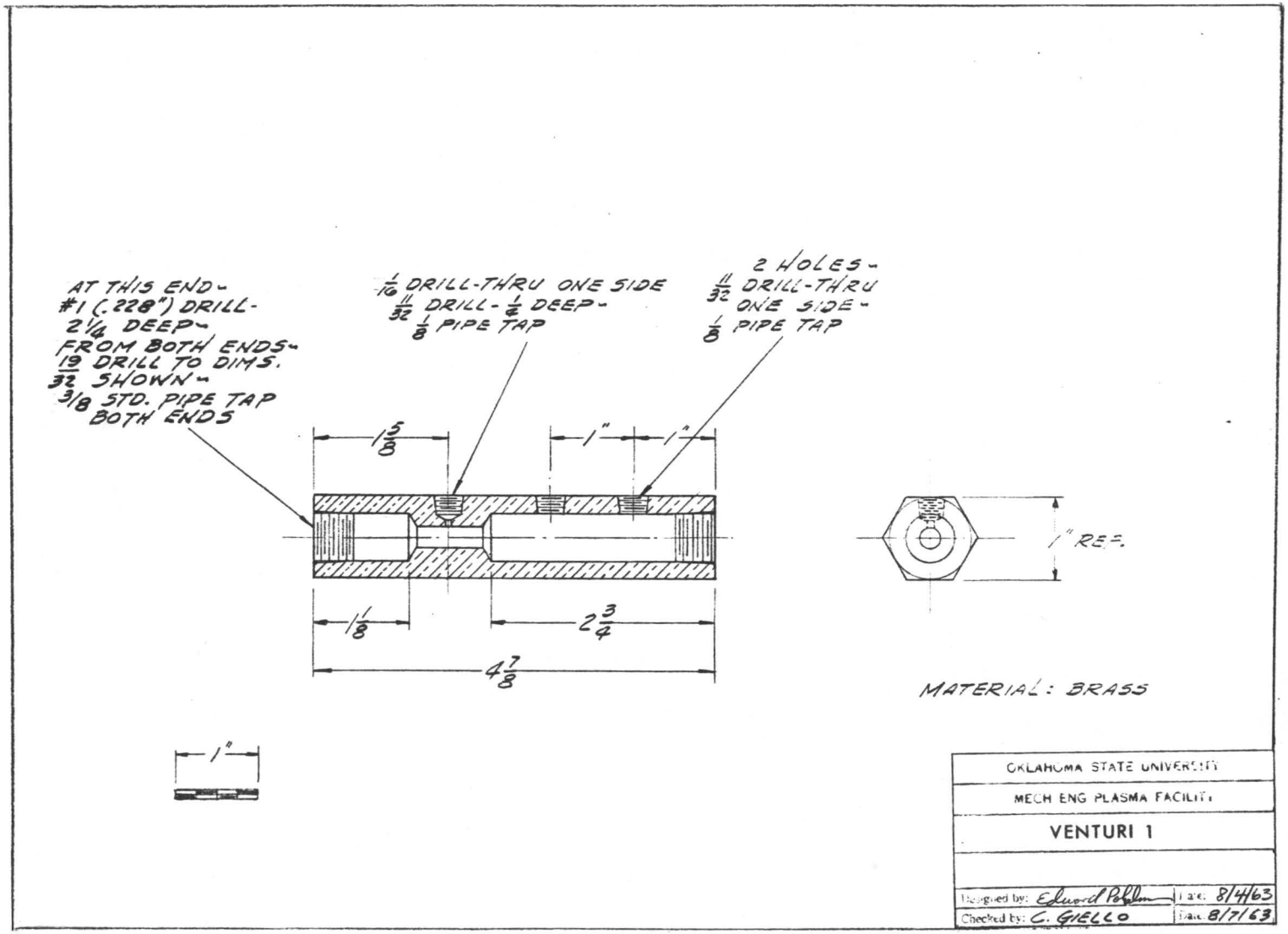

Figure 14 Venturi Details

CHAPTER IV

MULTIPLE ARC DEVELOPMENT

This chapter will be devoted primarily to a description of the experimental development leading to the successful multiple arc jet configuration. To facilitate the multiple arc studies a new design was developed to provide a chamber which could be quickly assembled and disassembled. In addition, it was the desire to design the main assembly so that the additional arc components could be easily attached to it. This design was discussed in Chapter III.

Multiple Arc

The multiple arcs are to be arranged electrically in series as shown in Figure 15 so that the large potential difference available from the power supply can be utilized while the same current passes through each arc. The idea is to take the plasma produced by the present facility in what is called the primary arc in Figure 15 and pass it through successive arcs. In this way it will be possible to add additional energy to a relatively small quantity of gas, and thereby raise its temperature and enthalpy above that presently possible from a single arc.

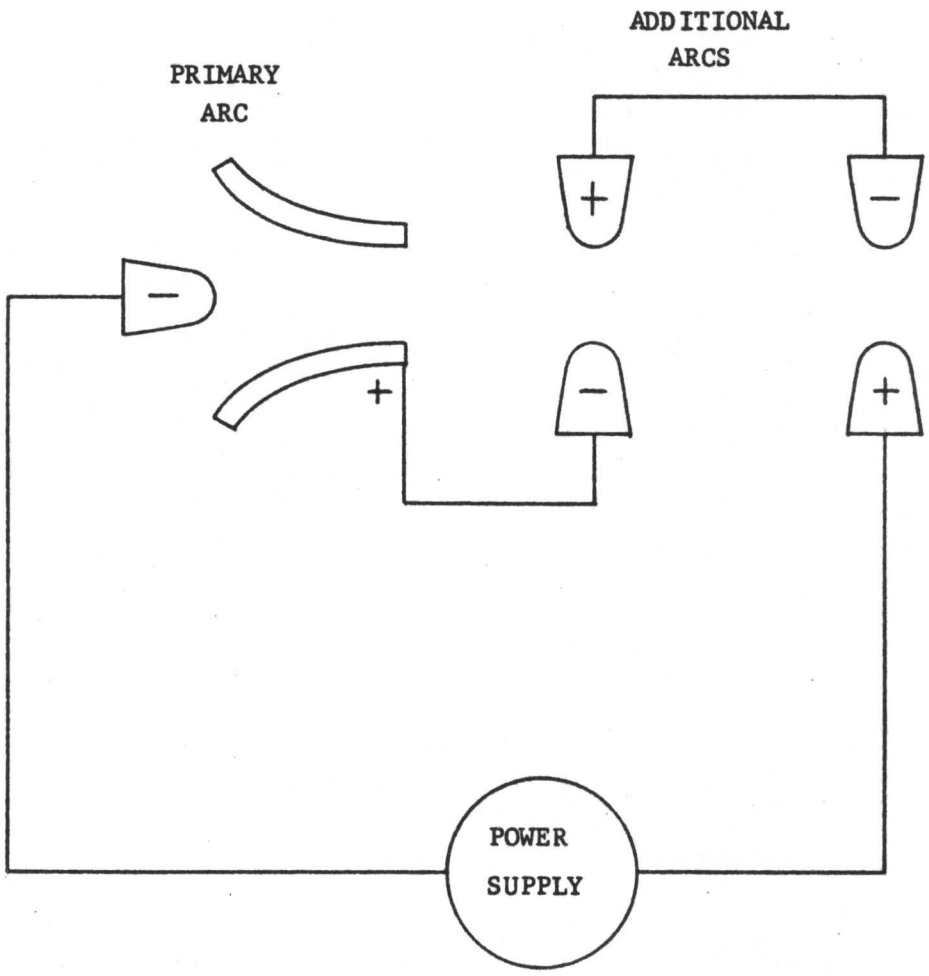

Figure 15 Multiple Arcs

Early in the investigation, a simple test was conducted to determine the feasibility of the additional arcs. It was feared that instead of adding additional energy to the jet stream, energy would be extracted in a sort of magnetohydrodynamic generator type of device. In this test a second pair of uncooled tungsten electrodes was placed about 2 inches downstream of the nozzle exit. These were short-circuited initially by a copper wire. The primary arc was initiated as before by means of the starter electrode and the high voltage impressed on it. After the main arc was started, the copper wire quickly melted because of the hot jet gas, and also because it could not carry the current passing through it. When the copper wire melted, a second arc was established across the efflux plasma from the primary arc. The voltage of the second arc was greater than about 30 volts, the limit of the meter in this particular case. The same current passed through both arcs and the total arc voltage was estimated to be at least 60 volts. This indicates that it is possible to double the input power to the gas, since the primary arc voltage was of the order of 25 volts. The positive electrode of the first additional arc electrode pair was observed to become extremely hot, and only a short run was possible. Since the idea proved feasible, the design of water cooled additional arc electrodes was undertaken.

The first design for the multiple arc is designated Model Z, and is illustrated in Figures 16 and 17. It was decided that the additional arcs should be arranged so that the jet would be completely confined. In this way, it was hoped, less energy would be lost from

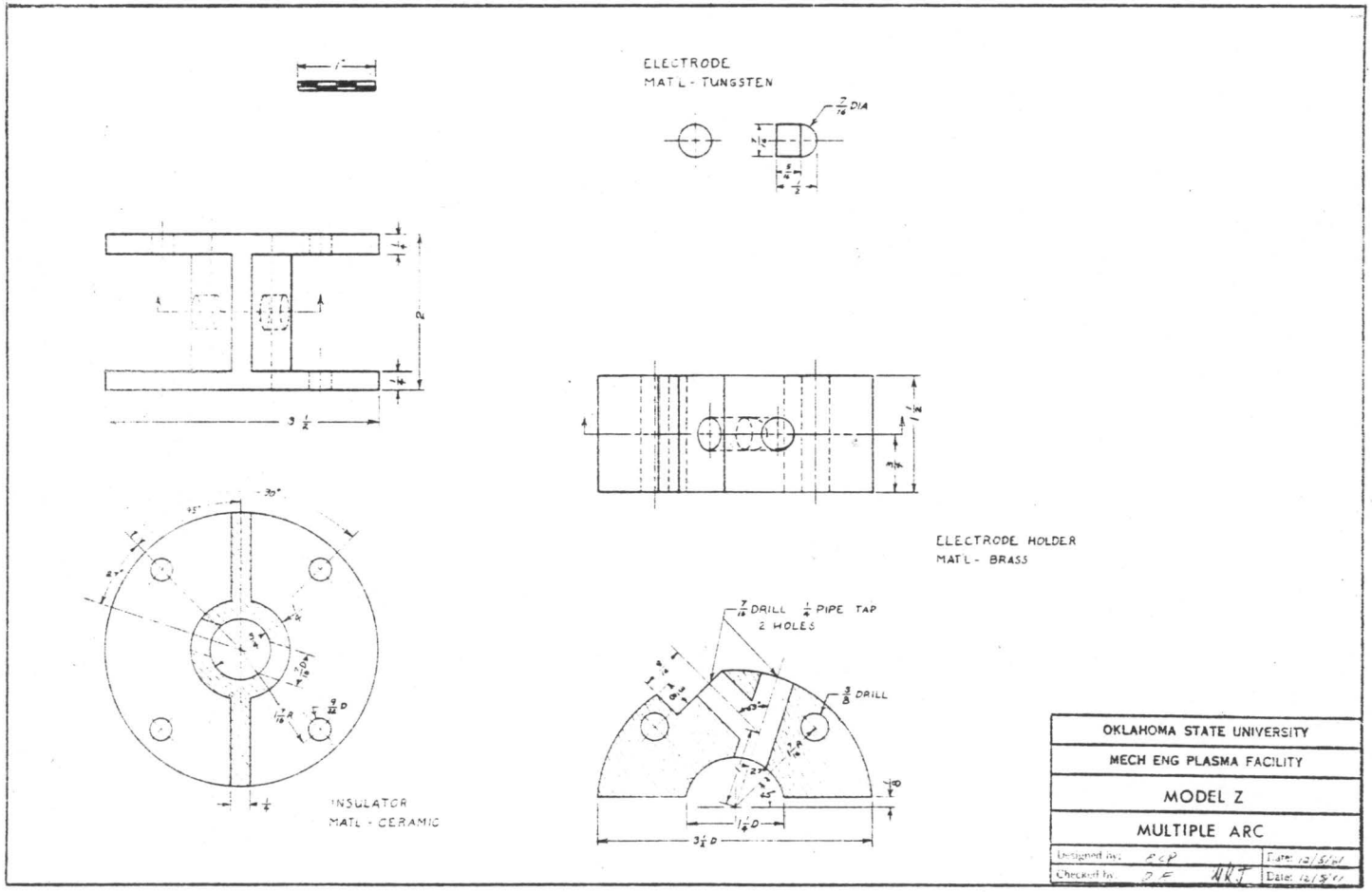

Figure 16 Model Z Details

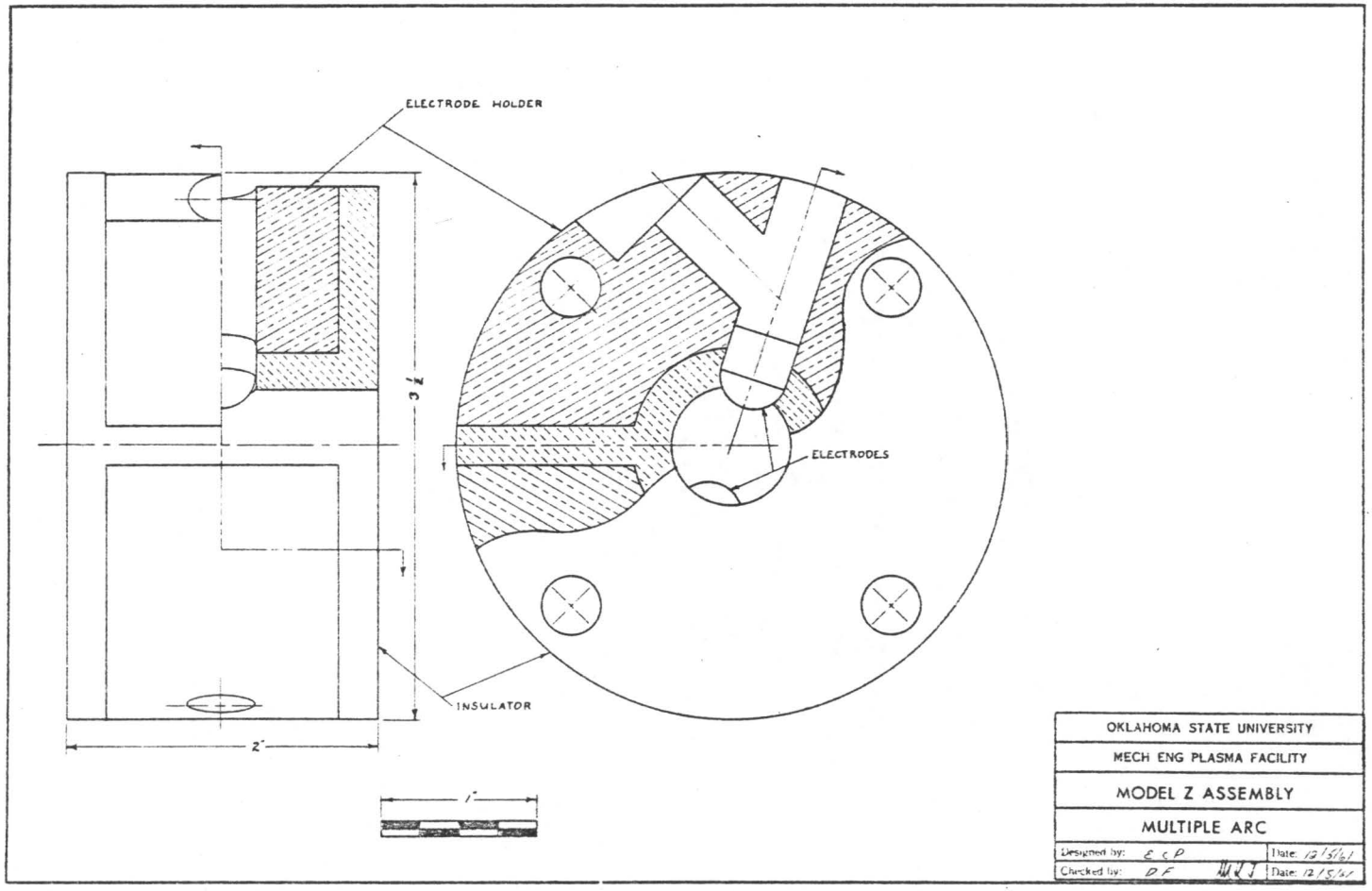

Figure 17 Model Z Assembly

the arc jet. As Figures 16 and 17 indicate, the Model Z additional arc design consisted of two elements. One is a ceramic shield made of aluminum oxide, and the other component is the electrode holder made of brass. Figure 16 shows the details of the design of this particular model, while Figure 17 shows the assembly of these components. As the assembly drawing shows, the ceramic piece is used to form the inside passageway for the jet and also to insulate the brass electrode holders from each other; since they are at different potentials, they must be electrically insulated. A copper or tungsten tip was soldered to the electrode holder in such a way that it just protruded through the appropriate opening in the ceramic insulator. The brass electrode holder was drilled and tapped for the purpose of cooling the electrodes. The assembly for the additional arcs was supported on four quarter-inch threaded nylon rods. The nylon was adopted so that the metal pieces could be insulated from each other. Model D was the primary chamber assembly used to supply the additional arcs with the plasma jet. An electrical arrangement of the additional arcs and physical location is shown in Figure 15. The additional arcs were transverse to the jet flow, and were arranged so that the tungsten electrode was the cathode, and the copper electrode was the anode.

The primary arc was started in the usual way by means of a high voltage impressed upon the starter electrode. After a brief warm up period, the multiple arc switch was moved so that the first

additional arc was placed in the circuit. Some arcing inside the trolley controller was heard during the switching process. The first two attempts failed to ignite the second additional arc, although when it did ignite, no audible arcing was observed from the switch. At low power levels, the primary arc and the number 1 additional arc operated satisfactorily with no apparent melting. However, when the second additional arc was included in the circuit, some melting occurred. At high power levels this melting became excessive and the operation was limited to a total of about 15 seconds in three short runs. During this time, the following data were recorded: main arc, 25 volts; number 1 additional arc, 15 volts; number 2 additional arc, 40 volts; current, 500 amperes through all three arcs, (assumed). Argon flow rate was 8 lbs./hr. If one assumes that 45% of the total input power is retained by the gas, then approximately 40 kilowatts of power were transferred to the gas. Corresponding to this, there is an estimated enthalpy of 7,700 BTU/lb. or a dimensionless enthalpy, H/RT_0, of 318. According to Cann and Ducati (41) this is equivalent to a temperature of about 10,700 °K at about 1 inch of mercury absolute pressure. This represents a considerable increase in enthalpy over the previous tests, although the temperature has not been increased very much.

The thermal stresses induced in the ceramic electrode holders caused them to crack in several places, but the electrical integrity was maintained. The first additional arc electrode was found to be in very good condition after the test. However, the copper tip of the

second additional arc was melted completely away, and part of its brass support was also melted. The tungsten cathode of the second additional arc was found to be undamaged. The only explanation for the low arc voltage of the first additional arc is that part of the current went directly from the anode of the main arc, i.e., the nozzle, to the anode of the first additional arc. After the test, the ceramic electrode holder insulator was reconstructed, as much as possible, by gluing the many pieces together. Some of the parts are shown in Figure 18. From these reconstructed parts, some useful information was obtained.

Streamers of molten ceramic existed on one side of the cathode opening but not on the other. This indicates that the first additional arc heated the gas to a temperature high enough to melt the ceramic and carry it downstream. However, there is negligible evidence of this molten ceramic entering the second additional arc opening. In addition,

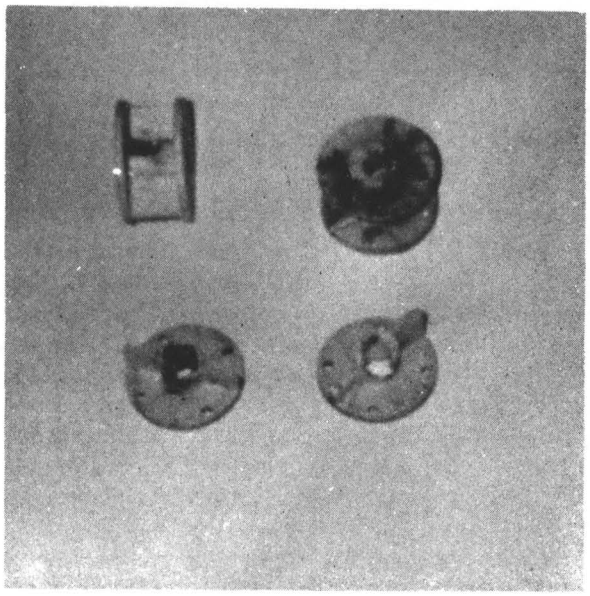

Figure 18 Model Z Ceramic Pieces

from the placement of the holder in relation to the main arc and the electrical connections to the additional arcs, the molten ceramic must be on the inlet side of the first additional arc holder. These factors and the low arc voltage indicate that the arc was established between the exit nozzle and the copper anode of the first additional arc as suggested previously. In this arrangement, the distance from the end of the nozzle to the anode of the first additional arc is the same as that separating the electrodes of the first additional arc. Since it is probably easier for the arc to follow along with the gas stream close to the wall, rather than to find its way across the stream, it is believed that this really did happen. However, the tungsten tip which was the cathode of number 1 additional arc, became hot enough to melt the ceramic close to it. Hence, some of the current must have passed normal to the gas stream. At one location near the opening for the tungsten cathode, a bubble of ceramic was formed. The electrodes themselves were in rather good condition. The copper anode appeared pitted as though a dull pointed object had been used on it. There was no damage to the brass parts. On the downstream side of the number 1 additional arc electrodes only a very thin layer, possibly 1/64 inch, of molten ceramic was observed.

The damage to the electrodes of the second additional arc was quite different from that observed for the first additional arc. The copper anode was melted almost completely away. The surrounding ceramic had melted and vaporized until the arc finally attached to the brass part and burned a hole about 1/4 inch in diameter, and

about 1/16 inch deep into the brass electrode holder component. Molten ceramic flowed out the end of the ceramic electrode holder and solidified forming icicles.

In general, the damage to both additional arcs and their respective components showed that (1) the ceramic insulators are too thick and cannot withstand this thermal stress, (2) the copper anode does not receive sufficient cooling, and (3) a spacer is needed so that the arc will not be established between the main nozzle and the succeeding electrode holder.

Another test was set up in which one ceramic piece was used as a spacer. In this test, the spacer was placed between the main arc nozzle and the first additional arc. The main arc was started in the usual way, and after several trials it was determined that the first additional arc could not be established until a current of at least 300 amperes existed. However, before switching to the first additional arc, the following data were observed: 300 amperes of current; 30 volts across the main electrode; -3 volts across the first additional electrode, and +6 volts across the second additional arc. Thus, it appears that a small amount of current was flowing through the first and second additional arcs. With the main arc and the first additional arc in operation, the following data were recorded: 300 amperes; 32 volts on the main arc; 22 volts across the first additional arc; and about 1 volt across the second additional arc. After this, the second additional arc was included into the circuit, and the following data were recorded: 120 amperes; 32 volts across the main arc electrodes;

7 volts across the first additional arc, and 36 volts across the second additional arc. Finally, the current was reduced to 60 amperes with 37 volts across the second additional arc. Between these runs there were brief periods of shut down. During the tests the ceramic pieces cracked as before, presumably from thermal stresses. It is believed that the electrical integrity was maintained. At the conclusion of this series of tests, the ceramic pieces were glued back together to the extent possible. From these reconstructed pieces, some useful information was derived.

The inlet of the spacer shows no signs of melting. The jet after leaving the main arc, expands from a 5/16 inch hole to a 3/4 inch hole. Thus, the plasma may never touch the walls of the spacer. The two holes in the spacer were not covered. During the operation no plasma hot enough to be visible was seen leaving the holes. However, the material around the holes was slightly melted on the inside, and the area in line and downstream of the holes was melted somewhat. The nylon rod outside the hole was melted into two parts. However, the other nylon rod, which could not see the other hole, and consequently the hot plasma was not melted as badly.

The inlet to the first additional arc was not melted very badly and only a small amount of ceramic material, corresponding to the contamination of the melted spacer, was observed. However, on the outlet side, there was considerable damage, particularly on the tungsten cathode side. Here it was found that the ceramic material had been melted away to the extent that the hole for the tungsten tip

was enlarged to about twice its original diameter. Furthermore, on the downstream side, the arc had become attached to the brass, melting the ceramic and leaving the brass part exposed. The ceramic piece was completely melted up to its flange. At this location, there is a deep trough eminating from the edge of the brass component and continuing to the second electrode holder. The copper anode of the first additional arc was burned and melted, and the wall thickness of the ceramic insulator was reduced from 1/4 to 1/8 inch.

The inlet to the second additional arc ceramic component had a very deep trough which was the continuation of the trough started in the first additional arc ceramic piece. This trough continued to the copper anode of the second additional arc, but became less shallow as it approached the copper anode. At this location, the trough was very shallow, and the wall thickness of the insulator was about equal to the original 1/4 inch. However, the molten material from the trough was pushed beyond the copper anode, and a ceramic icicle about 1 inch long formed at the outlet. It is believed that this trough was formed as a result of the arc being established between the cathode of the first additional arc and the anode of the second.

A third series of tests was conducted with the electrode holders fitted to new ceramic pieces so that the tungsten cathode of the first additional arc and the copper anode of the second were recessed about 1/16 inch below the surface. It was hoped that the arcing between the cathode of the first and the anode of the second arc might be eliminated in this way. To further assist in establishing the arc in

the proper place, the flow rate was reduced to approximately 1/4 of that used for the second series of tests. As before, about 300 amperes were required to establish the first additional arc. Again, a trough was burned from the tungsten cathode of the first arc to the copper anode of the second, and again the ceramic was completely burned away on the first, so that the arc eventually became attached to the brass electrode holder. Only moderate melting was observed on the second additional arc. Approximately the same total damage was observed, and it was concluded that recessing the electrodes was not effective in eliminating this problem. In addition, at the lowest gas flow rate used in this series of tests, the starter electrode was burned, apparently because the arc became attached to it instead of moving downstream and becoming attached inside the nozzle. After this series of tests, seven of the eight original ceramic pieces had been cracked and damaged and were no longer usable. Since these pieces could not withstand the high thermal stresses, it was decided to try a different design which might eliminate this problem.

Figure 19 is a drawing of Model Y electrode holder. In this design, the separate ceramic insulator has been eliminated and the brass holder coated with an aluminum oxide layer about .030 inch thick. The aluminum oxide coating is used to provide the electrical insulation. The coating is applied by means of a flame spray device. During the test of this unit, the arc jumped between the corner of the two electrode holders at the inlet side. This was originally believed to be due to a defect in the coating of the ceramic, but later tests indicated that

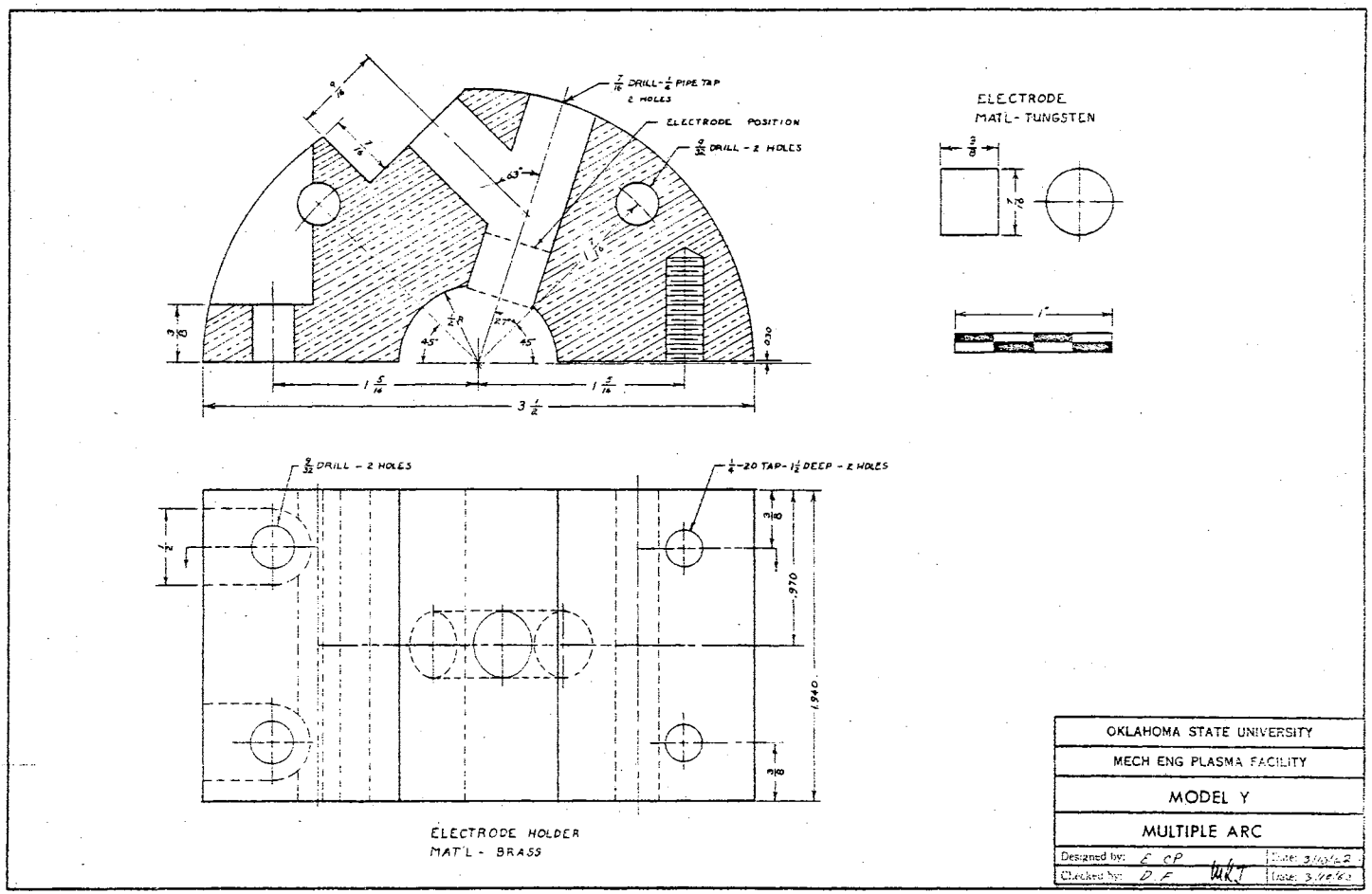

Figure 19 Model Y

this may not have actually been the case. At the time, it was believed that the ceramic melted and failed because it was improperly cooled. For this reason, a new Model X was designed with a more complete water cooling jacket. This is shown in Figure 20.

As the drawing shows, water enters the cooling jacket, cools the electrode, circulates around the passage, and leaves at the other end. The water jacket is sealed by means of a plate brazed over the opening on one side. This design was also coated with aluminum oxide and tested. The first trial of Model X lasted about 30 seconds. The electrodes for this test were exactly opposite each other. During the test, the arc became connected downstream of the tungsten cathode by penetrating the ceramic coating and attaching to the brass piece. The terminal point of the arc on the anode and the cathode could not be visually determined. The crack which developed in the ceramic coating was about 1/32 of an inch wide at its narrowest point, and progressed irregularly downstream from the cathode. A second trial of about 90 seconds duration was attempted with the Model X design. During this test, the anode was placed 2 inches downstream from the cathode, and the following data were recorded: 30 volts on the main arc; 40 volts across the first additional arc; current about 150 amperes. The arc was established between the base on the downstream side of the cathode and extended to the downstream side of the anode. A corner of the cathode was slightly melted.

After the ceramic burned away, the arc jumped and became attached to the brass holder. At the anode, the downstream corner

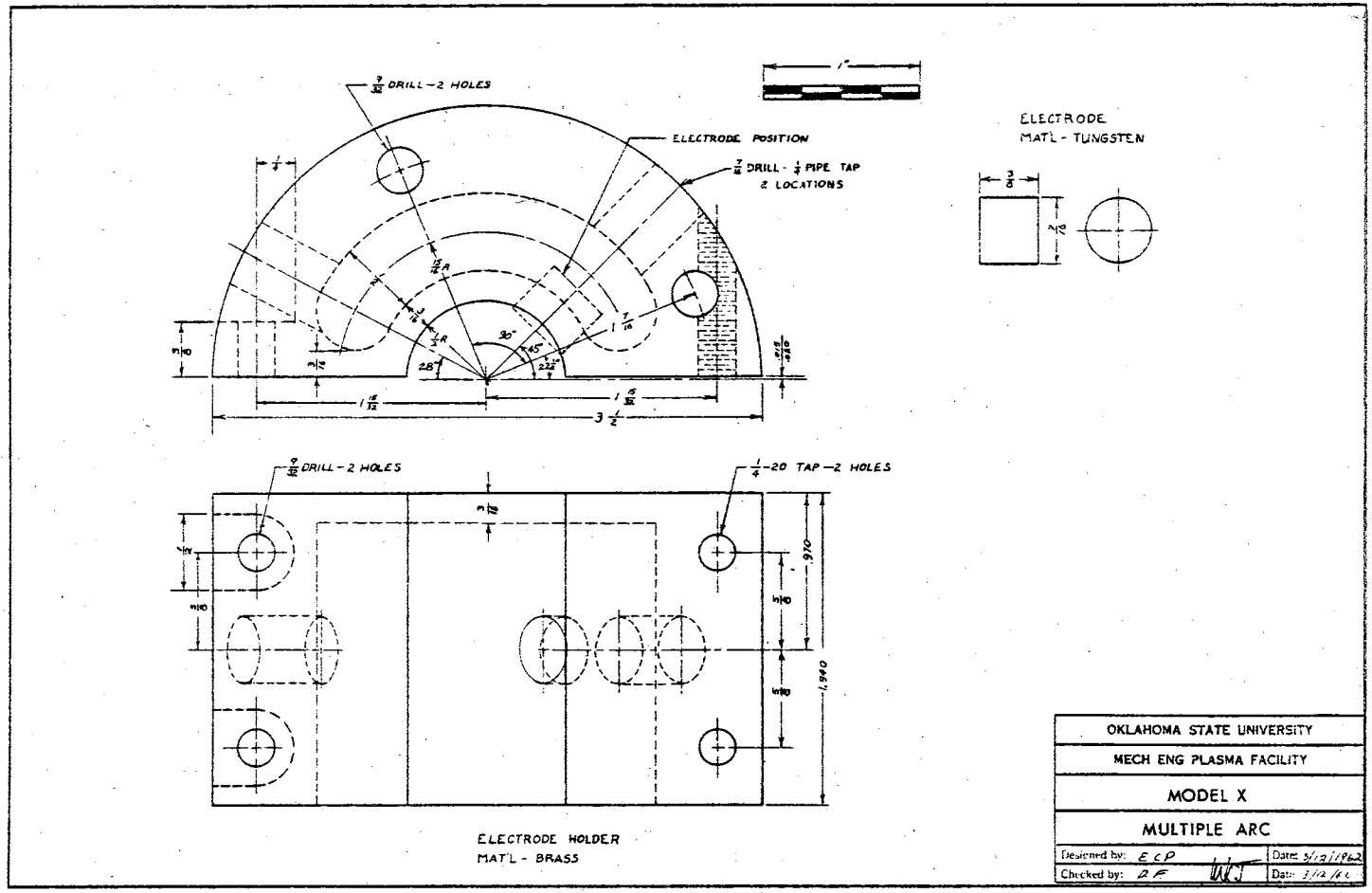

Figure 20 Model X

of the electrode was melted very slightly, but no erosion occurred. In addition, the ceramic on the downstream side of the anode was melted somewhat. After running in this manner for about 90 seconds, an arc was suddenly established between the two corners of the electrode holders. This phenomenon is similar to the one experienced with Model Y. It is now believed that after a period of time the ceramic material is weakened by the hot plasma jet so that it fails electrically, and allows an arc to be established across the relatively short distance separating the two brass electrode holders.

At this time, it was believed that the arc was being blown downstream by the action of the jet. Therefore, it was decided to build an electrode holder with a recess so that the electrodes could be placed out of the main flowing stream. In addition, it was believed that the sharp corners of the previous models contributed to the breakdown of the ceramic material and the arcing in the wrong place. Therefore, all the corners on the new design, Model W, were rounded. This design is shown in Figure 21. During the tests of Model W essentially the same thing happened; the ceramic broke down, and the arc was established at the shortest possible location (at the corners). The Model W components were also coated with aluminum oxide, but this time by means of a plasma spray gun. It was hoped that this technique would provide a denser coating, more firmly bonded to the brass, and in this way provide a better electrical insulation.

Experimentation with the confined multiple arc was suspended at this point, and attention was directed toward the development of an

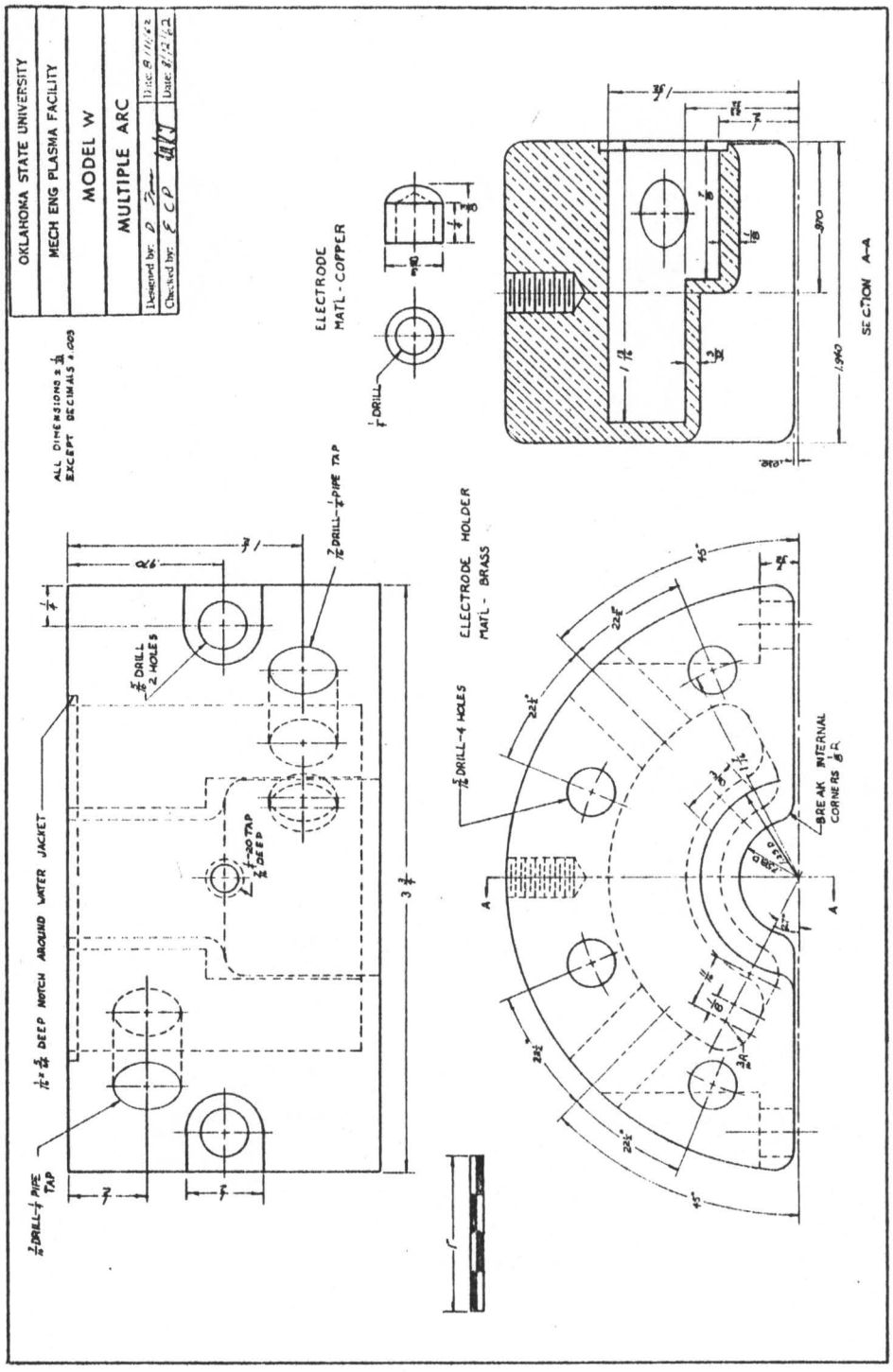

Figure 21 Model W

unconfined multiple arc. The details of this design, Model V, arc are shown in Figure 22. Two additional arcs were arranged as shown in Figure 15. In this configuration however, the arc again became connected between the cathode of the first and the anode of the second additional arcs. Even though the aluminum electrode holder and the electrode itself were coated with aluminum oxide, the improper arcing quickly damaged the components.

At this point is was decided to attempt multiple arc operation with only one additional arc. Generally, operation became acceptable. It was found that the separation of the additional arc electrodes in conjunction with their location downstream from the main nozzle is very important. If the spacing is not correct, the arc will jump from the main nozzle (acting as the cathode) to the anode of the first additional arc. Sometimes the arc seems to be partially attached to the cathode of the first additional arc but not to the anode. Both modes of operation are deemed unsatisfactory. The following detailed account of a series of tests reveals several interesting facts.

In the first test the electrodes were placed about 3/4 inch apart and were located about 2 inches downstream of the primary arc nozzle. When the additional arc was switched into the circuit, the arc was established from the rear of the primary nozzle to the anode of the first addition arc. It was possible to operate for more than a minute in this fashion at currents of about 150 to 200 amperes without seriously melting the nozzle. During this run, the chamber pressure was about 1 inch of mercury absolute.

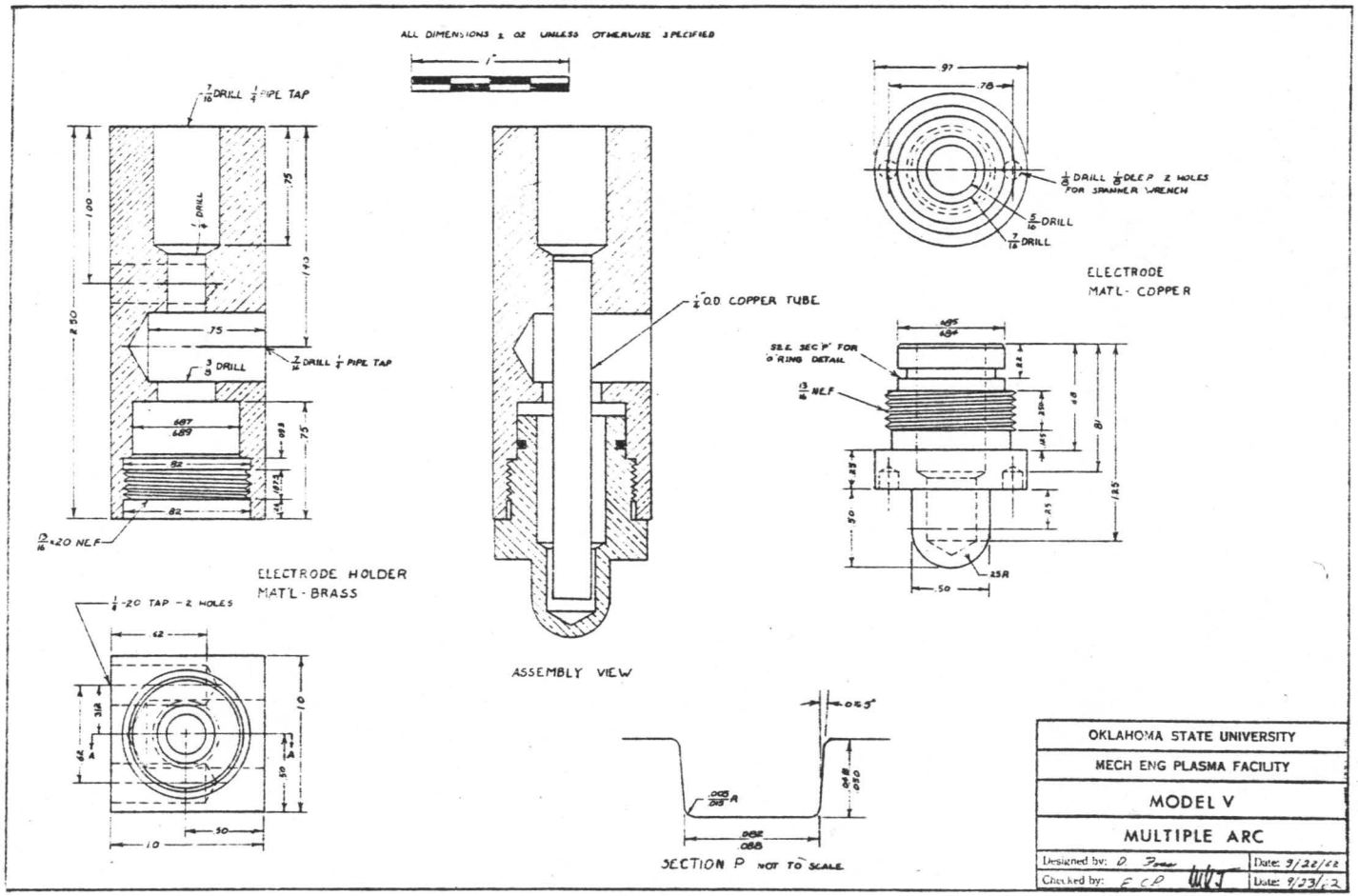

Figure 22 Model V

There was a small water leak in one of the inlet cooling water hoses, and water dripped down onto a lower hose. Because of the low initial temperature of the water and the low vacuum in the chamber, this water actually froze on the lower cooling water hose. The distance from the frozen water to the first additional arc and its associated plasma was not more than 3 inches. Apparently, the rate of heat transfer from the plasma and electrodes is very small; particularly the radiation must be small.

For a second test, the electrodes of the first additional arc were moved closer together so that the gap was only about 3/8 of an inch. Under these conditions the arc was established across the electrodes, and there was apparently little attempt by the arc to move upstream to the nozzle of the primary assembly. The arc definitely appeared to trail downstream from the electrodes as shown in Figure 23. The entire surface of the anode was surrounded by a glow which moved off downstream. However, on the cathode the glow was only on the downstream side. This indicates that the ions are the more important specie in determining the stability and location of the arc.

Fig. 23 Arc Distortion

The electrons, which are much more mobile, cause the glow to cover the anode completely. The heavier ions cannot move upstream so readily, and therefore the cathode glow appears only on the downstream side of the electrode. The flow rate was reduced to about 1/2 the initial starting value, with no affect on the position of the glow.

The current was increases to the maximum of the power supply, and it appeared at one time that the arc became attached more toward the upstream side, i. e., it appeared to straighten out somewhat. However, this phenomenon could not be reproduced. The facility was operated at 400 amperes continuously for about one minute with no appreciable melting or erosion of either electrode. During this time the primary arc potential was 20 volts and the first additional arc potential was 42 volts. Thus the input power was about 25 KW with argon. This represents an increase of about 75 percent over the single primary arc. At about 450 amperes the anode started to melt. Very brief runs at 600 amperes were possible but the anode melted and a flat spot quickly formed on the downstream side of the electrode.

From these tests and others similar in nature the following conclusions are drawn. (1) Model V is capable of passing a maximum of about 400 amperes without excessive erosion. (2) The positioning of the electrodes is very critical. (3) The unconfined arc is not the most suitable for adaption to a multiple arc jet. This last conclusion results from the fact that (a) a large amount of energy is lost to the surrounding by convection during the passage of the gas jet from the

exit of the primary nozzle to the electrodes of the first additional arc and (b) the jet is not at all well defined after it passes the first additional arc. In short, even though the energy input may be doubled, it is very doubtful that the gas flow from the additional arc is suitably directed or that its enthalpy is significantly increased.

Model V electrodes and holders were used by Eugene Fletcher in his study of arc voltage as a function of electrode separation (27). In these static tests, i.e., no gas flow, the electrodes performed fairly satisfactorily but eroded slowly during arc operation. Since a constant electrode separation was essential, the copper end was cut off and tungsten tips silver soldered in place. This modification proved very successful.

One of the problems with the Model V is the undesirable attachment of the arc on the downstream side of the electrode. In addition it was not possible to move the electrodes closer than about 2 inches from the primary nozzle. To overcome these difficulties Model T was eventually designed. With this model the electrode tips can be placed about one inch from the nozzle exit, and positioned so that the anode and cathode spots are on the end of the tips instead of on the sides. Further, the centerline of the tips need not be perpendicular to the jet axis as with Model V, but can be inclined to it at any angle from about 60° to 0° (electrode tips parallel to the jet). The Model T electrodes are used in conjunction with the Model V electrode holders. Model T is shown in Figure 24.

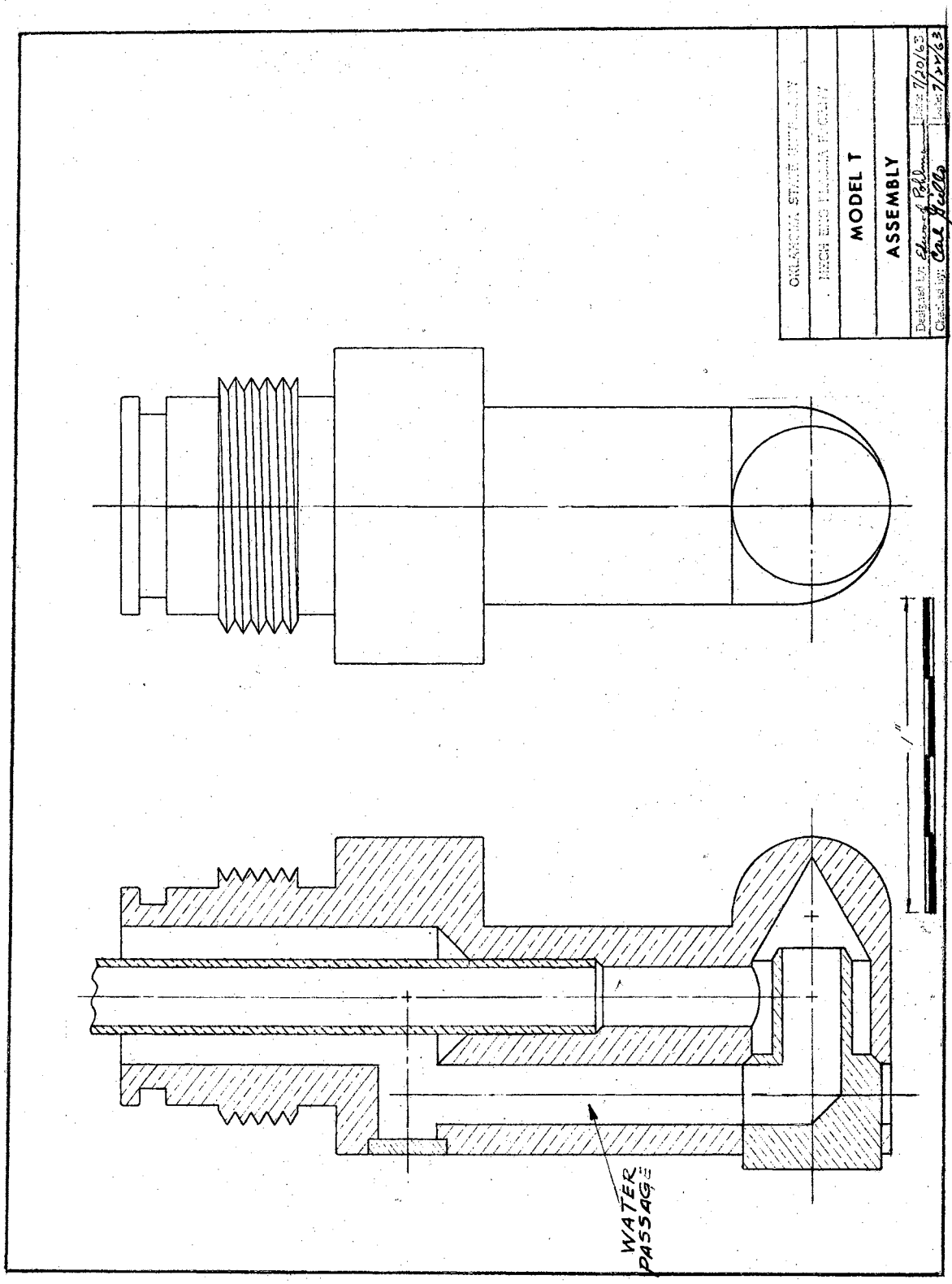

Figure 24 Model T

As it became obvious that an unconfined additional arc is not completely satisfactory for a plasma jet device, attention was directed again to the confined arc arrangement. Previous tests with Models W, X and Y indicated that an electrically neutral spacer should be placed between the electrode holder halves. Model X was so modified, and tested after all pieces, including the spacers, were recoated with aluminum oxide. The spacers eliminated the improper arcing from one electrode half to the other. However, the arc spot again moved downstream off the electrodes, eventually melting the aluminum oxide coating from the electrode tip to the exit of the electrode holder. The brass tended to melt under these conditions and the operation was deemed unsatisfactory.

Since it appeared that the arc spot was blown downstream by the plasma jet issuing from the primary arc nozzle, it was suggested that if the electrodes were recessed, the arc spot would not be blown away. To this end Model W1 was redesigned (Model W2) so that electrically neutral spacers could be used to insulate the holder halves. In addition the electrodes were set at 45° to the main flow. When tested, an arc became attached from the main nozzle to the anode of the first additional arc. This melted the spacers and the anode holder and rendered the holder useless for further testing.

At this point it was decided to investigate a confined longitudinal additional arc and to deemphasize the transverse, confined arc exemplified by Models W, X, Y, and Z. However, one final transverse, confined configuration, Model Q, shown in Figure 25,

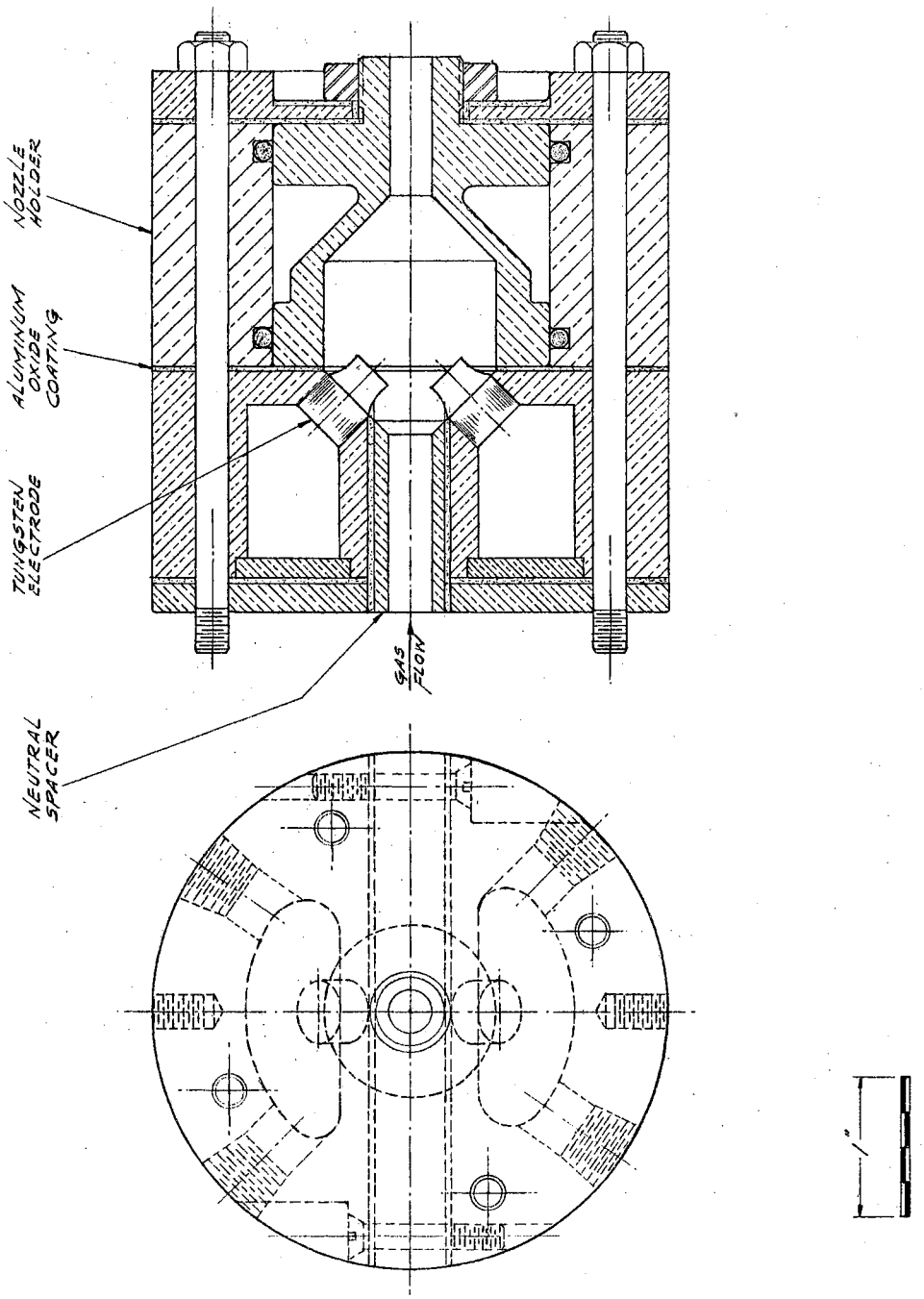

Figure 25 Model Q

was designed and built but not tested as the longitudinal confined arc was showing a great deal of promise.

Figure 26 shows an assembly drawing of Model S. In this configuration three tungsten tips form the cathodes of the first additional arc. These were mounted in a separate holder. The cathode, spacer and nozzle anode were attached to the main chamber by means of nylon studs. In the first test of this model the arc became attached to the wrong place and the nozzle was eventually burned. Figure 27 shows Model S in operation before it burned.

Finally, successful operation was achieved with Models R1 and R2 shown in detail in Figures 28, 29, and 30. Figure 32 is an exploded view of the main chamber and the Model R2 components. The tungsten tips of the cathode for the first additional arc were silver soldered in the end of the main nozzle (Figure 31) of the primary arc. The spacer was internally conical for Model R1, and cylindrical for Model R2. The nozzle used in R2 is identical to that used as the primary nozzle of Model D main assembly. Models R1

Figure 27
Model S in Operation

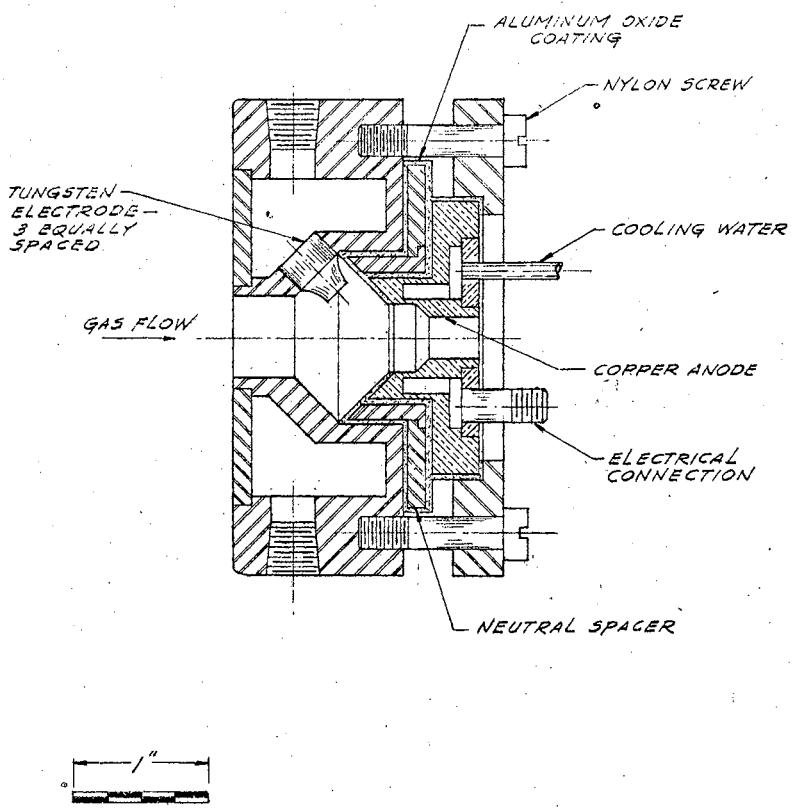

Figure 26 Model S

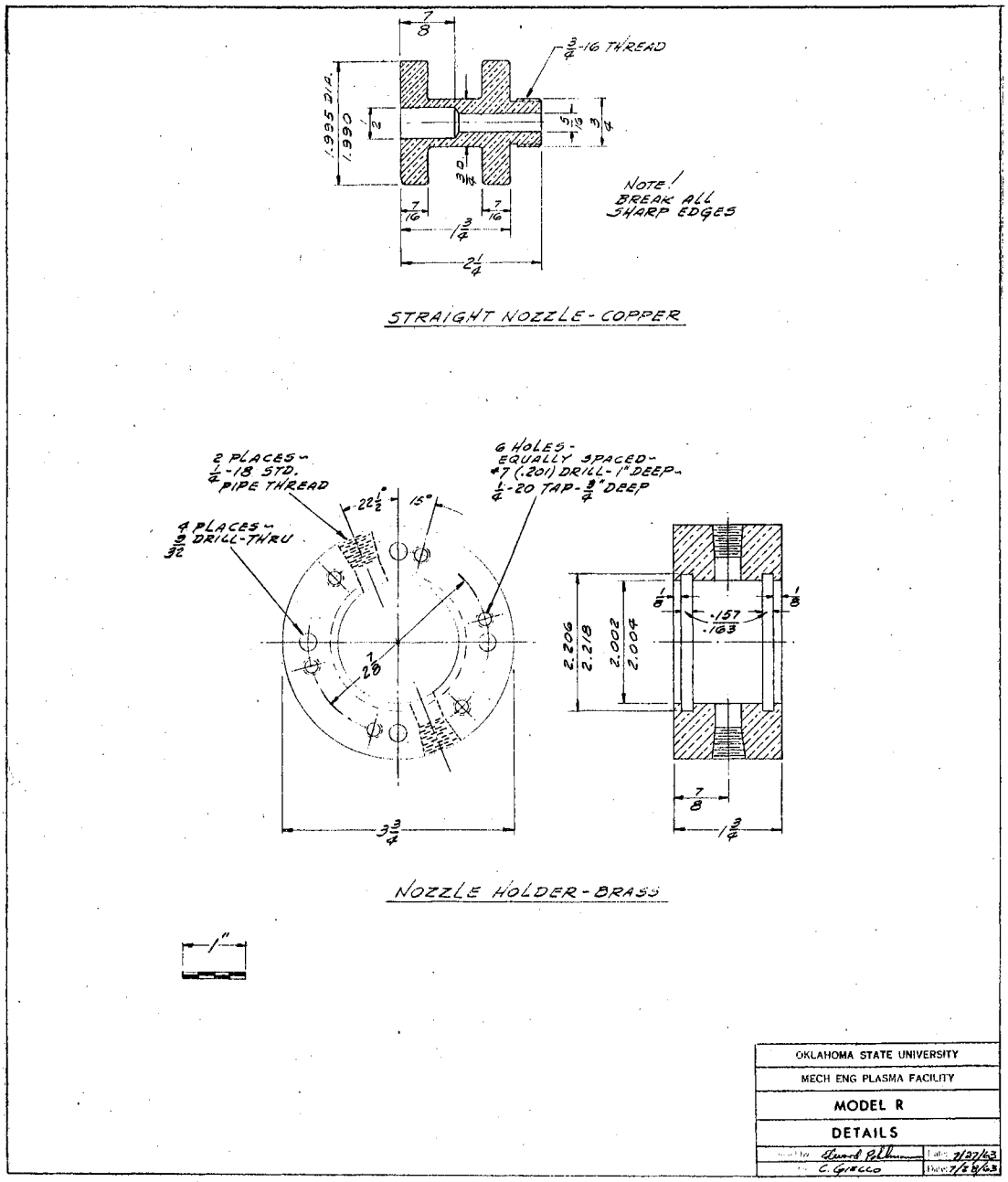

Figure 28 Models R1 and R2 Components

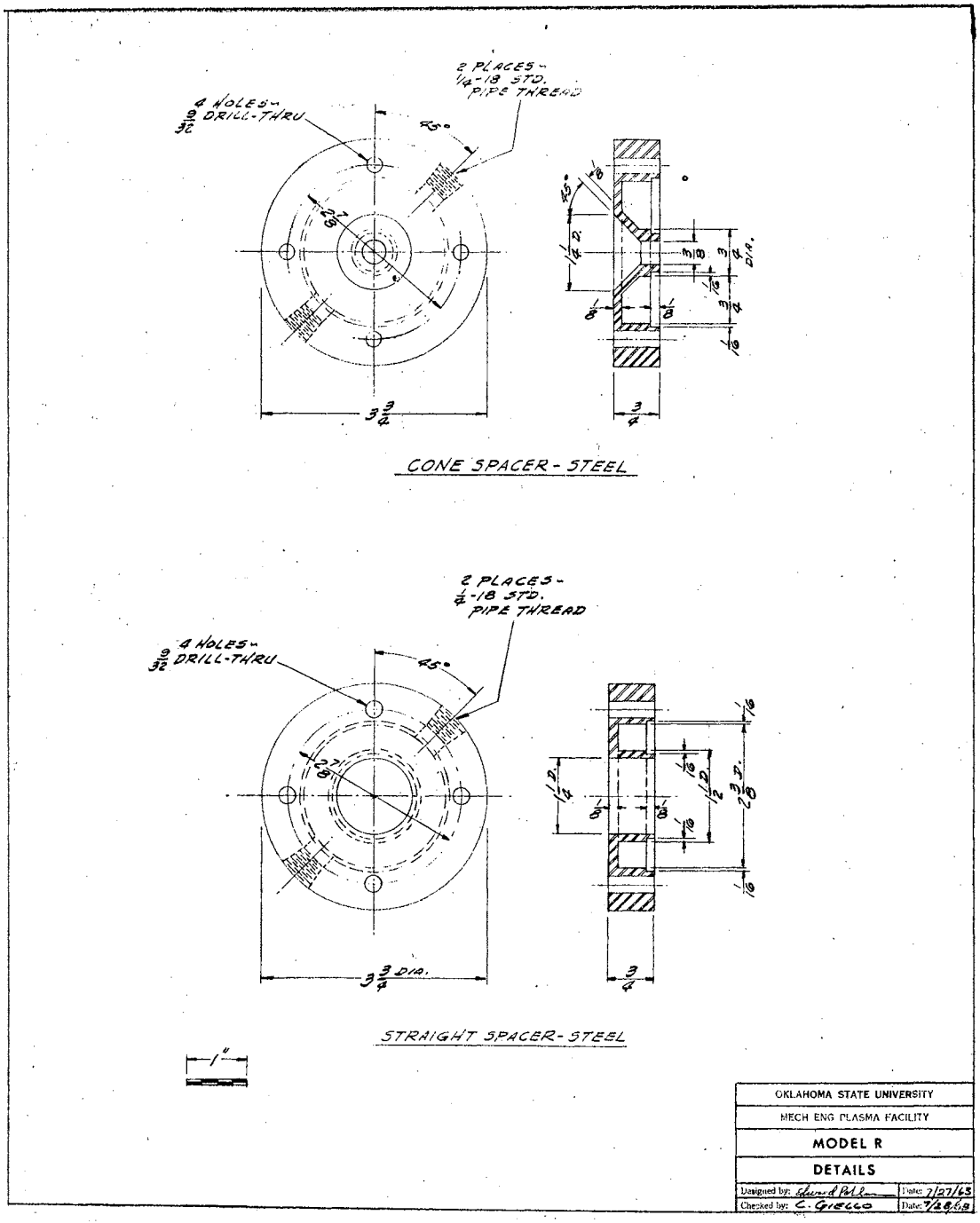

Figure 29 Models R1 and R2 Spacers

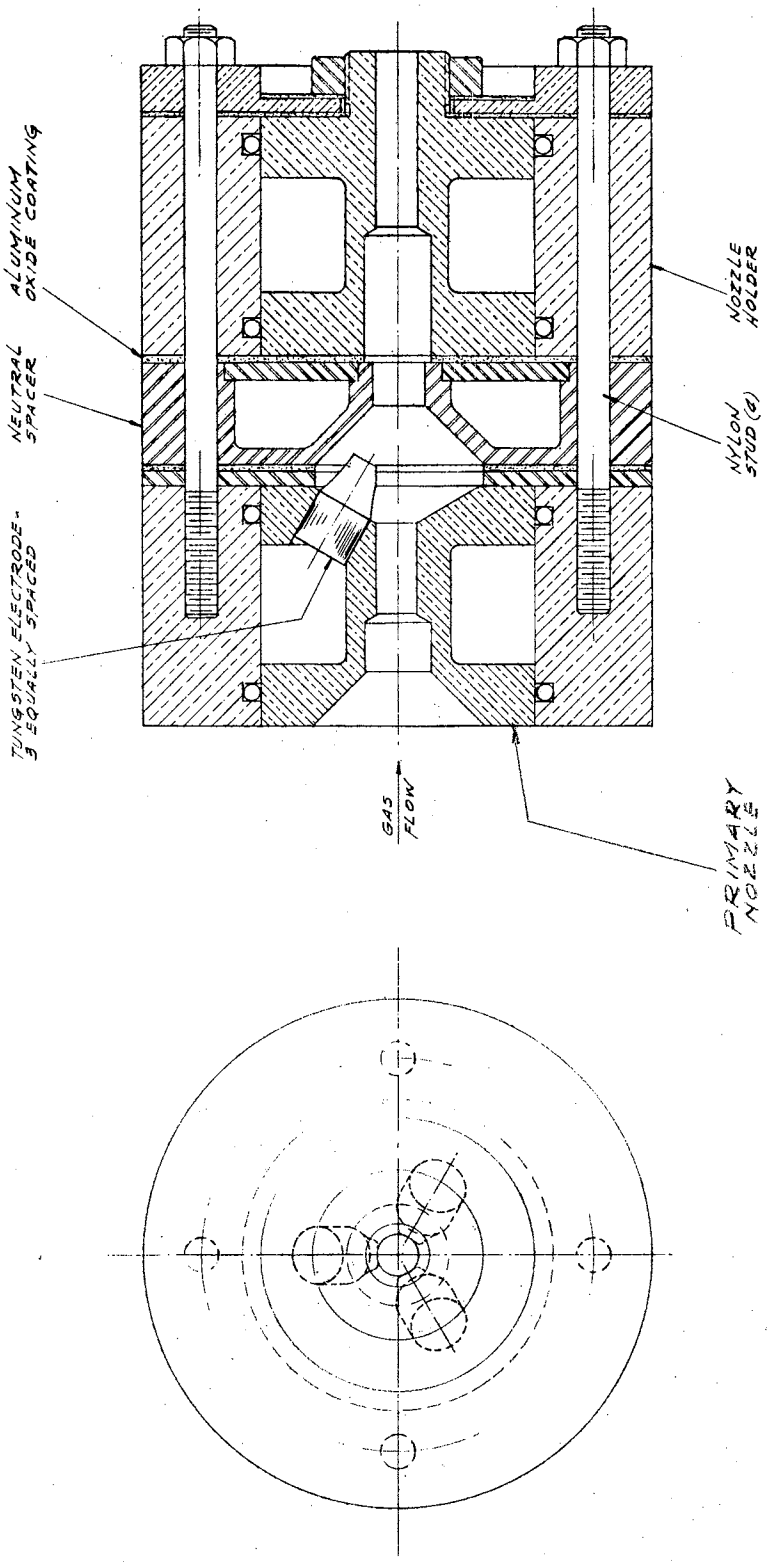

Figure 30 Model R1 Assembly

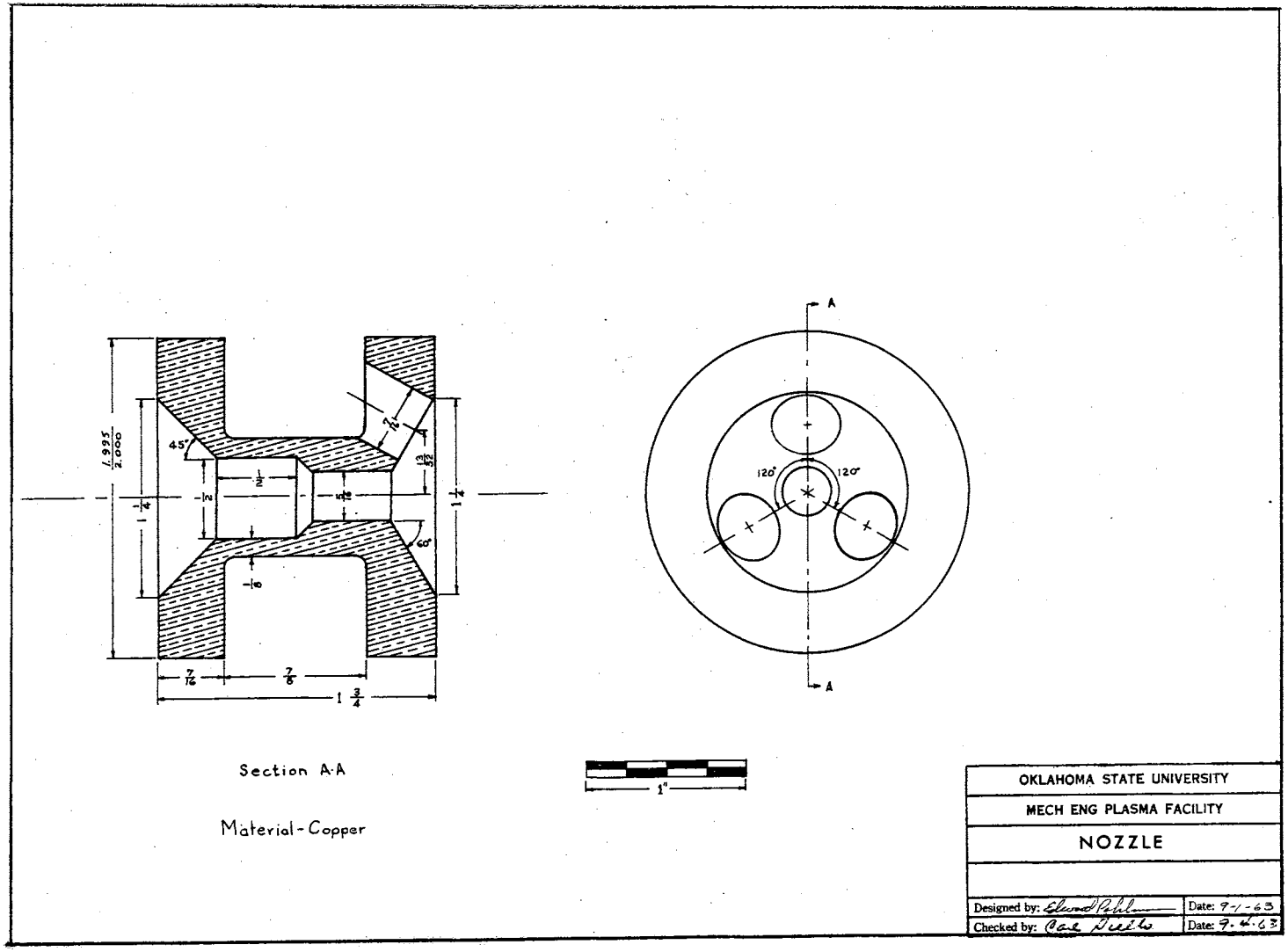

Figure 31 Nozzle

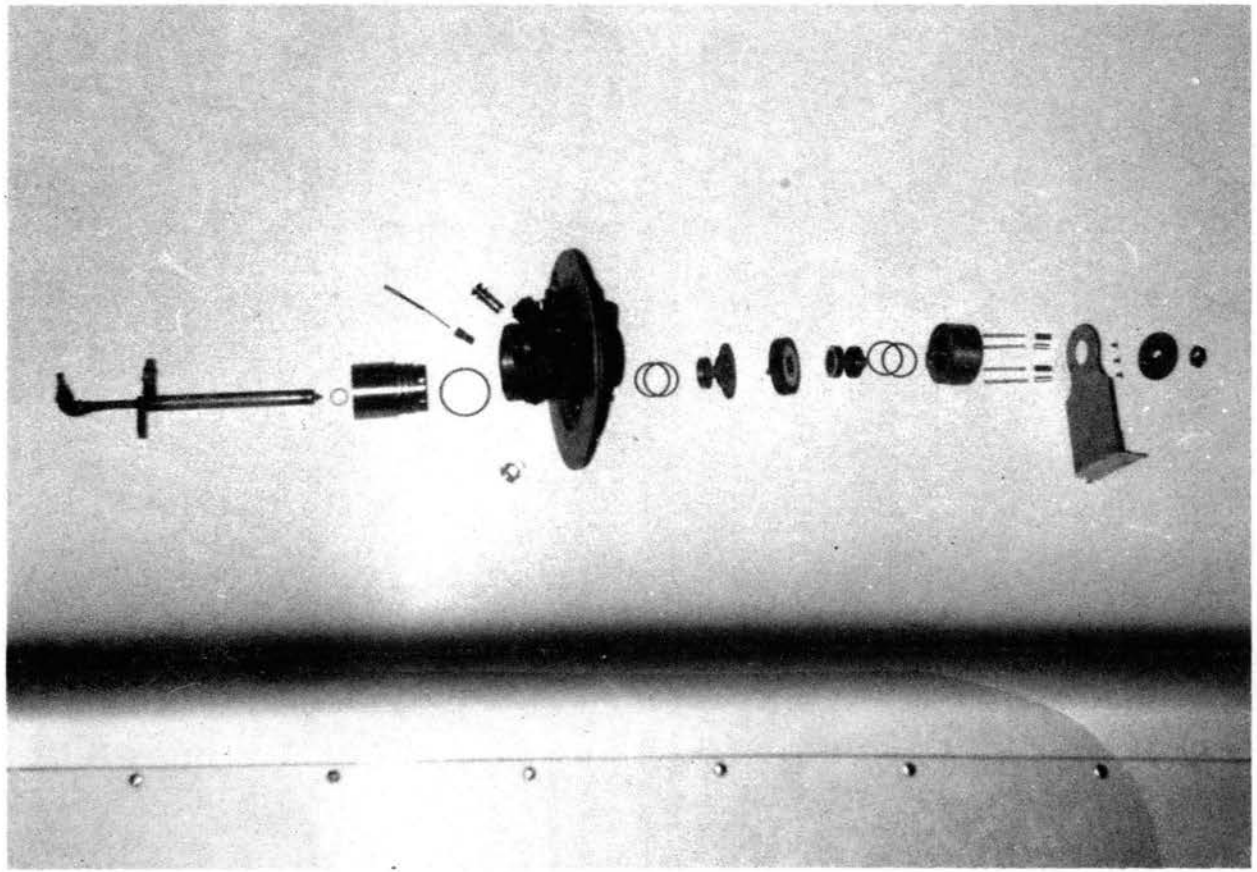

Figure 32 Exploded View of R2

and R2 operated very well and were used to obtain the final data.

Model R1 operated very effectively for a short period of time during which data points A1 through C1 inclusive were collected. (The data are presented in Appendix A) R1 is the configuration using the conical neutral spacer. In order for the second arc to be established the arc column must pass through the small hole at the exit of the spacer. It is believed that this is the reason for the unequal voltage distribution between the two arcs. As this data show, the second arc voltage was about five times that of the first arc.

The R1 configuration was the most effective in terms of energy conversion efficiency and gas enthalpy. Unfortunately, after a period of time the spacer became burned around the small hole, and the operation became so unstable that no further data were collected with Model R1.

Model R2 was now installed and tested. This is the model with straight spacer, and the standard Model D nozzle used as the anode of the second arc. During these tests two modes of operation were observed. At low current levels the arc voltage of the second was about four times that of the first. This is called the first mode and corresponds roughly to the operating characteristics of Model R1. The data points D1 through F2 inclusive except E4 are for mode I operation. Efficiencies, gas enthalpies, and total arc voltages are less with R2 mode I than they were with R1. It is believed that the arc column was attached inside the anode nozzle of the second arc assemble for mode I operation.

At currents of about 180 amperes the operation changed to mode II. This mode is characterized by a nearly equal distribution of potential between the two arcs and by a slightly larger potential drop across the first arc. It is believed that the arc moved upstream out of the bore of the second arc anode nozzle and became attached to the conical inlet surface of the anode.

Model R2 operated very satisfactorily during the tests. Only a small amount of burning and erosion occured during the tests, and the components of R2 were in relatively good condition at the conclusion of the tests. In terms of reliability R2 can be considered the most successful confined multiple arc design devised during this investigation. However, R1 is the most successful in terms of increasing the gas enthalpy.

CHAPTER V

EXPERIMENTAL METHODS AND DATA REDUCTION

The material presented in this chapter describes the detailed procedures for starting the Plasma Facility and adjusting the operational parameters such as power input level, gas flow rate, cooling water flow rates and test section pressure. The techniques used to record and reduce the data are given along with a sample data sheet and a sample set of calculations.

Operational Procedure

The overall operational procedure can be divided into three phases: (1) preliminary preparation, (2) main arc starting procedure, and (3) operational adjustments.

Preliminary Preparation

The preliminary preparation includes all operations which must be accomplished before the main arc is started. It is usually desirable to perform a few additional operations during the preliminary preparation. These preliminary preparations can be subdivided into three general areas: (a) the cooling system, (b) the electrical system, and (c) the vacuum and gas flow systems.

The cooling system is composed of water circuits and cooling

fans. There is one cooling water circuit for the main chamber assembly. The cooling water flows first through the rear electrode and then around the nozzle anode. The flow rate is controlled by a globe valve on the outlet side of the circuit. The pressure differential across a sharp-edged orifice is measured by a U-tube manometer filled with Meriam Indicating Fluid of 1.75 specific gravity. A calibration curve for this orifice is shown in Figure 33. Before the arc is started a flow rate corresponding to a total deflection of 15 to 20 inches should be established.

Another U-tube manometer filled with 1.75 specific gravity fluid is used to indicate the pressure differential in the venturi located on the outlet side of the multiple arc cooling water circuit. Three different venturis were designed, and the one used was selected on the basis of the number of multiple arcs used and the maximum allowable temperature rise. The details of the venturis are shown in Figure 15. The venturi is designated by the drill size of the throat. For all of the tests reported herein venturi 1 was used. A calibration curve is shown in Figure 34. The initial flow rate to the multiple arcs should be set to correspond to a total manometer deflection of about 20 inches.

There is a heat exchanger in the vacuum line ahead of the vacuum pump. The separate water circuit for this is adjusted to give maximum deflection of the manometer. In addition there is a cooling water line for the vacuum pump which should be turned on before the pump is started.

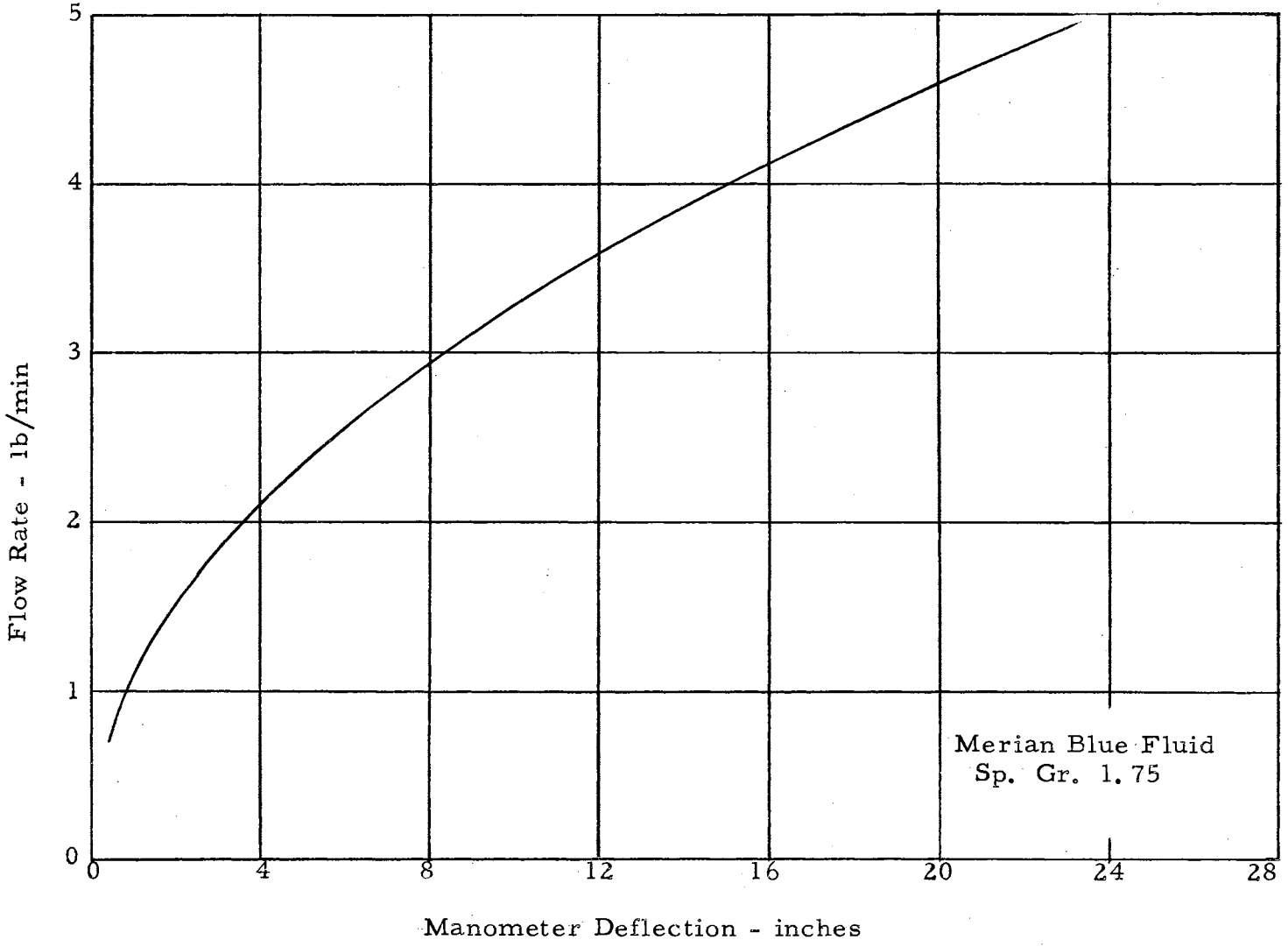

Figure 33 Main Chamber Assembly Cooling Water Flowmeter Calibration

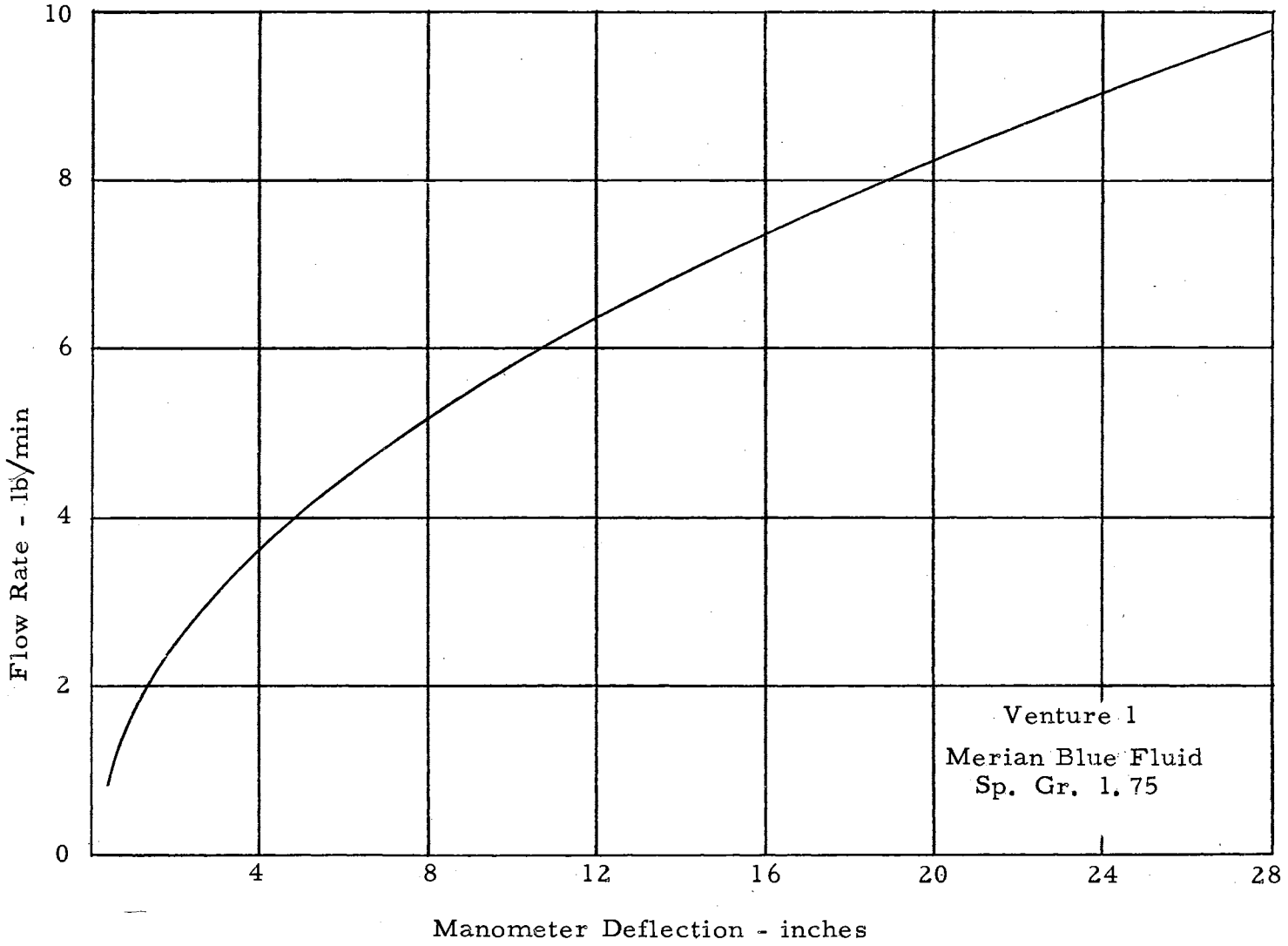

Figure 34 Multiple Arc Cooling Water Flowmeter Calibration

A cooling fan is provided for the ballast resistor, and must be turned on before the arc is started. Generally, the starting resistance bank does not require a cooling fan. However, if the starting resistance is to be used to augment the ballast resistor for long periods of time, a cooling fan must be used.

The electrical system is composed of all the controls associated with the MG set, the starting resistance by-pass relay, and the tesla coil.

The tesla coil is checked for proper operation. The starter electrode is positioned so that sparks of equal intensity eminate from the tip of the starter electrode and terminate on the rear electrode and the nozzle simultaneously. The starting resistance by-pass relay is checked. If it is not operational, the six volt storage battery will have to be charged or replaced.

The MG set can now be started, and the preliminary adjustments made. Both trolley switch levers are set to the off position. The voltage and current control rheostats on the control panel are set to their minimum positions. The load selector switch (the double pole-double through knife switch located in the blue box above the electronic control cabinet) is placed in the up position, thus connecting the DC generator power leads to the plasma facility. The main 440 volt, 3-phase AC power switch on the junction box near the MG set is closed. The green light on the control panel indicates the MG set is ready to start, and the actual starting of the MG set is accomplished

in the following order.

1. Push the MG start button. A red light on the left side of the control panel indicates the MG set is running.

2. Push the reset button.

3. Move the field switch to the forword position. The green light on the right side of the panel indicates that the MG set is now ready to deliver current.

4. Close the main contactor switch by means of the appropriate push button. The right hand red light is now on and indicates power into the trolley control switch.

5. At this point the volt meter which measures the total generator output voltage may indicate a definite voltage, even though all control rheostats are off. If this is the case, the current control and the voltage control should be moved to the maximum clockwise position. In a short time the voltage will drop to zero and begin to increase again. Only after the voltage starts to increase from zero can the rheostat be used to adjust the generator output voltage. The voltage should now be reset to zero, pending completion of the other preliminary operations. The current control can be left in its maximum (clockwise) position. The MG set is now ready to start the main arc.

The chart drive for the point recorder can be started.

The lubricating and sealing oil shut off valve on the vacuum pump is opened, and the pump can be started if desired.

The argon bottle shut off valve is opened, and the cylinder pressure regulator is set for a delivery pressure of 25 psig with a flow rate corresponding to about 10 inches deflection across the argon flow measuring orifice. This orifice was calibrated by a student laboratory group as part of their course requirements. Figure 35 is the calibration curve. The argon flow may be stopped at the

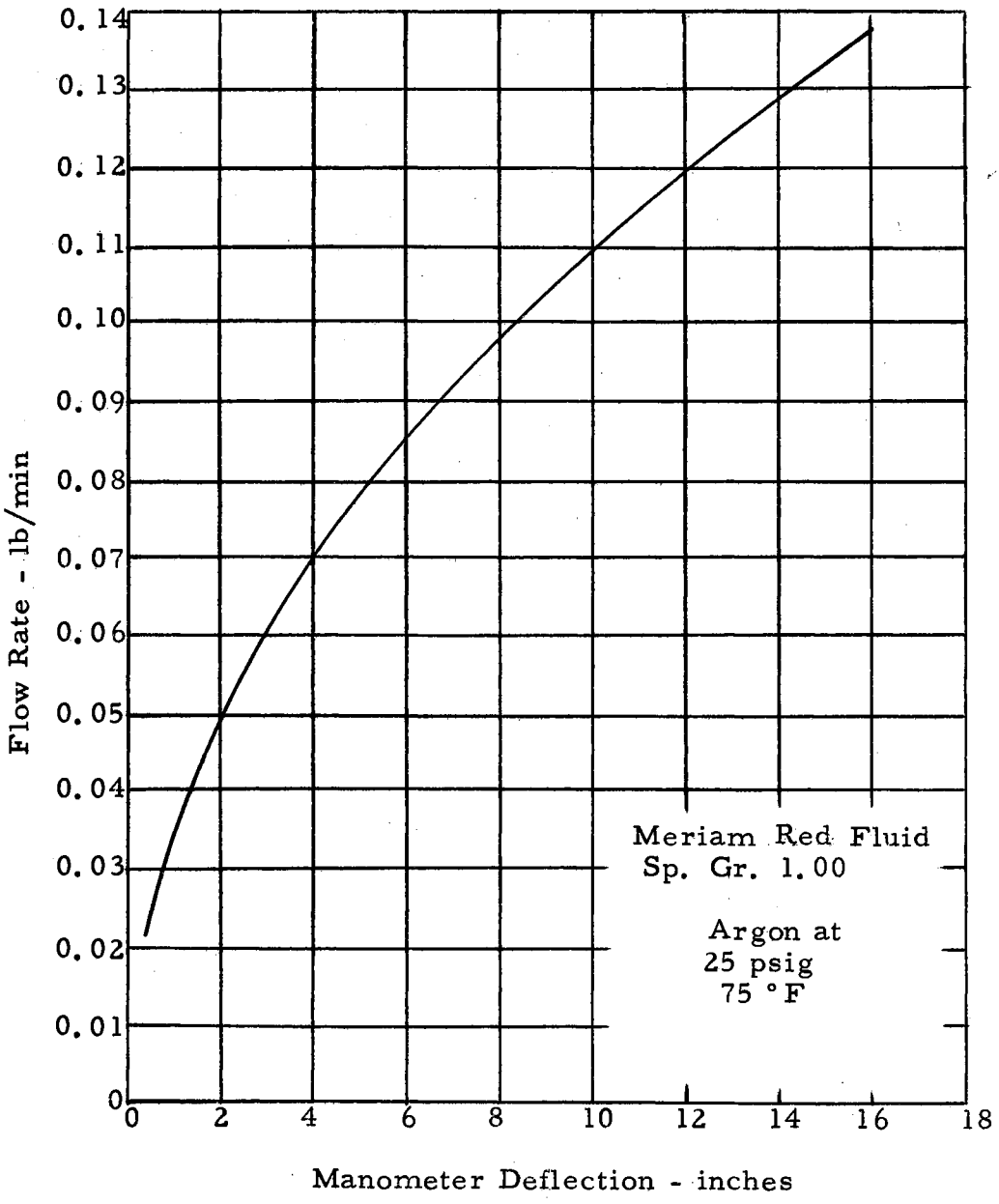

Figure 35 Argon Flowmeter Calibration

control panel until the actual start up time arrives.

Starting the Main Arc

After all of the above mentioned preliminary operations have been completed, the plasma generator may be started. The following sequence of operations should be adhered to.

1. Close the contactor switch, if this had not already been done.
2. Adjust the generator output voltage to give an open circuit potential of 150 volts.
3. Start the argon flow and adjust the orifice differential pressure to between 10 and 15 in. H_2O.
4. Move the resistance switch lever to the desired starting resistance (one or one-half ohm, i.e., first or second position, respectively).
5. Energize the tesla coil. The arc should start immediately.
6. Move the starting resistance control lever through its remaining positions, thus reducing the starting resistance to 1/16 ohm.
7. Close the starting resistance by-pass switch.
8. Adjust the voltage control rheostate to reduce the arc current to 300 amperes or less.

Operating Adjustments and Control

The main plasma generator is now operational. The argon flow rate is changed by adjusting the needle valve on the control panel. The arc current is changed by varying the voltage control rheostat. The chamber pressure was held fixed for these tests, but can be varied from 1 in. Hg to atmospheric by adjusting the blow-down valves on the vacuum tank.

During the tests the cooling water flow rates to the main chamber and additional arcs were adjusted to give a minimum temperature rise of 30°F.

The following procedure was used to start the multiple arc.

1. The main arc voltage was increased to about 300 amperes.
2. The trolley switch lever which controls the multiple arcs was moved with a quick, sure motion from the off position to the first additional arc position, and the second arc is ignited. If the lever is moved slowly, arcing will occur across the switch contacts.
3. Once the second arc is established it may be necessary to readjust the current. The multiple arc is now operational, and at least a five minute warm up period should precede the taking of data.

Data Reduction

Figure 36 is a sample data sheet. All pieces of data were recorded on the data sheet for each run except the multiple arc outlet water temperature which was recorded continuously on the strip chart recorder.

The calibration curve for the main arc voltage meter is given in Figure 37. A check of the mutliple arc voltmeters showed them to be sufficiently accurate, and no correction was applied to their readings. The calibration of the point recorder showed an error of about 2°F. Since a temperature difference is used in the calculations no correction was applied to the readings of the point recorder. However, it was necessary to add the appropriate correction to the

DATE 9/3/64 GAS A SIGNED Edward Poblano

	1	2	3	4
TEMPERATURES, °F				
Water In	80	80	80	80
Nozzle Out	112	115	123	125
Gas In	75	75	75	75
MA Out	127	132	119	127
BTU/min	465	520	433	500
FLOW RATES, Δ P				
Main Nozzle	10.3	10.6	10.1	10.4
MA	17.1	17.6	16.4	16.2
Stab. Gas	14.2	10	5	2.5
ELECTRICAL				
Amperes	175	180	175	180
Main Arc Volts	14	13.5	26	27
MA Volts	61	60	30	34
Power, Kw	13.27	13.36	9.80	10.98
PRESSURES, psig				
Gas In	25	25	25	25
Test Chamber	.7	.7	.7	.7

Figure 36 Sample Data Sheet

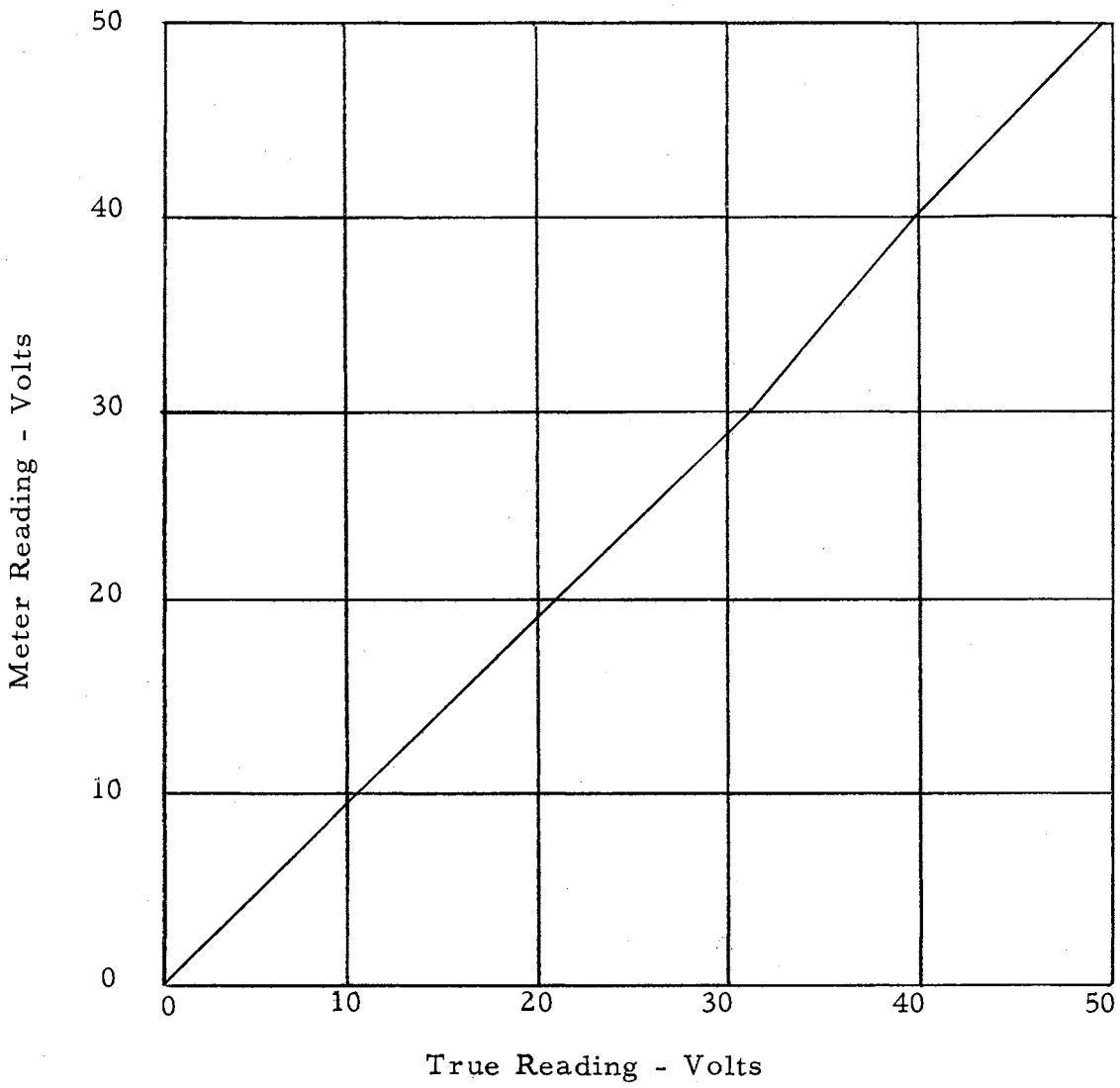

Figure 37 Primary Arc Voltmeter Calibration

strip chart temperatures. This has been done for the data of Figure 36. The calibration curves for the water flow meters were shown in Figures 33 and 34.

The data reduction process is not involved and relies primarily upon an energy balance. The data of Run No. 9 3 F2 will be used for a sample calculation.

The total power input is the product of the current and the total arc voltage.

$$180(14.3+60) = 13.36 \text{ kilowatts or } 760 \text{ BTU/min} \qquad (65)$$

The temperature rise of the main chamber cooling water is

$$115 - 80 = 35°F \qquad (66)$$

The deflection of 10.6 inches on the main chamber manometer corresponds to a flow rate of 3.38 lbs. H_2O per min. by Figure 33. Thus, the energy lost to the cooling water is

$$35 \times 3.38 = 118 \text{ BTU/min.} \qquad (67)$$

Similarly the energy lost from the multiple arc is

$$7.73 \text{ lbs/min } (132-80) = 402 \text{ BTU/min.} \qquad (68)$$

The total energy lost per minute is

$$118 + 402 = 520 \text{ BTU/min.} \qquad (69)$$

The energy retained by the gas stream in a unit time is

$$760 - 520 = 240 \text{ BTU/min.} \qquad (70)$$

The efficiency is

$$\frac{240}{760} = 31.6 \text{ per cent.} \qquad (71)$$

The gas flow rate is found from Figure 35 to be . 1098 lb/min. Hence, the gas enthalpy is

$$\frac{240}{.1098} = 2190 \ \frac{BTU}{lb} \tag{72}$$

CHAPTER VI

DISCUSSION OF RESULTS

The multiple arc was evaluated by comparing its performance with the performance of the single arc. Of particular interest are the gas flow rate, efficiency of energy conversion, gas enthalpy and total power input. In general, the input power was assumed to be the independent variable.

Data were collected for the single arc operating at flow rates ranging from .0346 to .127 lb per min argon, and currents ranging from 100 to 400 amperes. The data were plotted and smoothed so that values of efficiency, power input and gas enthalpy could be obtained at flow rates of .0346, .0546, .0774, .109, and .130 lb/min. These were the flow rates used for subsequent multiple arc studies. These data are presented in the appendix.

Figure 38 shows that for the single arc in general the efficiency of energy conversion increases with increasing power input. However, there appears to be a minimum efficiency with the lower flow rates. Also the figure shows that the efficiency is in general greater at the higher flow rates.

Figure 39 shows that the gas enthalpy increases with increasing power input but decreasing flow rate.

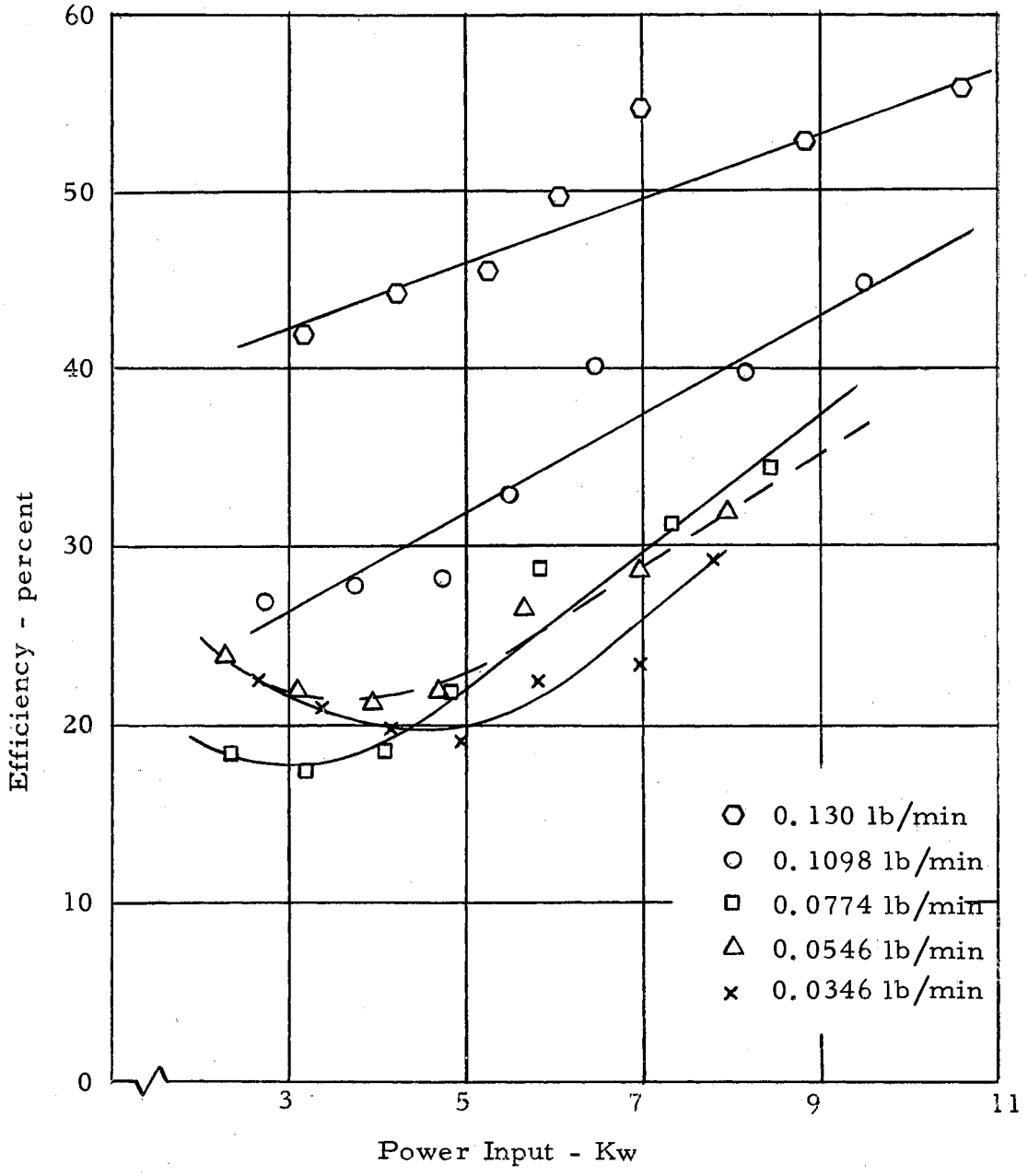

Figure 38 Efficiency Versus Power Input for Mono Arc

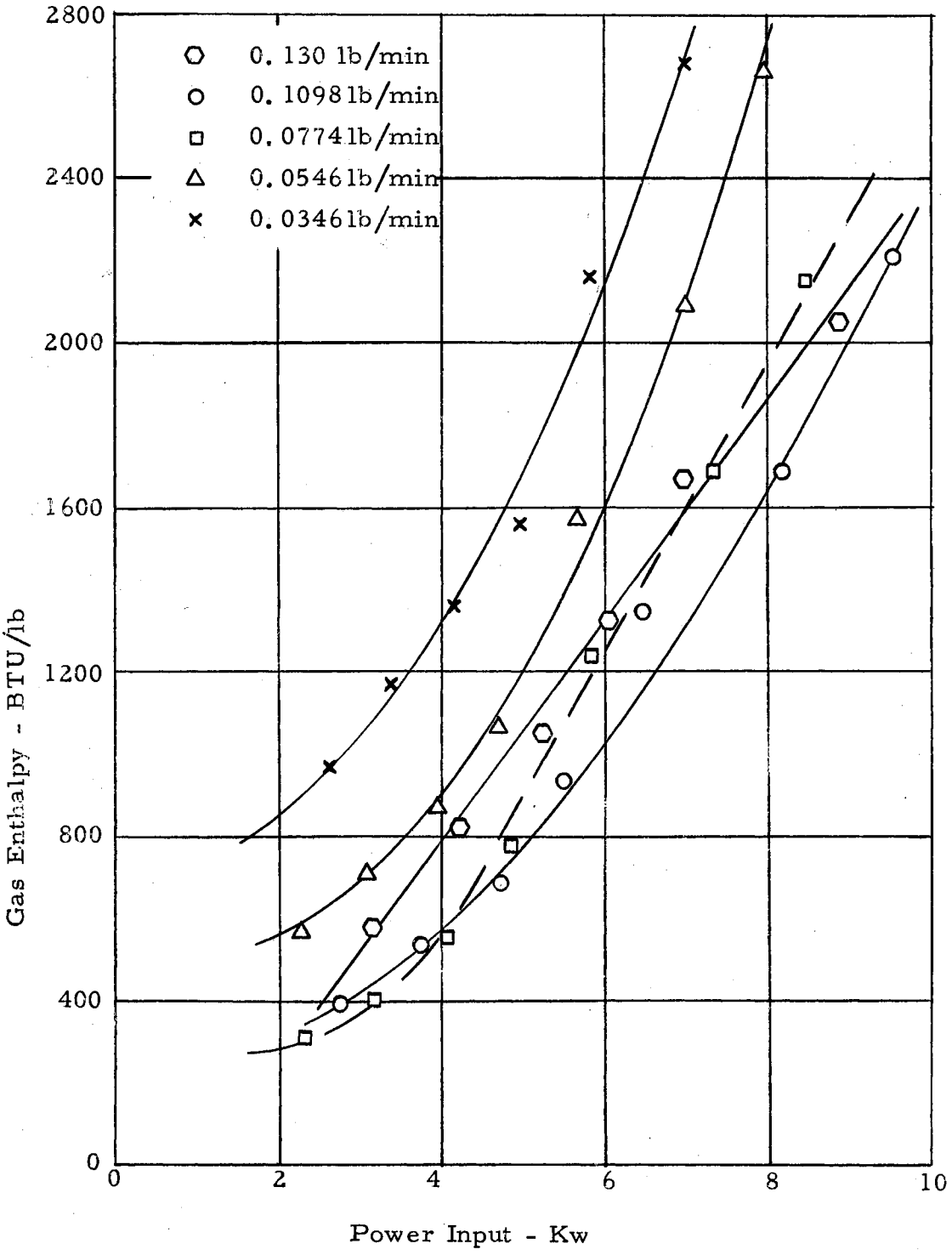

Figure 39 Enthalpy Versus Power Input for the Mono Arc

The general trends indicated by Figures 38 and 39 might be expected with the multiple arc configuration as well. However, a plot of the efficiency as a function of power input, Figure 40 reveals a different trend with the efficiency decreasing with increasing power input. In this figure the data points have been grouped according to the mode of operation, and the flow rates have not been taken into account. It is seen that in general the R1 configuration gives the highest efficiency, the R2 mode I gives efficiencies comparable to R1, and the efficiency of R2 mode II is the poorest. By definition, mode I operation occurs when the total arc potential is unevenly distributed between the two arcs; that is, when the voltage drop of the second arc is three or more times that of the first. Mode II occurs when the total arc potential is approximately equally divided between the two arcs. The data reveal that R1 configuration always operated mode I. The transition from mode I to mode II is not clearly defined by Figure 40 but appears to occur for power input levels between 8 and 14 kilowatts.

The existence of the two modes of operation is confirmed by a plot of the total arc potential as a function of power input, Figure 41 The cone spacer R1 operated with the largest potential difference while the straight spacer, R2, mode I has nearly as high a potential drop. Also note from the data points the relatively stable operation that is obtained with both these configurations. On the other hand, mode II appears much less stable, and the total arc potential is not

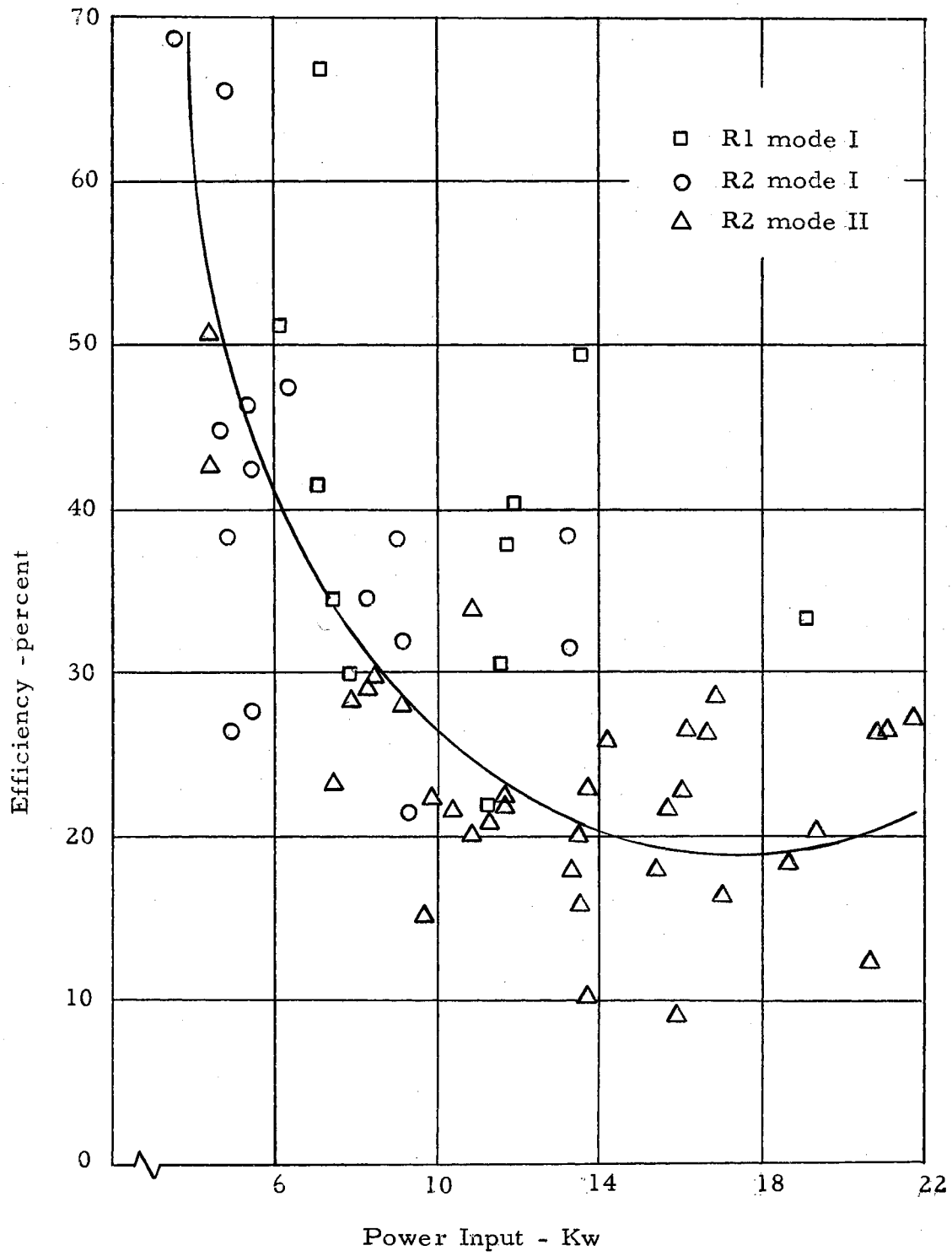

Figure 40 Efficiency Versus Power Input for Multiple Arc R1 and R2

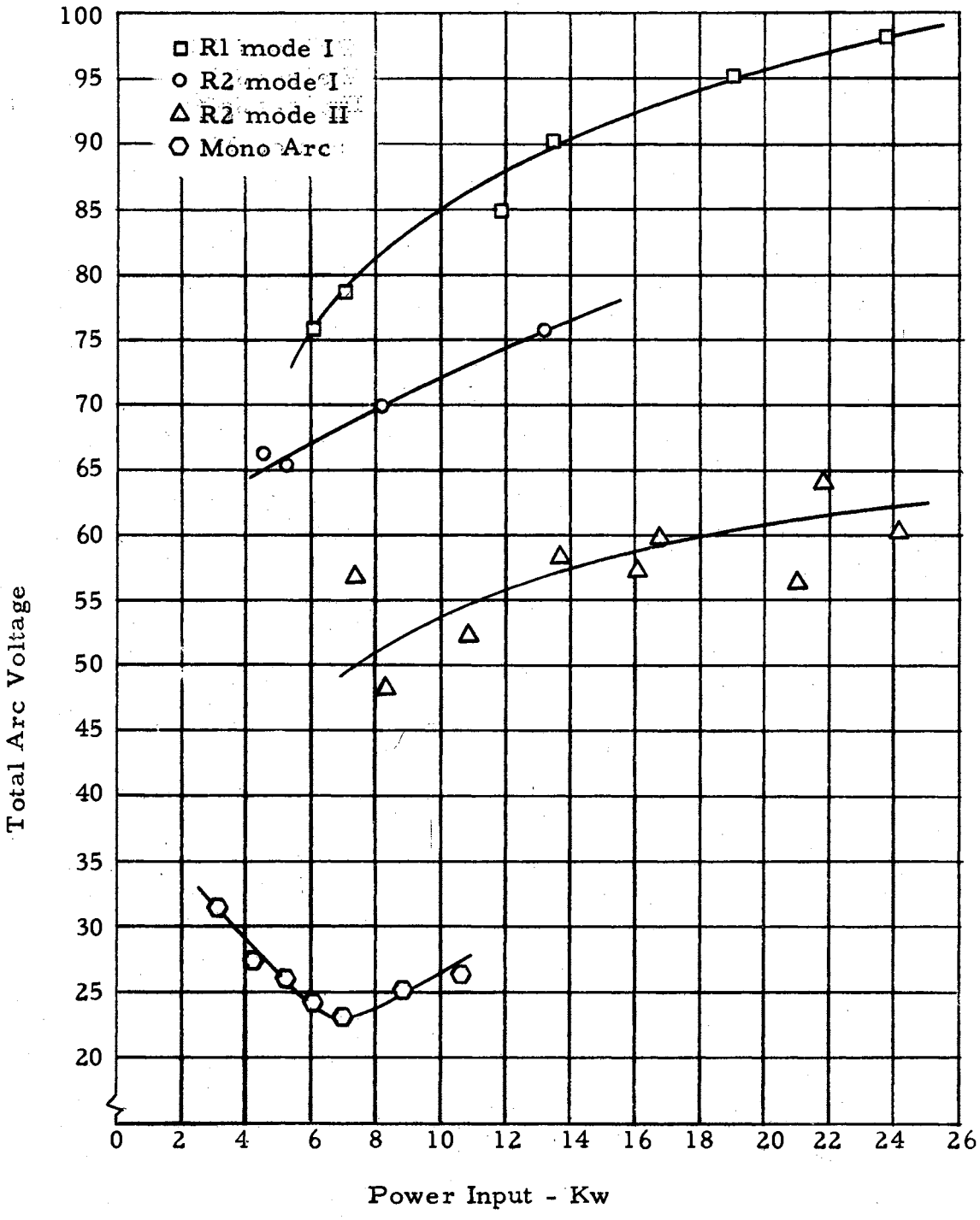

Figure 41 Total Arc Voltage Versus Power Input for Argon Flow Rate of 0.130 lb/min

nearly as high. In all cases, however, the total arc potential of the multiple arc is greater than the potential drop of the single arc. For Figure 41 only the data points for an argon flow rate of 0.130 lb/min were used. Figure 42 shows the effect of gas flow rate on the total arc voltage for the R1 configuration. Comparison of the two Figures 41 and 42 shows that the type of multiple arc configuration has a greater affect on the total arc voltage than the gas flow rate.

The operating characteristics of the multiple arc and the single arc can be more readily distinguished by plots of efficiency versus power input for a given gas flow rate. These plots are Figures 43, 44, 45 and 46. Here the two modes of operation are seen to overlap. At certain power levels both modes may be possible depending on how a given power level is reached. Thus, if the power is increased, mode I will exist in the transition region while if the power is decreased from a higher value, mode II will prevail into the transition region. The transition region exist from about 8 to 14 KW input power and is wider for larger gas flow rates. For the lowest gas flow rate the transition region appears very small and may not exist at all. In the transition region operation in mode I is more efficient (and hence the gas enthalpy is greater) than mode II operation. This is very nicely illustrated by data points E4 and E5, which were taken consecutively at almost identical conditions of gas flow (.130 lb/min) and current. E5 is mode I with 34.7 per cent efficiency and 1240 BTU per lb of gas, while E4 is mode II with only 23.3 per cent efficiency and 749 BTU per lb. Also note that a low power levels, the multiple arc is more

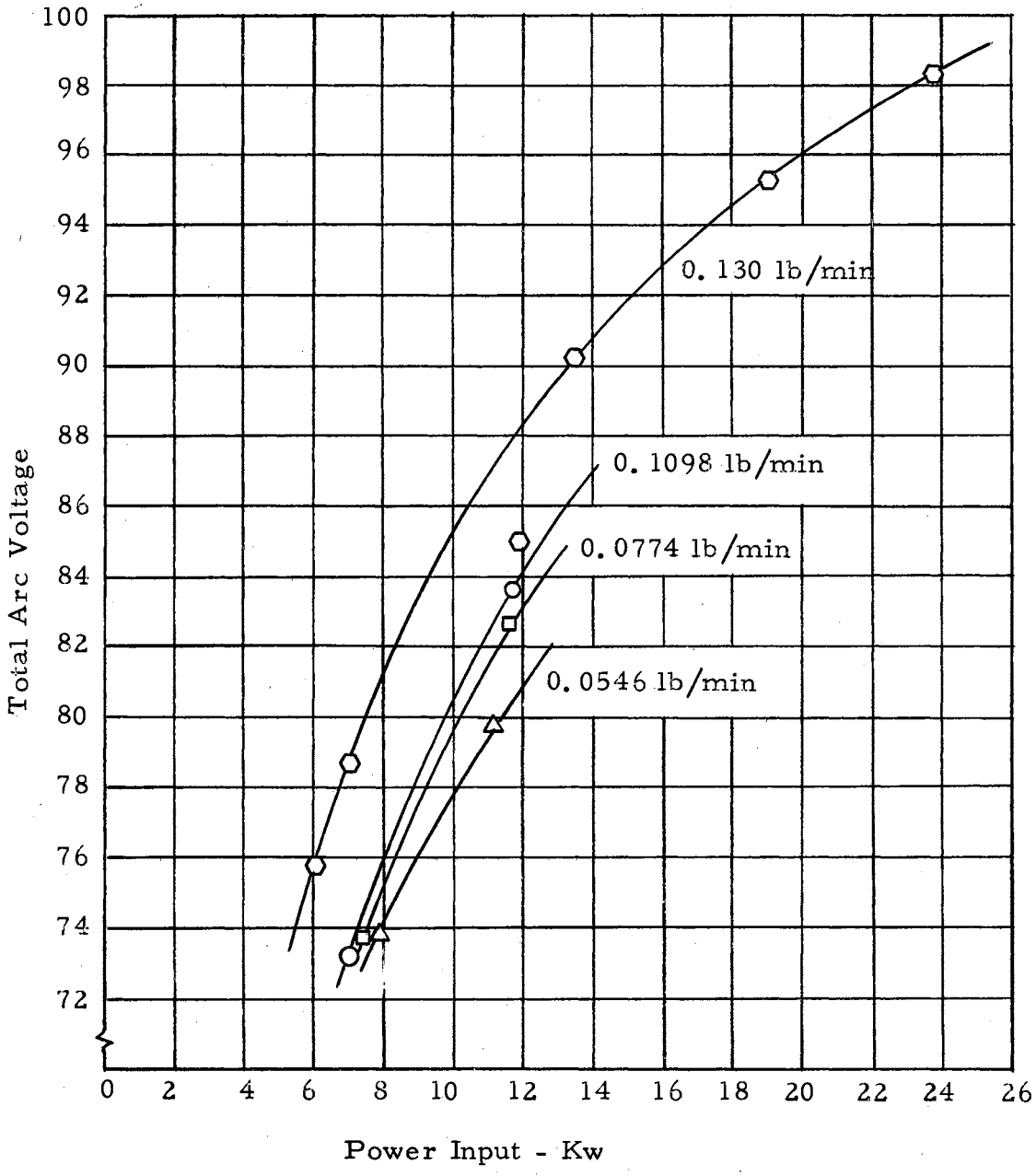

Figure 42 Effect of Argon Flow Rate on Total Arc Voltage

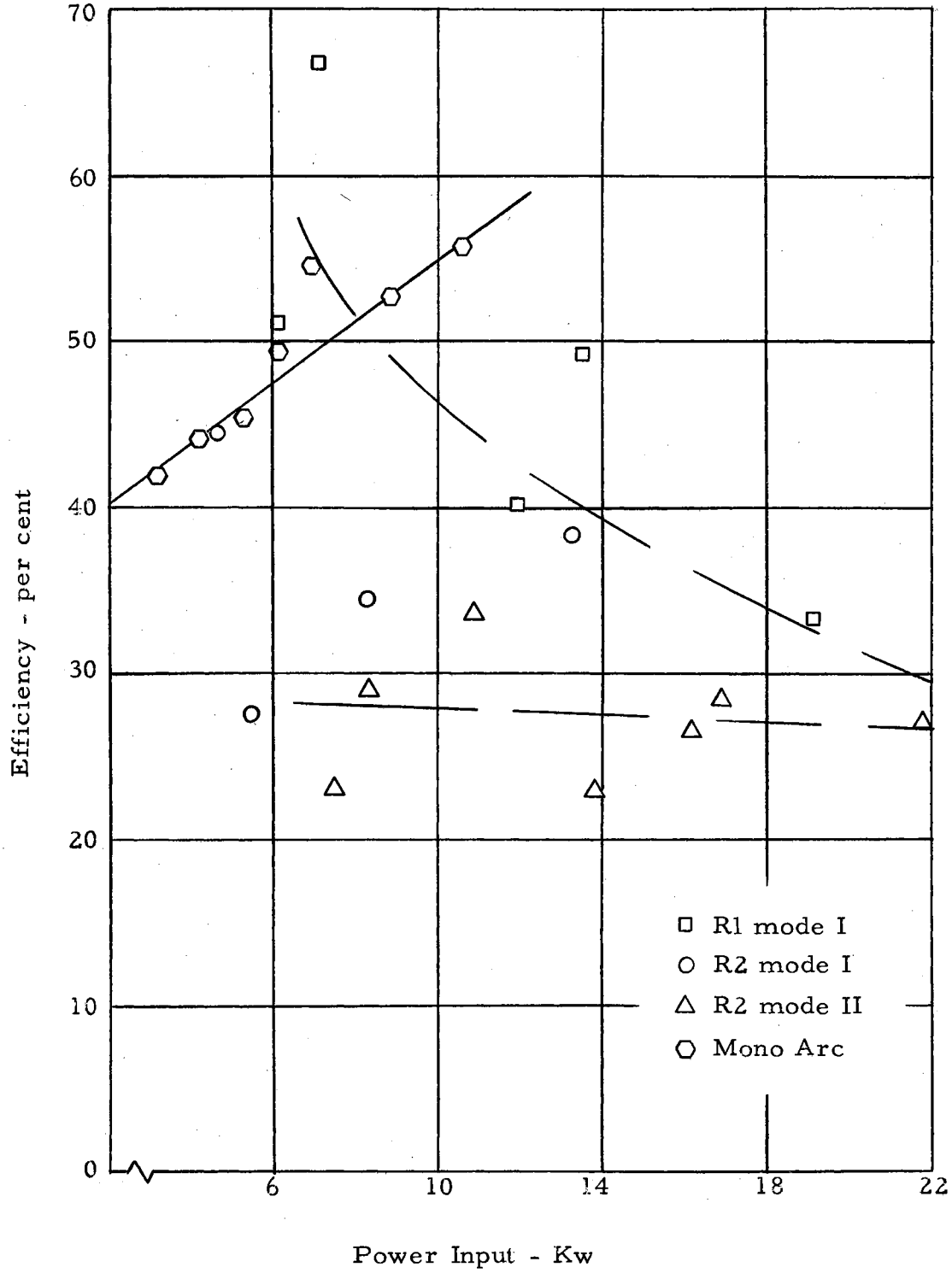

Figure 43 Efficiency Versus Power Input
0.130 lb/min Argon

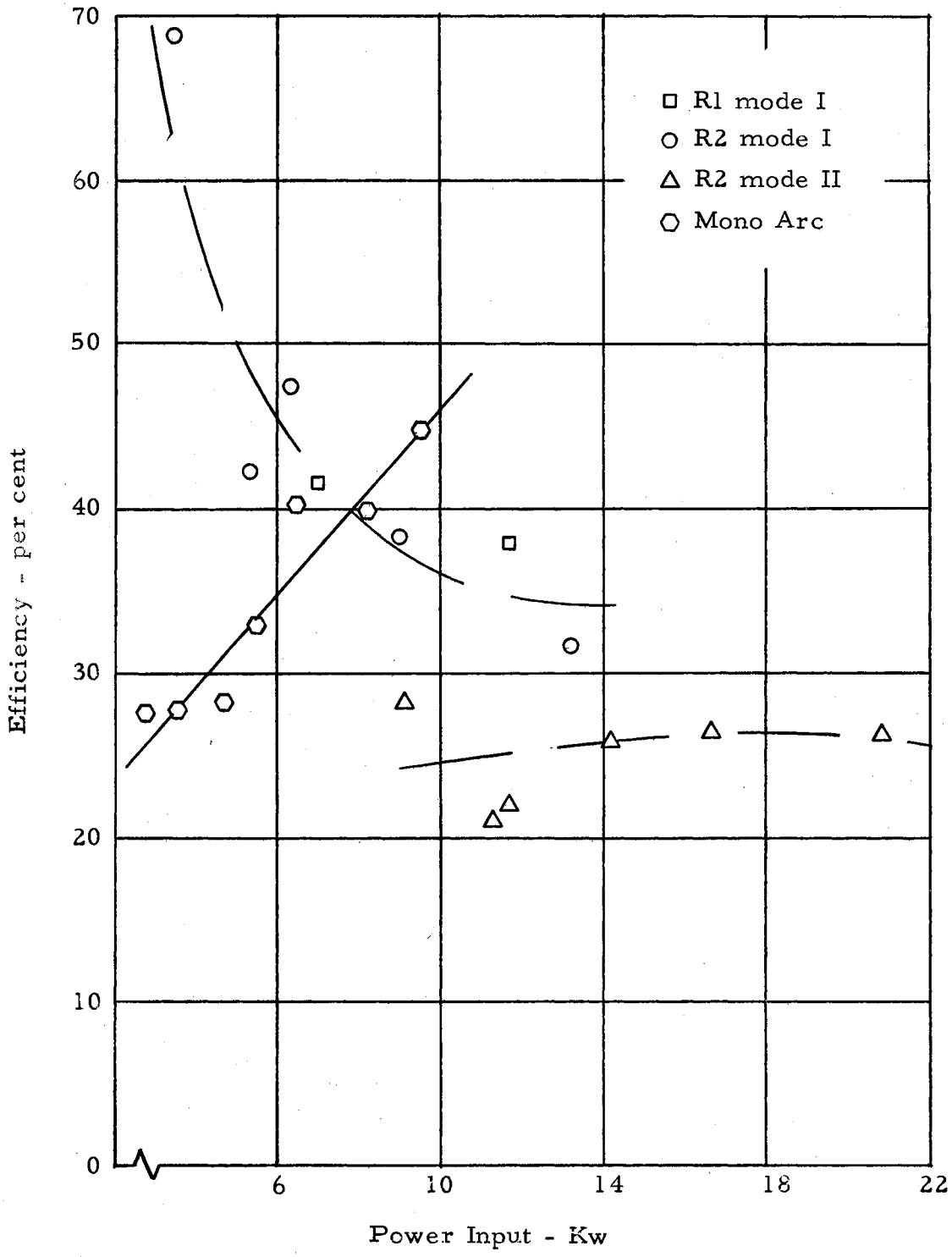

Figure 44 Efficiency Versus Power Input
0.1098 lb/min Argon

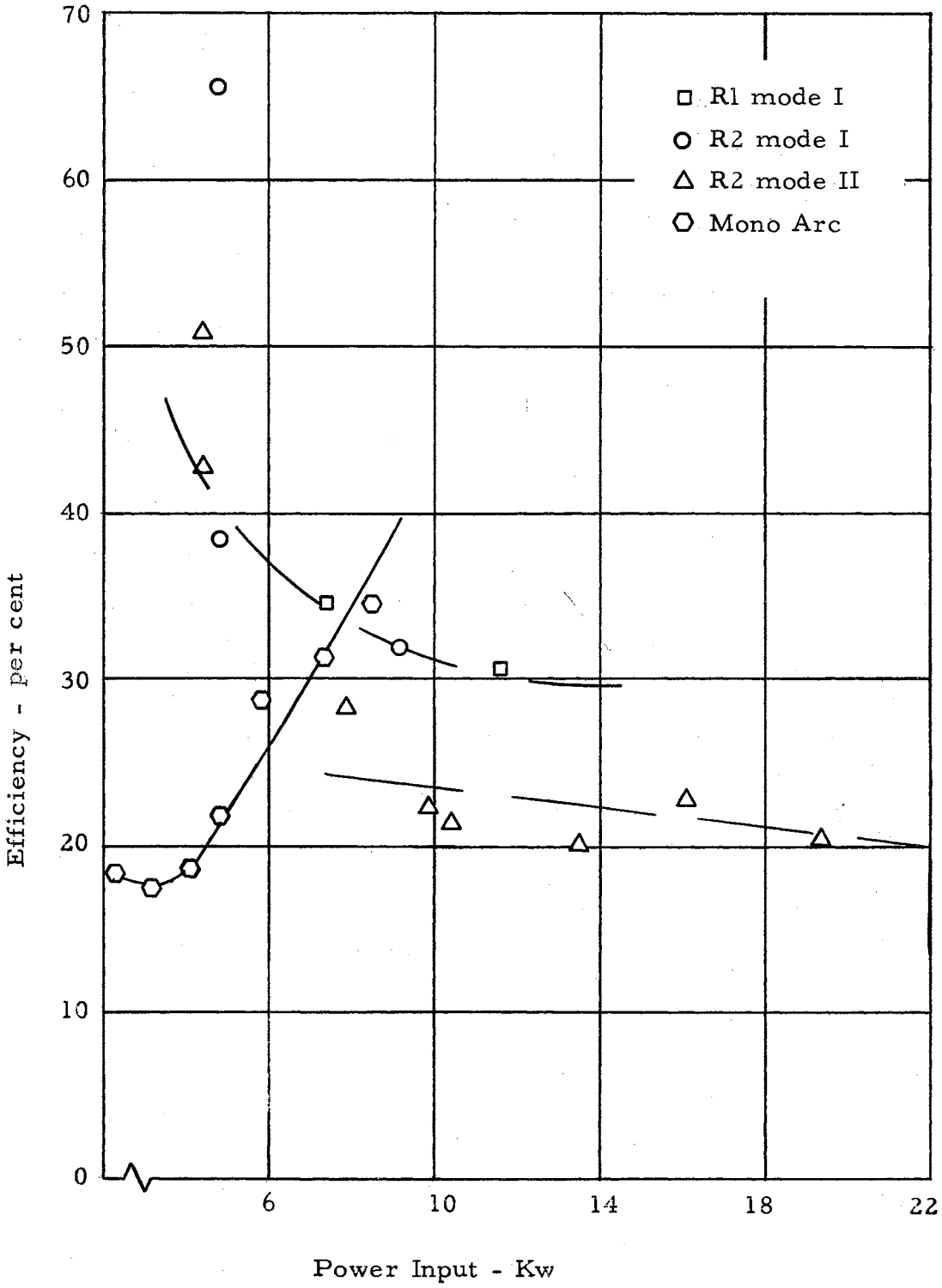

Figure 45 Efficiency Versus Power Input
0.0774 lb/min Argon

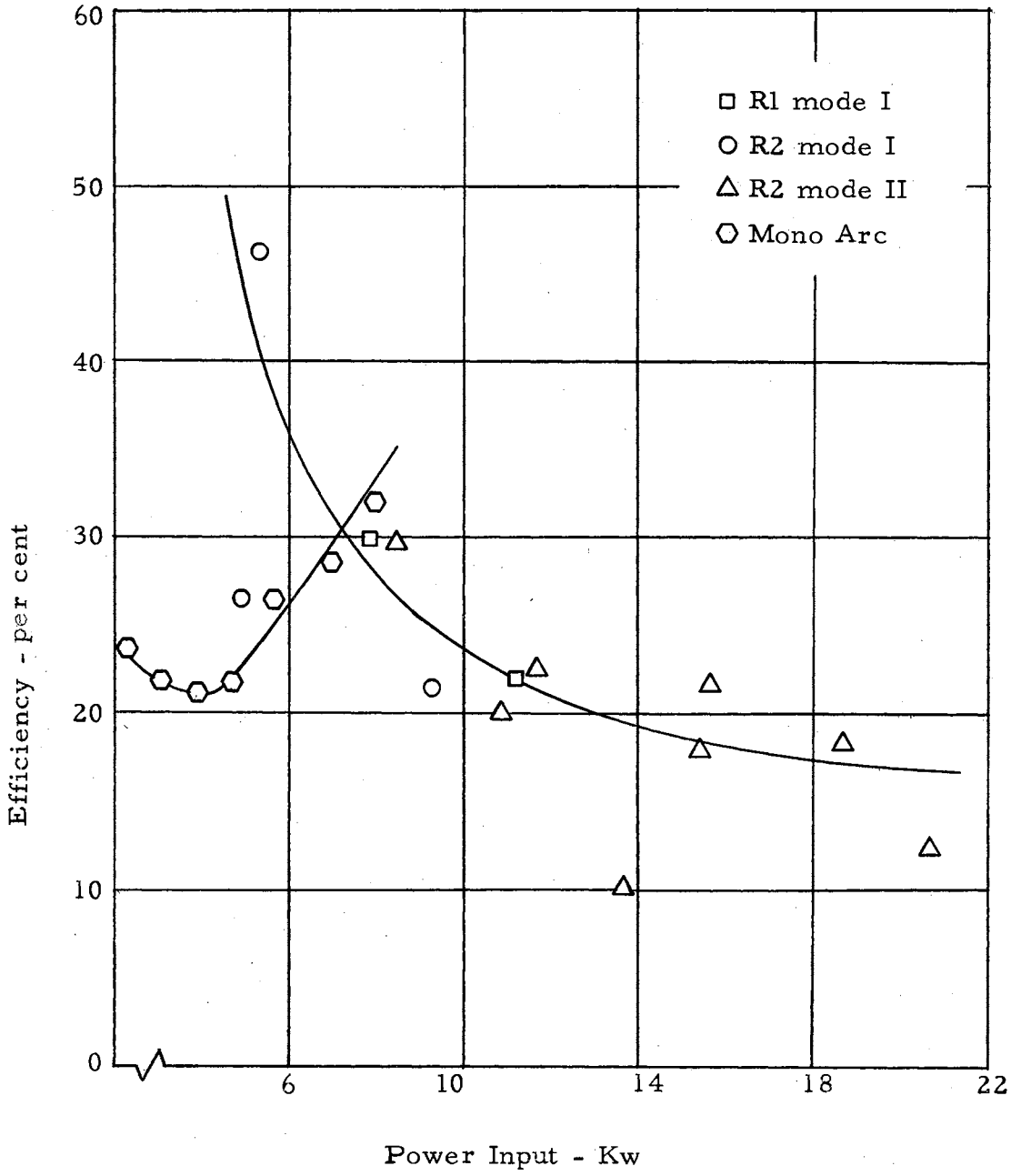

Figure 46 Efficiency Versus Power Input
0.0546 lb/min Argon

efficient than the single arc, and the cross over point is about 7.3 KW except for the highest gas flow rate where it is about 6KW.

Figures 47, 48, 49, and 50 show the gas enthalpy as a function of total power input at various gas flow rates. Again the two regimes of operation can be noted. Of particular interest is the fact that within the limits of the power supply, the gas enthalpy can be increased by means of the multiple arc, even though the operation is mode II. However, at intermediate power levels the single arc produces the highest gas enthalpies, and the multiple arc would not be used. At power levels less than about 7 KW input, the multiple arc again becomes the more effective in obtaining high gas enthalpies. For the highest gas flow rate, the single arc produces the highest gas enthalpies except for the highest power inputs which are beyond the capabilities of the single arc. In general then, the single arc is the best for intermediate power levels, but the double arc produces the highest gas enthalpies at low and high power input levels. It is also obvious from the figures that mode I operation yields a greater gas enthalpy at the same power input than mode II does.

Figure 51 shows the current required for a given input power. As would be expected the R1 configuration requires the least current with R2 mode I nearly as effective, while the single arc requires the most for the same input power.

Of more practical interest is the gas enthalpy which may be expected from a given current input. This effect is illustrated in Figure 52. For a given current the R1 configuration, with R2 mode I

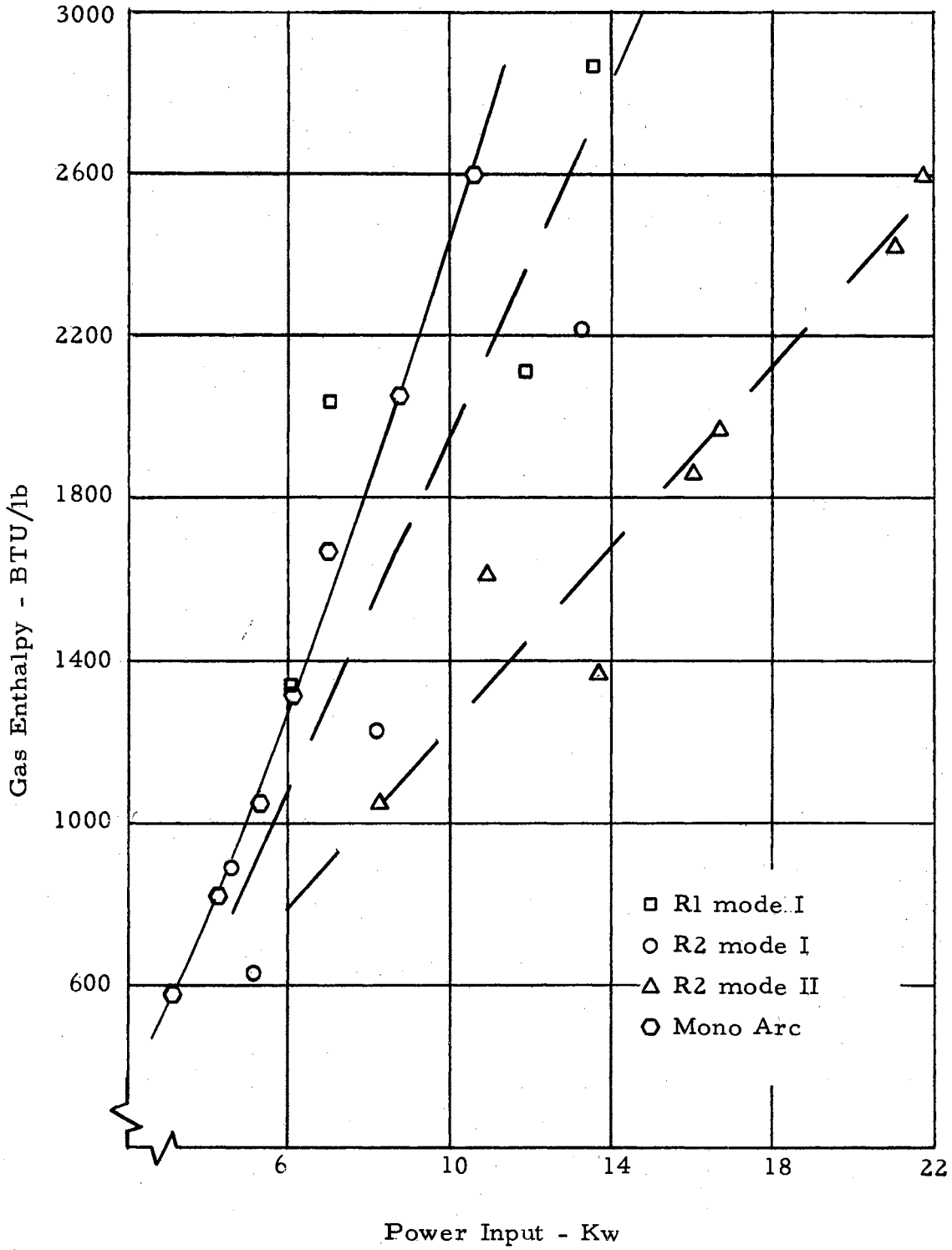

Figure 47 Enthalpy Versus Power Input
0.130 lb/min Argon

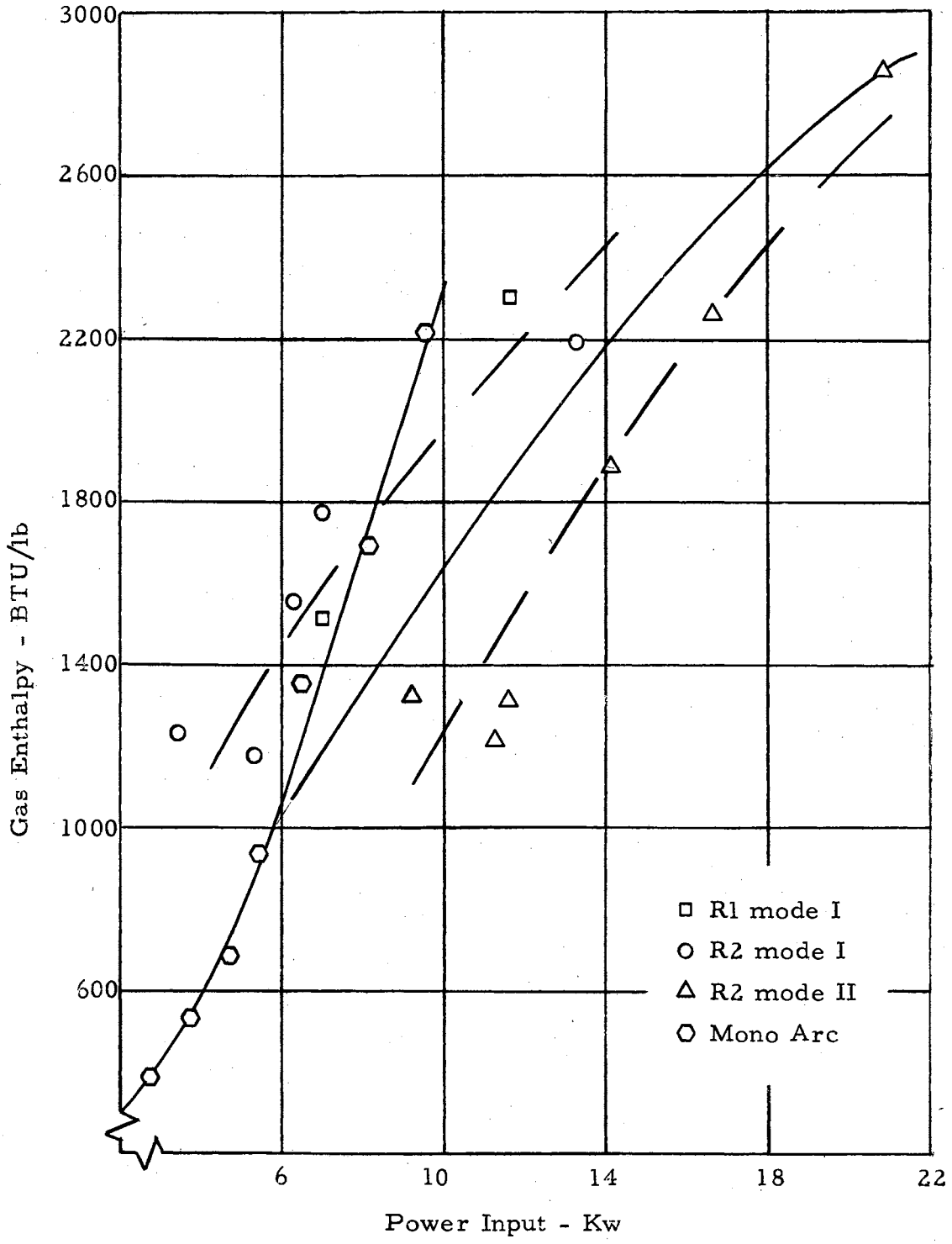

Figure 48 Enthalpy Versus Power Input
0.1098 lb/min Argon

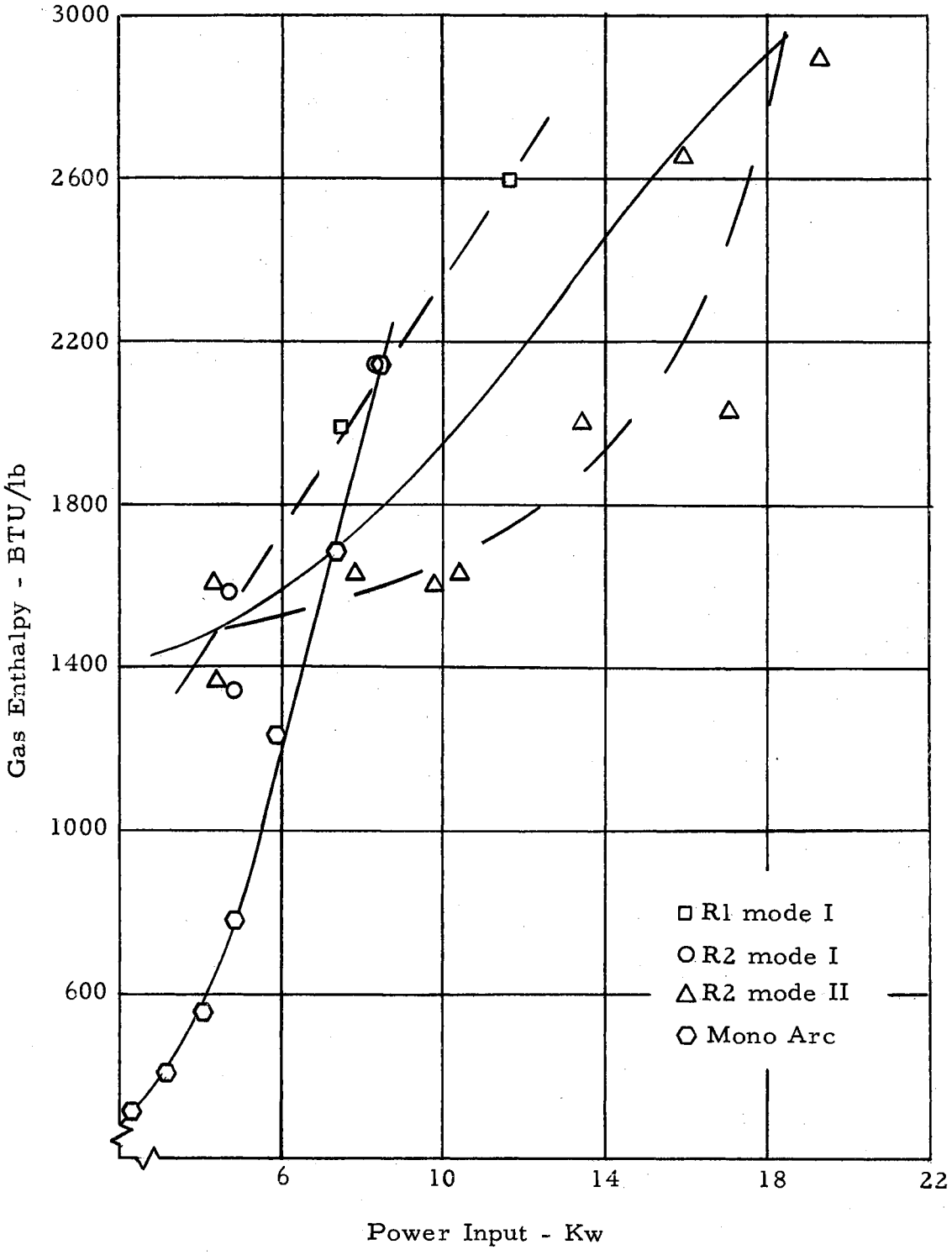

Figure 49 Enthalpy Versus Power Input
0.0774 lb/min Argon

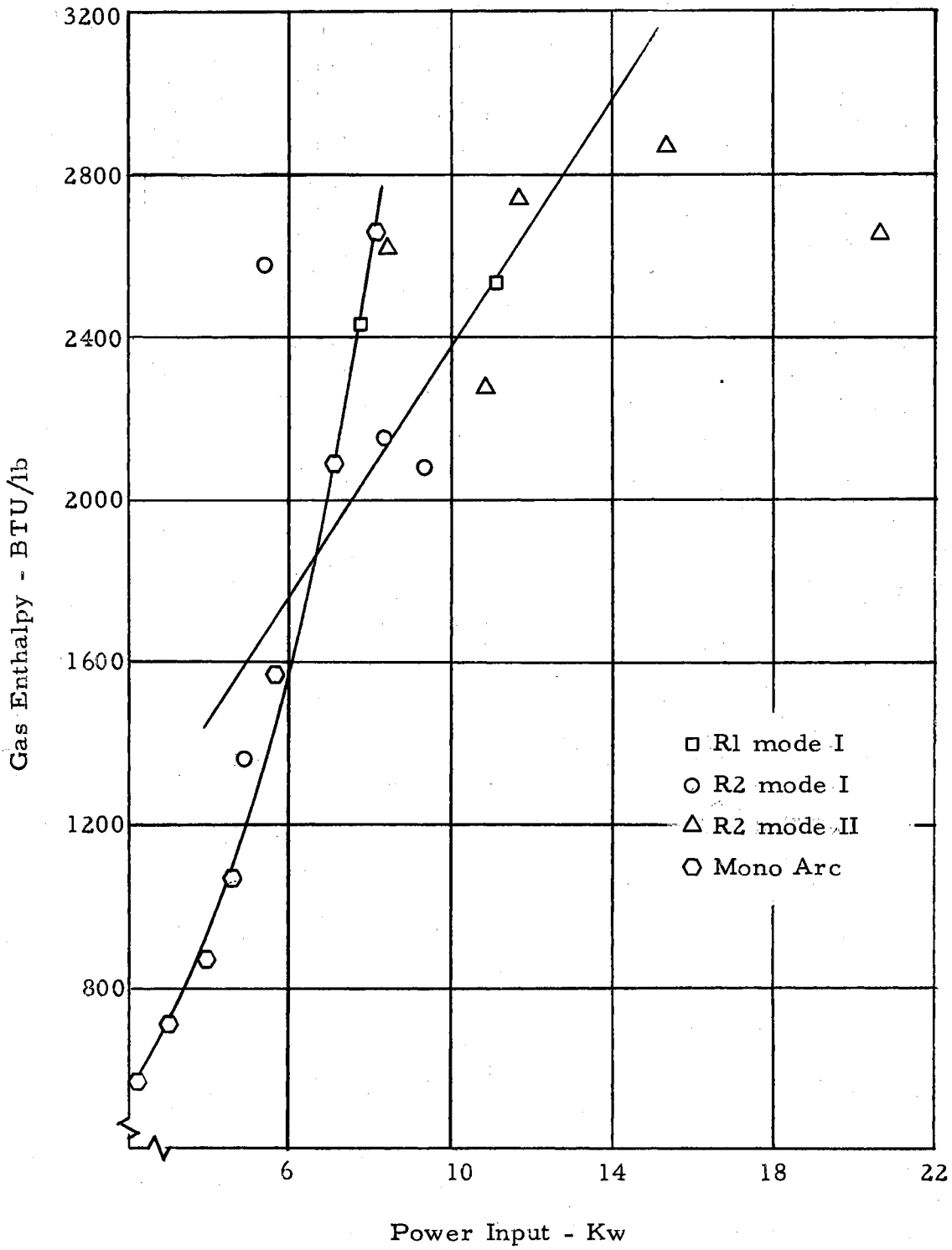

Figure 50 Enthalpy Versus Power Input
0.0546 lb/min Argon

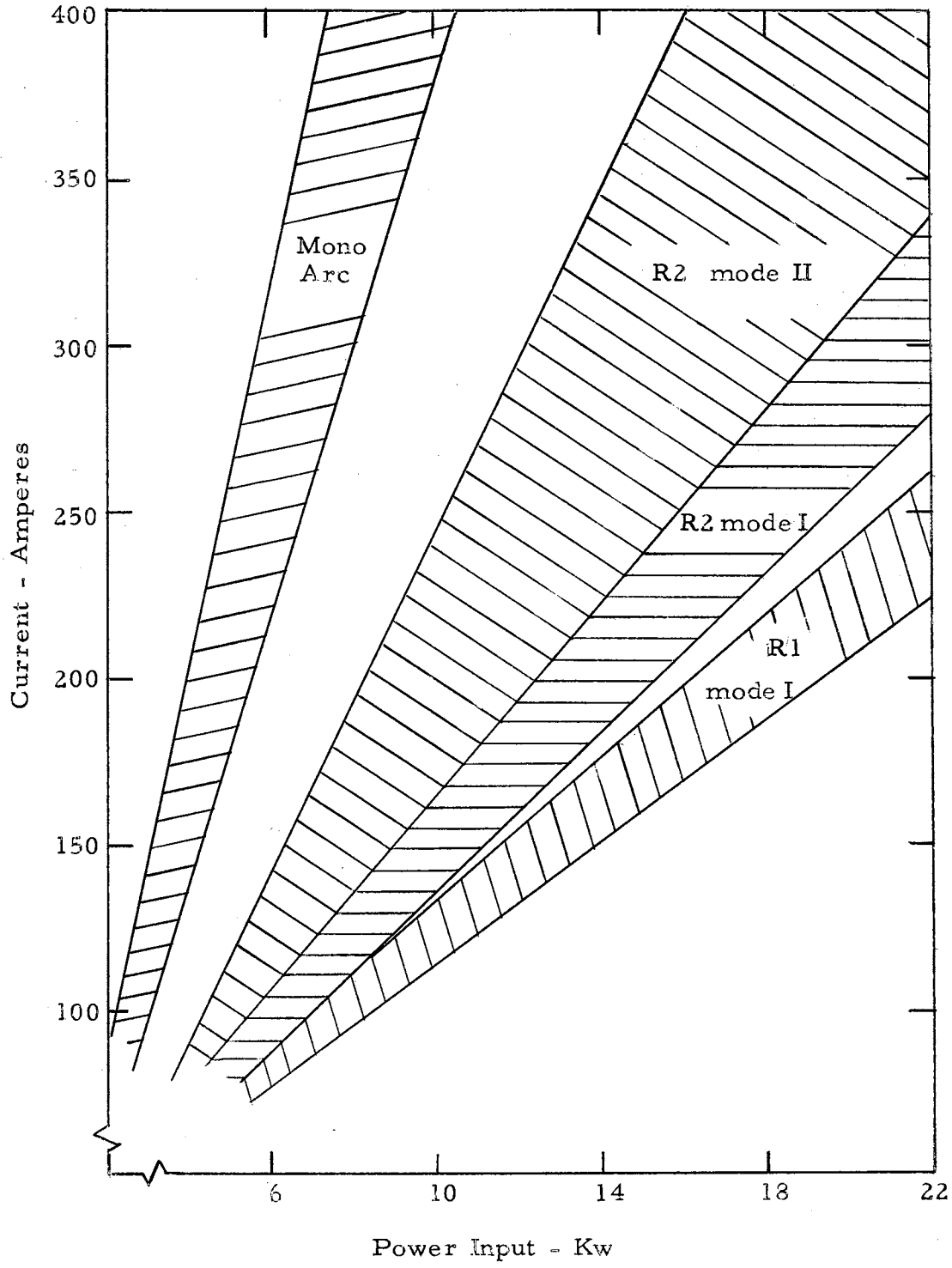

Figure 51 Regions of Required Current for a Given Input Power

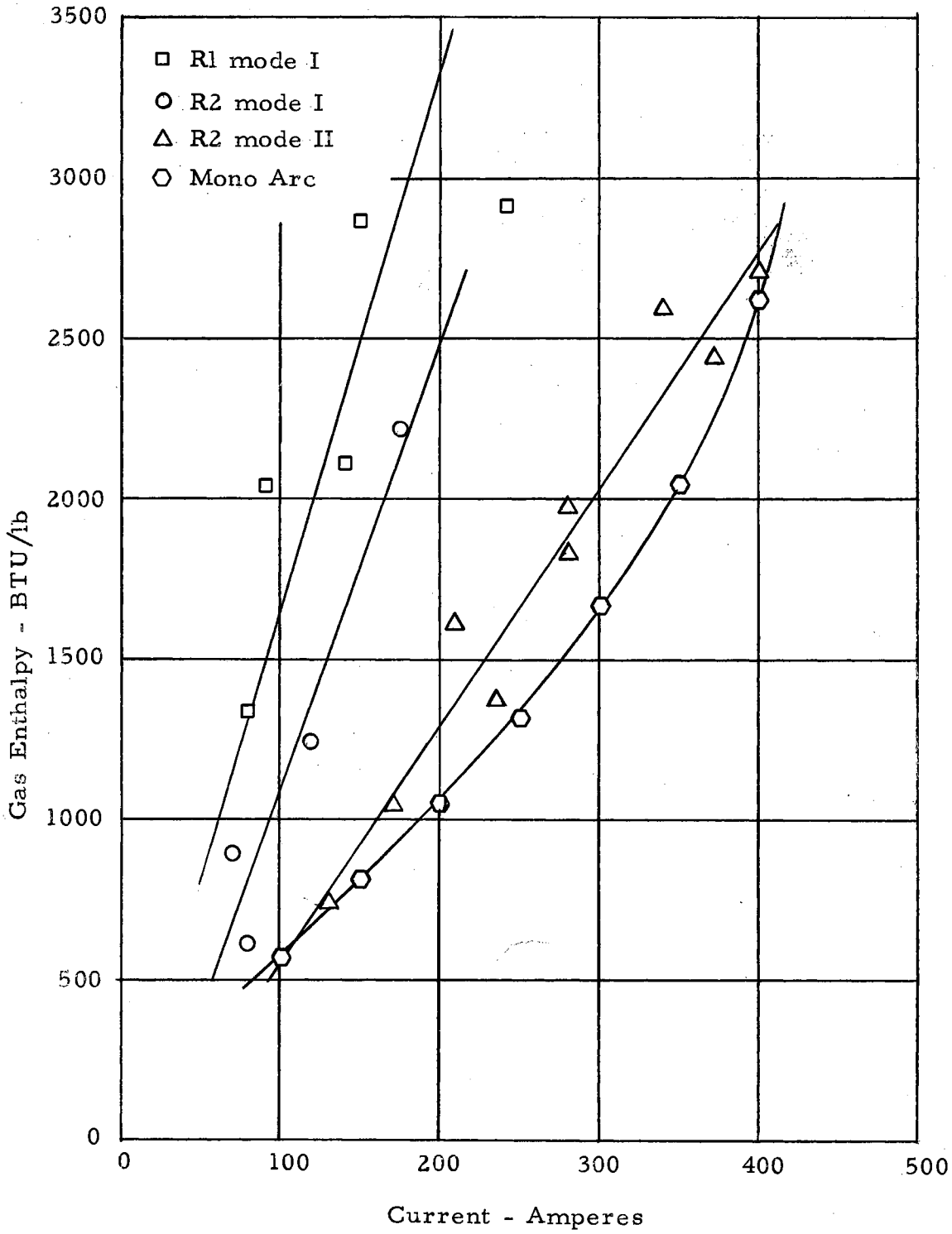

Figure 52 Gas Enthalpy for a Given Current
0.130 lb/min Argon

nearly as effective, produces the highest gas enthalpy, while the single arc gives the lowest gas enthalpy. For example at 200 amperes, the gas enthalpy with the single arc would be about 730BTU/lb on the average while a value of 3000 BTU/lb might be expected with the cone spacer configuration R1.

CHAPTER VII

CONCLUSIONS AND RECOMMENDANTIONS

Conclusions

It was the object of this research effort to build a multiple arc plasma jet for the purpose of increasing the enthalpy of the jet gas over that attainable from a single arc when the power supply has limited current capacity but not potential. The final multiple arc design was capable of fulfilling this objective. In comparison with the single arc the following conclusion can be drawn regarding the multiple arc.

1. Within the limits of the power supply the maximum gas enthalpy can be increased by as much as 50 per cent.

2. There is an intermediate range from 7 to 10 KW input power for which the mono-arc produces higher enthalpy.

3. For power levels less than 7 KW the multiple arc produces higher gas enthalpy, and at very low powers the enthalpy from the MA may be twice as great as that from a single arc.

4. For a fixed arc current the multiple arc is capable of producing four times the gas enthalpy possible from a single arc. Thus, the multiple arc is much more effective for producing a high energy gas jet when the current supply is seriously limited, i.e.,

below about 250 amperes.

5. For the multiple arc the efficiency of energy conversion decreases with increasing power input. This is contrary to the mono-arc efficiency vs. power input curve which has a positive slope.

The multiple arc has the following characteristics with respect to gas flow and power input.

1. The efficiency decreases as the current and total power are increases.

2. The gas enthalpy increases as the total power input increases. In the range of the experiments the efficiency is dropping more slowly than the rate at which the power input is increasing.

3. The efficiency increases with increasing gas flow rate at fixed input power. The highest efficiency recorded is 51.3 per cent.

4. The gas enthalpy increases with decreasing mass flow rates.

5. The total arc voltage increases with increasing power and fixed flow rate.

6. The total arc voltage increases slightly with increasing gas flow rate.

The multiple arc has two modes of operation. Mode I is characterised by an unequal distribution of potential between the two arcs. The second arc voltage is three or more times that of the first arc. The total potential is almost equally divided between the first and second arc during mode II operations, and the voltage drop is slightly larger across the first arc. Mode I is more efficient,

results in higher gas enthalpies, and operates more stably than mode II.

Recommendations

The R1 configuration described in Chapter IV showed the best efficiency and resulted in the highest gas enthalpy of any design tested in this work. The conical spacer was made of steel. Although a cooling water passage was provided, it is believed that the poor thermal conductivity of the steel prevented the surface of this component from being adequately cooled and as a result it failed prematurely. It is recommended that this component be fabricated of copper and R1 configuration retested. In general, it is recommended that multiple arcs of the R1 configuration be developed and tested since this appears to be the most promising design to date.

The appearance of the arc number and the concept of arc strength discussed in Chapter II are both interesting and promising. It is particularly recommended that further investigations both experimental and analytic be undertaken to learn more about the properties of the arc number. Experimental work should be conducted to determine what factors influence the arc number besides the gas properties.

BIBLIOGRAPHY

1. Hellund, E. J., The Plasma State, Reinhold Publishing Corp., New York, 1961.

2. Penning, F. M., Electrical Discharges in Gas, The MacMillan Co., New York, 1957.

3. Loeb, L. B., Basic Processes of Gaseous Electronics, University of California Press, Berkeley, 1960.

4. Cobine, J. D., Gaseous Conductors, McGraw-Hill, New York, 1941.

5. Von Engle, A., Ionized Gases, Clarendon Press, Oxford, 1955.

6. Von Engle, A. and Steenback, M., Elektrische Gasentladungen, Springer Verlag, Berlin, 1932.

7. Meek, J. M. and Craggs, J. D., Electrical Breakdown of Gases, Clarendon Press, Oxford, 1953.

8. Thomson, Sir J. J. and Thomson, G. P., Conduction of Electricity Through Gases, 3rd Ed., Vols. I and II, University Press, Cambridge, 1936.

9. Townsend, J. S., Electricity in Gases, Oxford University Press, 1914.

10. Handbuch der Physik, Vols. 21 and 22, Springer Verlag, Heidelberg, 1956.

11. Somerville, J. M., The Electric Arc, John Wiley and Sons, New York, 1959.

12. Elenbaas, W., "Ontladingen in Kwikdamp van Hoogan Druk," Ingenier 50, 1935.

13. Higham, J. B. and Meek, J. M., "Voltage Gradients in Long Gaseous Spark Channels," Proc. Phys. Soc. B63, 1950.

14. Craig, R. D. and Craggs, J. D., "Some Properties of Hydrogen Spark Channels," Proc. Phys. Soc. B66, 1953.

15. Ayrton, Hertha, "The Electric Arc," The Electrician Series, D. Van Nostrand Co., New York.

16. Haworth, D. R., "Development of a Plasma Facility and Spectrographic Determination of Plasma Temperature," (unpub. Ph. D. dissertation, Oklahoma State University, 1961).

17. Jovanovic, M. K. and Pohlmann, E., "The Development of a Plasma Facility," Oklahoma State University, Final Report to National Science Foundation on Grant No. 10161, 1961.

18. Ramberg, W., "Über den Mechanismus des Elektrischen Lichtbogens," Ann. d. Physik 12, 1932.

19. Richardson, O. W., "On the Negative Radiation from Hot Platinum," Cambridge Phil. Soc. Proc. 11, 1901.

20. Compton, K. T., "On the Theory of the Mercury Arc," Phys. Rev. 37, 1931.

21. Weizel, W. and Thouret, W., "Lightbogen mit und ohne Brennfleck," Z. Phys. 131, 1952.

22. Langevin, P., "Une Formule Fondamentale de Theorie Cinetique," Ann. de Chim. et de Phy. 5, 1905.

23. Loeb, L. B., The Kinetic Theory of Gases, McGraw-Hill, New York, 1934.

24. Brown, Sanborn C., Basic Data of Plasma Physics, published jointly by The Technology Press of The Massachusetts Institute of Technology and John Wiley and Sons, New York, 1959.

25. Morris, Alan D., "Analysis of the Direct Current Arc," Conference on Extremely High Temperatures, (H. Fischer and L. C. Mansur, Editors), John Wiley and Sons, New York, 1958.

26. Edels, H., "Properties and Theory of the Electric Arc," Institute of Electrical Engineers 108A, 1961.

27. Fletcher, E. C., "Experimental Investigation of the Variation in Arc Voltage with Electrode Separation," Oklahoma State University (Internal Report), 1963.

28. Palmer, G. M. and Paris, F. L., Jr., "An Experimental Study of the Operating Characteristics and Electrode Heat Transfer of a Direct Current Electric Arc in a Pressurized Argon Environment," Purdue Research Foundation Research Project No. 1717, Report No. A-59-10, August 1959.

29. Gibbs, E. F., "A Fundamental Study of the Tungsten Arc," Metal Progress 78, 1960.

30. Brode, R. B., "The Absorption Coefficient for Slow Electrons in Mercury Vapor," Proc. Roy. Soc. A125, 1929.

31. Compton, K. T. and Langmuir, I., "Electrical Discharges in Gases. Part I - Survey of Fundamental Processes," Rev. Mod. Phys. 2, 1930.

32. Nottingham, W. B., "A New Equation for the Static Characteristic of the Normal Electric Arc," A. I. E. E. Trans. 42, 1923.

33. Eddy, W. N., "Length-Voltage-Current-Pressure Characteristics of Normal Arcs for Different Electrode Materials," Gen. Elect. Rev. 25, 1922.

34. Grotrian, W., "Der Gleichstrom-Lichtbogen grosser Bogenlange," Ann. d. Physik 47, 1915.

35. Seeliger, R., Einfuhrung in den Physik der Gasentladungen, Barth, 2nd Edition, Leipzig, 1934.

36. Suits, C. G., "High Pressure Arcs in Common Gases in Free Convection," Phys. Rev. 55, 1939.

37. Doan, G. E. and Schulte, W. C., "Arcs in Inert Gases - III," Phys. Rev. 47, 1935.

38. Suits, C. G. and Poritsky, H., "Application of Heat Transfer Data to Arc Characteristics," Phys. Rev. 55, 1939.

39. Suits, C. G., "Current Densities, Lumen Efficiency and Brightness in A, N_2, He, H_2 Arcs," J. Applied Phys. 10, 1939.

40. McQuiston, F. C., "Design and Operation of a Plasma Generator Using Argon as the Stabilizing Gas," (unpub. M. S. thesis, Oklahoma State University, 1959).

41. Cann, G. L. and Ducati, A. C., "Argon Mollier Chart," AFOSR TN 59-247, ASTIA 212-227, Plasmadyne Corp., Santa Ana, Calif., 1959.

APPENDIX

TABLE I

MONO ARC - SMOOTHED DATA

Run	Gas Flow lb/min	Current Amperes	Arc I Potential Volt	Arc II Potential Volts	Total Power In BTU/min	Power Out BTU/min	Gas Enthalpy BTU/lb	Efficiency
6-12-1	0.1300	400	26.5	NONE	603	272	2800	55.9
6-12-3	0.1300	350	25.2		503	243	2050	52.9
6-12-5	0.1300	300	23.2		396	210	1670	54.7
6-12-7	0.1300	250	24.2		344	207	1320	49.7
6-12-6	0.1300	200	26.2		299	177	1050	45.6
6-12-4	0.1300	150	27.5		240	137	820	44.3
6-12-2	0.1300	100	31.5		179	106	580	42.0
6-31-1	0.1098	400	23.7		541	303	2210	44.9
6-13-2	0.1098	350	23.3		465	279	1390	39.9
6-13-3	0.1098	300	21.6		368	223	1350	40.3
6-13-4	0.1098	250	22.0		313	217	940	33.0
6-13-5	0.1098	200	23.6		268	152	690	28.2
6-13-6	0.1098	150	25.0		214	132	540	27.8
6-13-7	0.1098	100	27.6		157	116	395	27.6
6-13-15	0.0774	400	21.1		480	277	2150	34.6
6-13-16	0.0774	350	20.9		416	261	1690	31.4
6-13-17	0.0774	300	19.4		332	226	1240	28.8
6-13-18	0.0774	250	19.3		275	190	780	21.9
6-13-19	0.0774	200	20.2		232	157	560	18.6
6-13-20	0.0774	150	21.2		181	175	410	17.5
6-13-21	0.0774	100	23.2		132	91	315	18.4
6-13-8	0.0546	400	19.8		452	282	2660	32.1
6-13-9	0.0546	350	19.9		397	263	2090	28.7
6-13-10	0.0546	300	18.8		322	230	1570	26.6
6-13-11	0.0546	250	18.7		267	213	1070	21.9
6-13-12	0.0546	200	19.6		224	184	870	21.2
6-13-13	0.0546	150	20.6		176	139	710	22.0
6-13-14	0.0546	100	22.8		130	105	570	23.9
6-14-1	0.0346	400	19.5		443	310	3760	29.3
6-14-2	0.0346	350	19.9		398	288	2680	23.3
6-14-3	0.0346	300	19.4		330	248	2160	22.6
6-14-4	0.0346	250	19.7		281	228	1560	19.2
6-14-5	0.0346	200	20.8		237	191	1360	19.9
6-14-6	0.0346	150	22.5		192	154	1170	21.0
6-14-7	0.0346	100	26.2		149	127	970	22.5

TABLE II

CONE SPACER - MODE I

Run	Gas Flow lb/min	Current Amperes	Arc I Potential Volt	Arc II Potential Volt	Total Power In BTU/min	Power Out BTU/min	Gas Enthalpy BTU/lb	Efficiency
9-1-A1	0.1322	80	13.8	62	345	168	1340	51.3
8-31-1	0.1325	90	13.2	65.5	403	133	2040	67.0
9-1-B4	0.1290	140	13.0	72	677	403	2120	40.4
8-31-2	0.1325	150	14.3	76	771	390	2870	49.4
9-1-C1	0.1283	200	14.3	81	1085	613	3680	43.4
8-31-3	0.1325	242	15.3	83	1355	968	2920	28.6
9-1-A3	0.1098	96	13.3	60	401	234	1515	41.5
9-1-B3	0.1098	140	12.7	71	667	414	2300	37.9
9-1-A4	0.0774	106	12.7	61	445	291	2000	34.6
9-1-B2	0.0774	140	12.7	70	659	458	2600	30.5
9-1-A5	0.0546	106	13.8	60	445	312	2430	29.8
9-1-B1	0.0546	140	13.8	66	636	497	2540	21.8

TABLE III

STRAIGHT SPACER - MODE I

Run	Gas Flow lb/min	Current Amperes	Arc I Potential Volt	Arc II Potential Volt	Total Power In BTU/min	Power Out BTU/min	Enthalpy BTU/lb	Efficiency
9-3-D1	0.1319	70	13.3	53	264	146	899	44.8
8-29-13	0.131	80	13.5	52	298	216	630	27.7
9-3-E5	0.1311	118	14.8	55	469	307	1240	34.7
9-3-F1	0.1306	175	14.8	61	755	465	2220	38.4
8-23-2	0.1098	60	11.1	47	199	62	1244	68.8
9-3-D2	0.1098	92	14.3	44	306	176	1182	42.4
8-23-1	0.1098	110	10.6	47	361	190	1555	47.4
9-3-E3	0.1098	130	13.3	56	513	317	1780	38.2
9-3-F2	0.1098	180	14.3	60	755	520	2190	31.6
9-3-D3	0.0774	79	13.8	47	273	167	1353	38.4
8-37-6	0.0774	80	15.8	43	268	92	1598	65.6
9-3-E2	0.0774	135	12.7	55	522	355	2150	31.9
9-3-D4	0.0546	83	14.8	44	278	204	1355	26.6
8-29-5	0.0546	104	14.2	37	304	163	2580	46.4
9-3-E1	0.0546	135	13.8	55	528	415	2080	21.4

TABLE IV

STRAIGHT SPACER - MODE II

Run	Gas Flow lb/min	Current Amperes	Arc I Potential Volt	Arc II Potential Volt	Total Power In BTU/min	Power Out BTU/min	Gas Enthalpy BTU/lb	Efficiency
9-3-E4	0.1306	130	31	26	422	324	749	23.2
8-29-12	0.131	171	26	22.5	472	335	1050	29.2
8-29-11	0.131	208	29	23.5	622	410	1615	34.0
9-3-G4	0.1293	235	33.5	25	783	605	1380	22.8
9-3-H1	0.1293	280	35	25	956	700	1980	28.6
8-29-10b	0.131	280	33.5	24	916	672	1862	26.6
9-3-I1	0.1300	340	39.7	24.5	1242	904	2600	27.2
8-39-10a	0.131	372	35.0	21.5	1200	880	2440	26.6
9-3-J4	0.1271	400	37.4	23	1375	1030	2710	25.1
8-23-3	0.1098	174	18.3	34	518	372	1327	28.1
8-23-4	0.1098	230	18.9	30	640	517	1218	20.9
9-3-G3	0.1098	253	31	25	806	600	1890	25.8
9-3-H2	0.1098	275	35	25.5	947	698	2260	26.2
8-23-5	0.1098	280	19.4	22	660	516	1312	21.8
9-3-I2	0.1098	340	38.2	23	1185	871	2860	26.4
9-3-J3	0.1098	420	35.8	23	1410	1090	2900	22.6
8-27-5	0.0774	87	22.6	27.5	248	142	1368	42.7
8-27-7	0.0774	91	18.3	28.5	248	122	1624	50.8
9-3-F3	0.0774	175	26	30	558	433	1610	22.4
8-27-1	0.0774	180	19.1	24.5	447	320	1640	28.4
9-3-G2	0.0774	240	26	30	765	645	1560	15.7
8-27-2	0.0774	250	19.4	22	589	462	1640	21.6
9-3-H3	0.0774σ	280	31	26	908	703	2660	22.8
8-27-3	0.0774	324	19.4	22	765	609	2000	20.2
9-3-I3	0.0774	345	34	22	1100	874	2900	20.4
8-27-4	0.0774	400	20.9	21.5	965	808	2030	16.3
9-3-J2	0.0774	430	33	22.5	1360	1098	3370	19.2
9-3-F4	0.0546	180	27	34	620	501	2280	20.0
8-29-4	0.0546	185	21.9	23.7	480	338	2620	29.7
9-3-G1	0.0546	240	25	32	778	700	1440	10.1
8-29-3	0.0546	250	22.9	24	668	518	2740	22.4
9-3-H4	0.0546	290	29	24	875	719	2870	17.9
8-29-2	0.0546	341	22.6	23.5	895	700	3560	21.7
9-3-I4	0.0546	345	32	22	1060	866	3540	18.3
8-29-1	0.0546	419	24.5	24.7	1175	1030	2660	12.4
9-3-J1	0.0546	430	31	22.5	1310	1040	4890	20.4

VITA

Edward Charles Pohlmann Jr.

Candidate for the Degree of

Doctor of Philosophy

Thesis: SOME INVESTIGATIONS OF A MULTIPLE ARC PLASMA GENERATOR

Major Field: Mechanical Engineering

Biographical:

Personal Data: Born in Chicago, Illinois, March 18, 1931, the son of Edward C. and L. Marita Pohlmann.

Education: Received the Bachelor of Science degree from Newark College of Engineering, Newark, New Jersey, with a major in Mechanical Engineering, in June 1953; received the Master of Science degree from Northwestern University, Evanston, Illinois, with a major in Mechanical Engineering, in August, 1954; completed requirements for the Doctor of Philosophy degree in May 1964.

Professional experience: Research Engineer with IIT Research Institute (formerly Armour Research Foundation), Chicago, Illinois, from September, 1957 to August 1960 and from September, 1963 to present; Instructor in Mechanics at Illinois Institute of Technology, Chicago, Illinois, from January, 1959 to June 1960; Instructor in Mechanical Engineering at Oklahoma State University from September, 1960 to August, 1963.

Professional organizations: Member of Pi Tau Sigma; Associate member of Sigma Xi.